Fakultät für Elektrotechnik und Informationstechnik
Technische Universität München

An enhanced methodology for energy system modeling including life-cycle analysis

Hydrogen as Power-to-X element

Kay Bareiß

Vollständiger Abdruck der von der Fakultät für Elektrotechnik und Informationstechnik der Technischen Universität München zur Erlangung des akademischen Grades eines

Doktor-Ingenieurs (Dr.-Ing.)

genehmigten Dissertation.

Vorsitzender:
Univ.-Prof. Dr.-Ing. Dr. h. c. Ralph Kennel

Prüfende der Dissertation:
1. Univ.-Prof. Dr. rer. nat. Thomas Hamacher
2. Univ.-Prof. Dr.-Ing. Ulrich Wagner

Die Dissertation wurde am 10.06.2020 bei der Technischen Universität München eingereicht und durch die Fakultät für Elektrotechnik und Informationstechnik am 17.11.2020 angenommen.

Abstract

This doctoral thesis is written in a large extent within the framework of the Kopernikus research project P2X and can be thematically classified in the field of energy systems modeling. In the scope of this research, hydrogen is utilized as the central sector-coupling element, which is produced by using surplus electricity from renewable energy sources. At first, the ecological footprint of hydrogen production from PEM water electrolyzer is evaluated through a life-cycle assessment (LCA). A surprising result of this analysis is that, across all modeling scenarios, over 90% of the global warming potential results from only the electricity demand of the electrolyzer. A comparison of the two different modeling approaches - LCA and energy system modeling - reveals that the respective results are not equivalent. This is caused by the different implementation method of CO_2 emissions for renewable energy technologies. It is shown that a dynamic consideration of these emissions throughout the lifetime of the technology is essential for a realistic assessment of PtX technologies in future energy systems. By using the multicrystalline silicon solar cell as an example, it is shown that a static modeling of emissions produce wrong results with respect to CO_2 balance. The novel approach presented in this work, depicts the dynamics of energy and material flows endogenously. Therefore the accuracy of energy system modeling is significantly increased. The model results also show, that from 2050 onwards, hydrogen could not only contribute substantially as a storable energy carrier, but also as a reducing agent in PV production for achieving the energy transition goals.

Zusammenfassung

Die vorliegende Doktorarbeit entstand größtenteils im Rahmen des Kopernikus Forschungsprojektes P2X und ordnet sich thematisch in den Bereich der Modellierung von Energiesystemen ein. Dabei dient Wasserstoff als zentrales Element für die Sektorkopplung unter der Ausnutzung des Dargebotes von Strom aus erneuerbaren Energiequellen. Zunächst wird der ökologische Fußabdruck von Wasserstoff aus der PEM-Wasserelektrolyse mithilfe einer Lebenszyklusanalyse (LCA) bewertet. Ein überraschendes Ergebnis ist, dass der für die Wasserspaltung benötige elektrische Strom, über alle Szenarien hinweg, über 90% des Treibhauspotentials verursacht. Bei einem Vergleich der unterschiedlichen Modellierungsansätze - LCA und Energiesystemmodellierung - fällt auf, dass die jeweiligen Ergebnisse nicht vergleichbar sind. Als Grund ist die methodisch unterschiedliche Implementierung von CO_2 Emissionen für erneuerbare Stromerzeuger zu nennen. Es wird gezeigt, dass eine dynamische Betrachtung dieser Emissionsquellen essentiell für eine realistische Bewertung von PtX Technologien in zukünftigen Stromsystemen ist. Am Beispiel der multicrystallinen Silizium Solarzelle wird gezeigt, dass eine statische Modellierung von Emission jedoch zu falschen Ergebnissen bezüglich der CO_2 Bilanz führt. Der vorgestellte neuartige Ansatz bildet die Dynamik von Energie- sowie Materialflüssen endogen ab, wodurch die Aussagekraft der Energiesystemmodellierung signifikant gesteigert wird. Die Modellergebnisse zeigen, dass Wasserstoff ab dem Jahr 2050 nicht nur als speicherbarer Energieträger sondern auch als Reduktionsmittel einen wichtigen Beitrag für die Energiewende leisten wird.

Contents

1 Introduction

1.1 Motivation

Icebergs melt, polar caps break apart and the habitat of living creatures disappears. Industrialization has not only heralded a new way of life, but has also initiated a profound change in our environment. Due to the increased use of fossil energy sources in heat engines, the amount of emitted CO_2 is increasing rapidly from combustion. Since 1800, the concentration of carbon dioxide in the atmosphere has risen by 45% percent [1]. It is estimated that beyond a concentration of 450 ppm CO_2, serious changes take place on our planet. Various climate models show possible future scenarios characterized by their different extremes [2]. However, they agree on the result of a rising temperature on earth due to the anthropogen greenhouse effect. This is associated with a rise in the sea level leading to further consequences, such as a slow down of the Gulf Stream [3]. In summary, humanity is expected to experience a drastic loss of habitat, an abundance of weather extremes and thus an increase in famines [4] in the decades to come. Politicians have already recognized these problems and are trying to counter them in international collaborations.
The United Nations Framework Convention on Climate Change (UNFCCC) which took place in the year 1992 already had on their agenda, the consequences of the antrophogenic climate change [5]. With the "Kyoto Protocol" signed in 1997 an additional module is added to the climate protection by defining the green house gases such as CO_2, CH_4 and N_2O [6]. The following international summits set more specific requirements to the models and made them more complex. In the agreement of Paris (2015), 195 states agreed to the objective of limiting the global warming to 2 °C over the pre-industrial time and striving to keep temperature increase within 1.5 °C [7]. The dramatic situation is strengthened by a publication where the globally available CO_2 budget was calculated [8]. In 2016, EU defined their goals of a 55% reduction for CO_2 emissions in 2030 and 80%-95% until 2050 based on 1990 [9] (also the reference year for the Kyoto protocol) which was then adopted by Germany [10]. Germany in particular, currently counts as a pioneer in climate protection with plans for a radical transformation from a fossil based electricity generation towards one using renewable energy. Currently, Germany contributes as the 31^{th} largest CO_2 emitter per capita, with roughly nine tonnes of global emissions, every year [11]. However, Germany is still on the sixth rank among the world's largest CO_2 polluters and thus contributes with 730 Mt per year to two percent of worldwide emissions [12].
Due to the current EU goals, years of interest are often set to 2030 (Paris agreement) and 2050 [13]. For the year 2050, CO_2 scenarios are mostly defined with a 80 or 95% reduction with respect to 1990 which leads to promoting renewable technologies by reducing the use of fossil fuels. Besides, Germany also has individual goals as stated in the "Erneuerbare-Energien-Gesetz-EEG 2014" [14] which claims an increase of the renewable energy share in the gross electricity demand at least up to 80% until 2050.
Thus Germany initiated a change in energy supply, the "Energiewende" and started a

variety of research projects to implement this intention. Several CO_2 reduction goals were defined along the path for the years 2020, 2030 and 2040 until the years 2050. However, despite the efforts and promises made by the German government, the climate protection goals for the year 2020 will not be kept. But more ambitious targets for 2030 have already been set. This failure, as well as the thematization of climate change on media, led to numerous demonstrations. Particularly noteworthy is the "Fridays for Future" movement, in which thousands of school children and students demand radical climate protection actions from politics.
In order to meet the 2030 targets, many measures are currently being implemented in the course of climate protection by the German government. Low-emission electricity generation plays the central role in achieving sustainable and far-reaching decarbonization by linking with other sectors. For this reason, in addition to pricing climate-damaging technologies, efficient technologies are also being subsidized by politics. Monetary bonuses for battery-electric-vehicles or feed-in tariffs for electricity generation from photovoltaics are few among them on a citizen level.
On the research level, long term solutions, beyond 2050, such as the nuclear fusion are still on today's research agenda. Thus, having in mind that climate protection and the accompanying measures have on the one hand a long time perspective but are also very urgent as time is running out, a variety of research projects were initiated by the German government.
One among them is the Kopernikus research initiative to tackle the urgent climate protection goals until 2050. It consists out of four Kopernikus projects and is equipped with a total budget of 400 million euros for the duration of 10 years. Among them, the hydrogen-based future-oriented paths are being researched within **Kopernikus - P2X** to offer new technologies to prevent climate change. If produced in a largely climate-neutral way, hydrogen theoretically offers the potential to decarbonize several sectors such as industry, heat, agriculture and transportation to a large extent. In contrast to power-to-heat, power-to-gas and other techniques of sector coupling, PtX preserves the unique selling point of a far-reaching penetration of various sectors "X", via the key element, hydrogen.
Hydrogen from proton exchange water electrolysis is used in this thesis as a representative for P2X concepts and implemented in sector-coupled energy scenarios, until an 80 to 95% CO_2 reduction target in the year 2050. It is noteworthy, that in this work a **distinction** is made between the project P2X and the method of using PtX, denoted by the different way of spelling.

1.2 Kopernikus project

The federal government of Germany started the Kopernikus initiative to explore the central questions of the "Energiewende" by means of 4 research projects. One among these is the P2X project funded for a time frame of 10 years and separated into 3 phases. The first phase, spanning 3 years, is equipped with a budget of 38.3 million euro. The consortium consists out of 50 organizations from different fields, including 20 research institutes, 26 partners from industry and 2 civil society organizations. The relevance of this topic for industry is indicated by the sector's contribution of 8.3 million euro towards the budget of the project. The project coordination is led by DECHEMA e.V.,

as a representative of the chemical industry. The following three different application cases were defined during the project work [15]:

- The use of PtX technologies for sectors which cannot competitively or technically be substituted in big scale such as industrial heat, fuel for aviation or ships, chemicals, electricity supply, just to mention few. Some industries need fossil feed for their process, for example, carbon is needed to harden steel. Another example is the porcelain manufacturing, where reductive or oxidant atmosphere is necessary during the burning process to ensure quality.
- Sectors which stand in direct competition with direct electrification, such as heavy duty vehicle freight transportation on roads, or supplying process heat for industry.
- Increasing the flexibility in the electricity grid by adding an additional load using the PtX technologies could help in the transformation process of the energy system. Using synthetic fuel or hydrogen for private transportation delivers an opportunity to reduce emissions in these sectors. Especially in these sectors, social aspects are another important factor, as e.g. increasing prices for fuel will have a direct impact on civilians. However, this wide field does not lie in the scope of that work and thus will not be covered.

The primary target of the project was to take advantage of available surplus power potential from renewable energy sources (RES) during hours of an overproduction of electricity. Thus, different PtX technologies can use this energy to produce during that time. The products of these technologies then are stored and can be used either for reconversion or further applications. When used for reconversion, e.g. hydrogen, they can be burned in a fuel-cell, thus electricity will be supplied during time of shortage. PtX products can also be used as an energy carrier and transported to locations where it is needed. A short video from the kick off seminar of that project shows a concept for that target [16]. It sketches the principle of using electricity, which is defined with as over production from RES, and converting it into a PtX product and e.g. reconverting it in time of lacking electricity or using it as a fuel. Following Figure 1.1 shows the this principle, where surplus power is used to produce a PtX product for later reconversion when electricity is needed. the electricity production from renewable energy sources is represented by the gray area. The blue area needs to be covered, as it represents the electricity demand. Surplus power (green area) can be shifted as a PtX product to fill gaps (yellow shape) which satisfies energy demand.

Preferably, the products resulting from PtX should be storable and easily transportable for later use, regardless of where they were produced. The stored energy, converted by PtX should also be quickly made available in time of supply deficit in the electricity grid (e.g. via reconversion of hydrogen). Such occurrences are more likely to happen in presence of an increased share of RES in the electricity sector, as opposed to conventional power production. In this project, hydrogen is used as the **central element** to store surplus power, and shift the usage in place and time. For this purpose, a holistic approach is pursued by using hydrogen as an energy carrier as well as a primer for the chemical industry.

In the first phase of the P2X project, three hydrogen paths were defined, each with an upstream process, which supplies a following downstream process with pure hydrogen

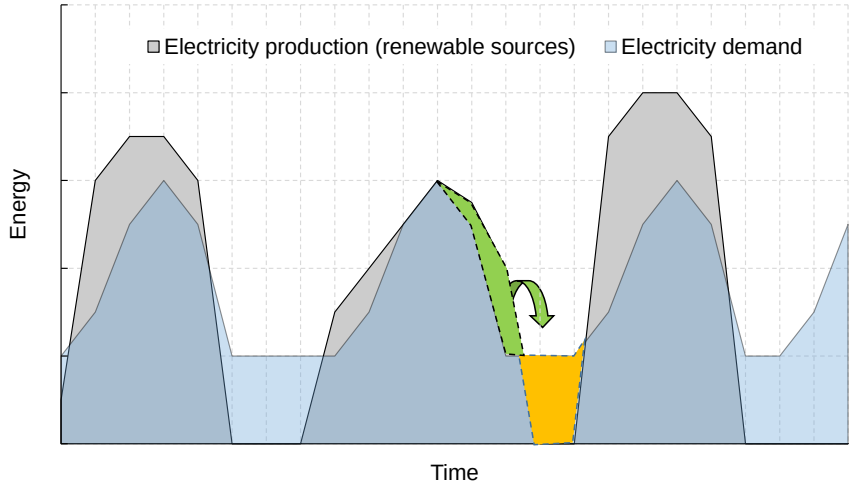

Figure 1.1: Sketch of an energy system in which surplus power is used from renewable energy sources for later use when energy is needed, as presented in the P2X kick-off clip [16].

or hydrocarbon (CxHy) compound. Whereas the upstream process delivers a product which is of use in versatile applications, the downstream process addresses specific fields to be substituted. Each process is performed by an individual technology. The upstream process provides the reactant that a downstream process uses to produce the end product. Following three paths can be distinguished:

1. PEM Water Electrolyzer + LOHC
2. LT electrolysis + Butanol / Fischer-Tropsch / Fermentation / hydrocarbons
3. HT electrolysis + OME

Figure 1.2 sketches the path of resources needed for a process. This way of depiction is called *reference energy system* and is read from left to right. On the left side, a range of resources are available which are consumed during a specific process (rectangles) to create a product (right side). The different electricity generating technologies such as power plants, PV or windturbines provide a power mix which is used by the PtX technology. The PtX technologies are highlighted in green and the respective reference processes for the upstream processes are shown in blue. For example, the upstream process proton-exchange-membrane water-electrolyzer (PEMWE) uses water as well as electricity as elementary input variables to produce hydrogen (H_2). This H_2 can already be used in this pure form for some applications. A possible reference process is steam methane reforming (SMR), which is based on the use of natural gas. A possible downstream process for pure hydrogen is the hydrogenation of hydrogen via creating of liquid organic hydrogen carriers (LOHC). As indicated before in the enumeration, LOHC was chosen as the fitting downstream process for the production of pure H_2 via PEMWE. This downstream process offers a new transportation technology. Usually hydrogen is compressed or liquefied by heavy cooling to increase energy density and make transportation of hydrogen more efficient. In the case of LOHC, hydrogen is linked to an carrier molecule in the hydration process for easy transportation similar

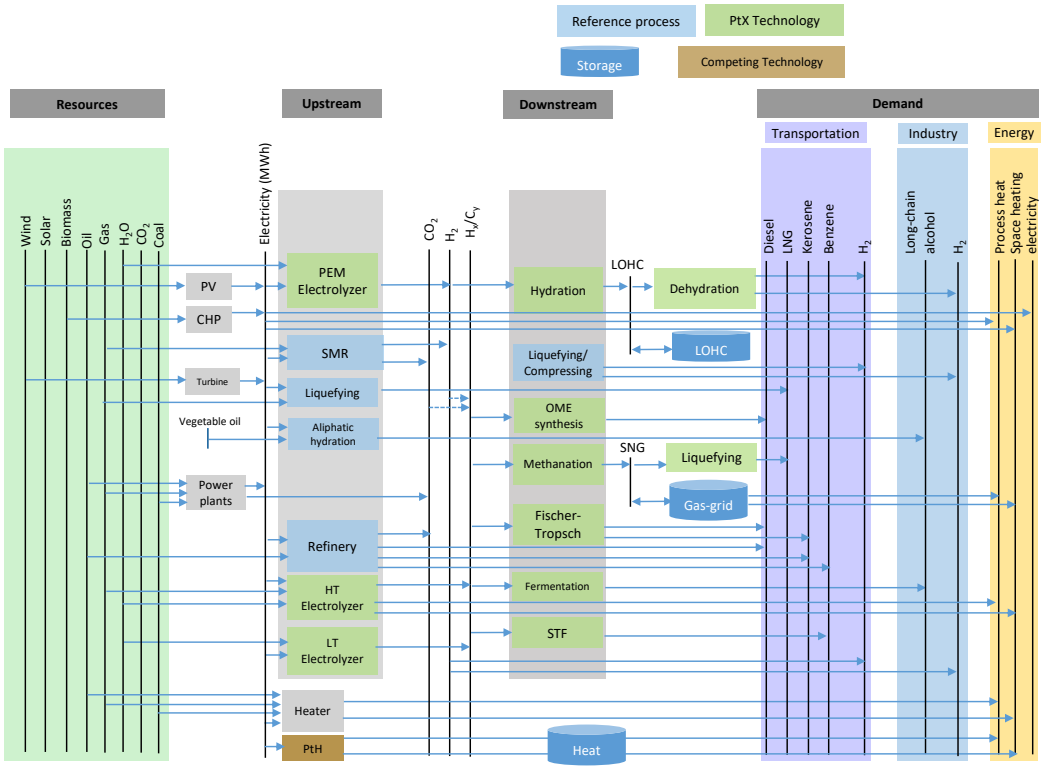

Figure 1.2: Overview of the PtX process chains and products that have undergone an evaluation within the Roadmapping.

to other liquid energy carriers such as petrol. At its destination, by applying heat, hydrogen can be extracted from the carrier. The respective product is then available for a variety of applications. In the case of hydrogen, it can be used in the transportation sector for hydrogen-powered fuel cell vehicles. On the other hand, already a hydrogen demand exists nowadays in industry. This dissertation deals explicitly with the first path, i.e. the PEM electrolyzer with a strong focus on hydrogen application. The PEM electrolyzer is described in detail in the Chapter 2.3.4 and its significance in a future power system is evaluated. The other PtX processes are briefly presented in the following for completeness.

The **low-temperature (LT) electrolysis** uses electricity to reduce carbon dioxide to carbon monoxide on the cathode side. On the anode side, water is oxidized to oxygen, producing small amounts of hydrogen as a by-product. In a further process (cold box), the main product (CO) can be broken down into its components by the different boiling temperatures. With the addition of H_2, a specific synthesis gas mixture of CO + H_2 is produced depending on the requirements. Here, biogas is used as a environment friendly CO_2 source in the P2X project. One possible application is the production of long-chain alcohols such as butanol. Conventionally, butanol is currently produced on a petrochemical basis or using vegetable oils. The synthesis gas mixture is fed to microorganisms, which can then produce butanol or hexanol by fermentation. The advantage of this technology is the flexibility of the products which can be adjusted by the plant design and the gas admixture. The current research focus within the P2X

project is currently on the development of novel electrodes and cell designs for the production of synthesis gas. In addition, the second step, the production of butanol by fermentation, is to be carried out in three process steps (eq. 1.1-1.3), which in principle have already been proven [17].

In the first step of the fermentation process, the bacteria *Clostridium autoethanogenum* ferment a mixture of CO and H_2 to acetate and ethanol:

$$\mathrm{CO} + \mathrm{H_2} + \text{bact. Clostridium autoethanogenum} \longrightarrow \text{acetate} + \mathrm{C_2H_5OH} \tag{1.1}$$

In the second step the bacteria *Clostridium kluyveri* is producing butyrate and hexanoate:

$$\text{acetate} + \text{ethanol} + \text{bact. Clostridium kluyveri} \longrightarrow \text{butyrate} + \mathrm{C_6H_{12}O_2} \tag{1.2}$$

In the last step butyrate + hexanoate are fermented by bacteria *Clostridium autoethanogenum* to produce butanol and hexanol:

$$\text{butyrate} + \mathrm{C_6H_{12}O_2} + \text{bact. Clostridium autoethanogenum} \longrightarrow \mathrm{C_4H_{10}O} + \mathrm{C_6H_{14}O} \tag{1.3}$$

The **high-temperature (HT) electrolysis** or solid oxid electrolyzer cell (SOEC) is the upstream process of the third path, which produces synthesis gas or hydrogen at high-temperature co-electrolysis. Especially in P2X, a container solution is being researched which can be designed as a stand-alone plant but also used in large-scale industrial plants. In the Co-electrolysis, two reactions take place simultaneously in a reverse water-gas shift reaction. The advantage of this system is that it requires less equipment compared to the separate production of H_2 and CO. By varying operating parameters such as temperature and pressure, different synthesis gases can be produced which differ in their composition. Electricity, preferably from renewable energy sources, is used as input to guarantee the pressure and temperature level. A CO_2 source is used to provide the carbon for the synfuel. Good sources are steel production, ammonia synthesis or direct-air capture (DAC) plants. In steel production, CO_2 is produced primarily due to the use of coal in the blast furnaces. In ammonia synthesis (Haber-Bosch process), CO_2 is not emitted directly during the reaction of nitrogen and hydrogen to the product ammonia. However, the hydrogen is first extracted from natural gas, which produces the greenhouse gas.

In the DAC plant, air from the environment is enclosed in a chamber via several turbines. A sorbent is enriched with CO_2 and CO_2-free air is separated as a product. After the sorbent has been enriched with CO_2, the sorbent is reactivated at around 100°C for the next cycle. Future energy consumption is given as 500 kWh electricity and 1500 kWh heat consumption per ton of CO_2 captured [18]. If a synthesis gas ratio (H_2/CO) of 2:1 is used for the HT-Co elektrolyzer production, methanization is a possible following downstream process. This allows synthetic natural gas (SNG) to be produced for e.g. the transportation sector. SNG can either be fed into the gas network, transported via pieplines or liquefied to LNG in a further downstream process. Another possible downstream process is the production of oxymethylene ethers (OME) which is nowadays produced via the Methanol and Formaldehyde path [19], [20]. In principle, these can be used as substitute fuel for diesel. Typically, however,

the OME are used as blends and added to the fuel. Using a blend of 22% of OME, soot emissions can be reduced by up to 75% and NOx emissions by about 43% [21]. With this single technology, the diversity of technologies and reduction potentials of different pollutants within the P2X project is already noticeable. In addition to using a syngas, pure hydrogen can also be used from PEM electrolysers, for example, and CO_2 from DAC plants can be synthesized in a methanol synthesis to SNG and later to OME.

The question of a sustainable source of electricity and energy arises for all PtX technologies. Since these processes are based on electricity and replace existing petrochemical plants, they must of course create sustainable added value. Fossil power generation is out of the question, as no emissions would be saved due to higher conversion losses. The electricity requirement must therefore be covered by renewable energy sources. Since the focus of the P2X project is primarily on the use of surplus power from fluctuating renewable generation, wind and PV are the suitable power generators. This fluctuating electricity production leads to fluctuations in production of PtX technologies, which is unfavorable for some processes. Especially high temperature processes, such as HT-Co electrolysis are only of limited use for dynamic operation, that follows the supply of electricity, due to the heating losses. For this reason, there is also the question of the environmental friendly provision of electricity through a constant plant operation. These questions will be answered in the following chapter by using an energy system model. In addition to the German electricity consumption, a PEM electrolyser will also be implemented as an exemplary PtX technology for hydrogen production.

In addition, however, it must also be discussed to what extent emitting additional fossil carbon is avoided in the production of syngas. There are two different points of view here. On the one hand, carbon can be obtained from DAC plants or from the sustainable cultivation of biomass. According to this, the CO_2 concentration in the air does not increase further due to PtX plants. Another position is the use of already existing CO_2 point sources from industry. These are primarily steel or cement plants, glass production or power plants. The advantage is obvious here, since the concentration of CO_2 in a point sources is considerably higher (20% CO_2 in a cement plant) [22], less air mass has to be moved than with a DAC process (400 ppm CO_2 in air) to extract carbon from air. Although carbon dioxide is finally emitted into the environment, an additional **second cycle** takes place. A reduction of CO_2 emissions is thus possible if, for example, the rate of consumption of fossil diesel can be reduced. Nevertheless, both with the sustainable thought and with the second life approach, the power source is again an important factor, since the purification of CO_2 is associated with an energy expenditure. An overview of some different technology paths of the project is presented in Table 1.1

Although the products of the individual PtX technologies are different, they have in common that they are all energy carrier. Since the added value of a fuel is high due to the current willingness to pay for fuel, an evaluation in the project P2X is made between the individual products in the transportation sector. Hydrogen from PEMWE can be used in many ways and is a basic prerequisite for a variety of further processes. Moreover, in the transportation sector, hydrogen can be used directly from the upstream process without any further downstream process. The use of hydrogen in fuel

Table 1.1: PtX systems from project work and their parameters [23].

Technology	**reactant**	**product**	**demand** [1] **kWh/kg**	**power rating**	η	**startup time**
PEMWE	H_2O	H_2	55	1 MW	0.6	sec
NTEL	CO,H_2O	CO	6	1 MW	0.6	n/a
HTEL[2]	CO_2,H_2O	H_2:CO	9	150 kW	0.75	min
LOHC[3]	H_2	$C_{21}H_{20}$	0.65	1 MW	0.7	sec-min
FT[4]	H_2,CO	Diesel	26	1 MW	0.6	min
OME[5]	CH_3OH	OME	8		0.8	n/a
Methanation	H_2,CO	CH_4	63-70	1.25 MW	0.7-0.8	n/a
Fermentation	H_2,CO	$C_4H_{10}O$	n/a	1 MW	n/a	n/a

[1] Energy demand per 1 kg of product
[2] A syngas ratio between H_2:C of 2:1 is chosen
[3] assumption that 1 kg H_2 can be stored/extracted in/from 16 kg LOHC ($C_{21}H_{20}$) using 1.4 kWh_{el}, 9.1 kWh_{th}.
[4] efficiency goal, when using waste heat from HTEL, FT LHV = 12.2 kWh/kg, HTEL η= 0.75, methanation η= 0.8
[5] OME_1 LHV=6.3 kWh/kg [24, 20]

cell vehicles with an efficiency of about 50% is predestined for this. However, since hydrogen has a very low volumetric energy density of about 3 kWh/m³, it is usually liquefied or compressed [25]. LOHC is another possibility of liquefaction, which can bind 620 m³ H_2 per m³ LOHC and thus increases the volumetric storage density of hydrogen to about 2 MWh/m³ LOHC [26].

In the case of Fischer-Tropsch, for example, diesel is produced via HTEL as the upstream process and a FT synthesis in the donwstream. The advantage of this product in contrast to hydrogen is that existing combustion engines can still be used. However, by combustion, CO_2 is emitted, which was previously bound in the FT Diesel. Production costs of various synthetic fuels have recently been reported in a literature review with a wide cost range between 45 € to 3500 € per MWh fuel [27]. In this review paper also additional scenarios of the corresponding author were developed, where the production costs vary between 130 € to 770 € per MWh fuel, depending on assumed electricity prices, carbon capture costs and plant utilization.

Fermentation, in this project, aims at a product with a high energy density, which conventional combustion engines can use without modification. Butanol with a LHV of 8 kWh/l is produced with bacteria [28] and is next to the FT Diesel another type of synfuel.

As already mentioned, carbon has to come from either renewable sources or point sources of anyway emitted CO_2 from fossil fuel, to be sustainable. However, this might start a controversial discussion about the accounting of the emissions. Either emissions can be allocated to the source as they would have emitted anyway and carbon is just used for a second cycle. Another view is that emissions are allocated to the emitter who burnt the initial fuel. This however starts a next debate as car manufactures have to achieve certain fleet goals regarding their CO_2 emissions [29]. For estimating

the environmental impact occurring from the different technologies in the project, life-cycle assessment (LCA) were conducted, each presented in the latest roadmap of the Kopernikus P2X project [30]. Currently, research efforts in the reduction of catalyst loading of PEMWE is performed at the TUM. As PEMWE catalyst made out of material from platinum group, which is rare and defined by the EU as critical material. The list of critical materials is updated periodically and depends on several parameters. The most important are the security of supply, considering their governance performance and trade aspects of the EU and the economic importance in means of the cost of material substitution (SIEI Index) [31], [32].
The LCA of the PEMWE was performed by the author and presented in this dissertation. As PEMWE mainly runs on electricity and water, a energy system model was developed to estimate the amount of surplus power in future. This model was adopted by all LCA partner of the project which ensures a harmonized electricity mix which is the first step for a comparable assessment of the different PtX technologies. At this point it should already be mentioned that LCA as it is currently used has led to effects worthy of discussion in this project. These effects will be discussed in detail in this thesis and a new methodological approach will be developed as a proposed solution.

Currently, due to the high diversity of products, a large number of applications are possible for PtX technologies. On the one hand, this is a positive phenomenon, but this makes it difficult to compare them with each other among the project, since there is not one specific reference product all technologies can be compared with. In summary, the first project phase has succeeded in creating a good uniform basis for comparing the individual PtX technologies. A cornerstone is the energy system model, which was developed in the context of the dissertation and was used for the entire project. Details of this model are presented in the following of this work for different scenarios. Another finding from this modeling was that PtX technologies are perceived as additional consumers in the electricity system. In order to achieve an impact, sizes of the plants must also be correspondingly large. In the energy system model, a scenario was developed in which about 1/3 of the vehicles of the individual transport are supplied with PtX technology. It reveals, that for this amount of energy (ca. 50 TWh end energy of fuel-cell vehicles) the currently curtailed electricity can only account for about 10%. Thus, the primary target of using unused energy from renewable electricity producing technologies (surplus power) to decarbonize different sectors is not possible. Furthermore, did project results showed, that surplus power can not be seen as a "free" available resource. Moreover, with the new consumers, this surplus power will gain a value through the market mechanism of supply and demand. This electricity is therefore a scarce commodity that is not available to such an extent that it can supply all potential sectors identified by DECHEMA. In the 1st project phase a total of about 2 PWh of electricity was determined for PtX technologies in the transportation sector. This electricity demand already includes conversion losses to substitute fuels for car fuel, rail transportation, kerosene and fuel for shipping. However, this potential is not to be understood as a goal to be redirected, since it is also possible to switch to more efficient technologies such as fuel cells or battery electric vehicles. Further possible areas of application are low-temperature heat (1.5 PWh electricity demand) and industry with about 1 PWh. In the latter case, a high potential is seen for process heat [33].

Electricity used for PtX technologies is therefore the key input parameter for the subsequent LCA regarding the greenhouse gas emissions. This method serves as evaluation for the individual PtX technologies on a standardized basis. Following impact categories where selected to be examined: Global warming potential (GWP), metal depletion (MDP), photochemical ozone creation potential (POCP) and water depletion (on an inventory level). In addition to the impact categories, the cumulative energy demand by renewable and non-renewable sources was reported. The following Figure 1.3 shows a snapshot of the corresponding technology paths based on the GWP evaluation criterion in the current electricity grid. The interpretation of these LCA results are explained in depth for the PEMWE technology in later chapters. At this point it serves as an overview of all technologies and is listed for completeness.

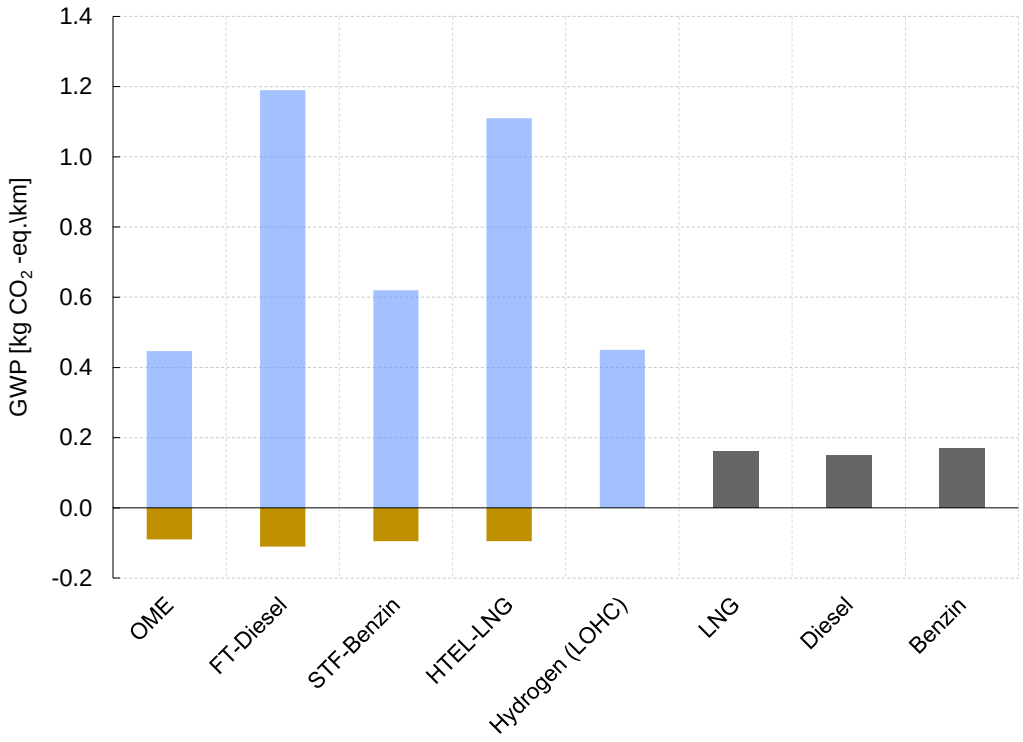

Figure 1.3: Global warming (GWP) impact category for all P2X paths of the different technologies in the project for the year 2018. The negative bars represent a credit as fossil carbon is stored from a source in the product. This carbon is released during use phase in a middle class car per driving distance of 1 km and represented by the blue bars. the reference products are shaded in gray (data from [30]).

In this case, a functional unit of 1 km distance with a medium-sized car is selected for the impact category GWP. The impact of the product when converted into kinetic energy with a vehicle is thus shown in the corresponding graph. The utilization phase, the manufacturing impact of all components as well as the value chain are summed up in the blue bars [30]. These values are valid under the assumption of the corresponding PtX technologies in the electricity system as simulated for the year 2018. It is therefore clear that none of these technologies are environmental friendlier than their corresponding reference product (gray bars), from today's point of view, as the current electricity mix emits approximately 500 g of CO_2 per kWh of electricity. For the production of

electricity-based fuels, further technology specific conversion losses are added, which leads increase the specific emissions. In case of the produced hydrogen via PEMWE, an additional transportation to a hydrogen filling station is modeled via trucks over 250 km distance in hydrogenated. This LOHC will be dehydrated at its destination and is assumed to be distributed via the existing petrol station infrastructure. For this reason, it was decided within the project to compare the hydrogen demand in a fuel cell vehicle with that of a combustion engine (gasoline).

1.3 Outline

As this dissertation is conducted during the P2X project, its structure follows the same chronological order, as the research questions was strongly connected to the P2X Roadmap process. A flowchart provided at the end of this chapter, outlines in Figure 1.4 the different stages of this dissertation, as they appear in the corresponding chapters stated on the vertical and the modeling horizon on the horizontal. This work starts with the introduction of the sector coupling methodology overview, especially power-to-heat and power-to-hydrogen. For the latter, an energy system for Germany is modeled to calculate the potential of energy used for hydrogen production and to examine the system behaviour. To investigate the global warming effect of sector coupled produced hydrogen by using electricity, a life-cycle-assessment is conducted. Research questions are describes, which occur during project work and solutions are provided. The content exclusively focuses on the first phase of the P2X project, and covers especially the impact of PEMWE as a new technology in the future energy system.

During the project work in P2X, the following **research questions** were addressed by the author:

- Development of sector-coupled energy systems under a constant reduction of CO_2 emissions, until 2050, referring to the German climate protection goals; in particular using hydrogen.
- The life-cycle assessment of electrolytically produced hydrogen via PEMWE.
- The implementation of a dynamical approach of introducing the ecological footprint of renewable energy technologies in energy systems models.

The current chapter (Chapter 1) describes the P2X project in which this work was conducted and also classifies it in the current situation regarding climate change.

The second chapter, **Power-to-X** describes some methods for utilizing surplus power from renewable energy-sources to supply further sectors. First of all, terms such as surplus power, or the different PtX methods are clarified. In contrast to PtH, Power-to-Hydrogen is presented as another method which is very flexible and can address further sectors. In addition, several technologies are introduced for hydrogen production.

Chapter 3 describes the different premises set for modeling an energy system in which PtX technologies play a significant role. A model generator is used and described for building a linear optimization problem which is solved by its cost optimal solution.

The optimal solution of the energy system is given by minimizing the overall system costs for the different scenarios developed. Two case studies are conducted:

- PtH is chosen to show an efficient way of strongly reducing carbon emissions in the heating sector of the municipality of Greifswald by using high share of wind energy.
- An electricity-mix was provided for the P2X project to decarbonize the individual transportation sector. This is model is further used within the P2X project to provide the energy-mix and utilization period of PtX technologies in an energy system of the future [15, 30].

The evaluation of the ecological impact for all PtX technologies in the P2X project is carried out by conducting a LCA for each scenario. Since no literature is available, providing insight to the materials used for a PEMWE, an inventory list is developed in Chapter 4 in coordination with ZAE Bayern. This inventory list is used to conduct a LCA on PEMWE which is the first published [34] and compared with the conventional hydrogen production. To track a development of the different impact categories of assessing hydrogen from PEM, the electricity mix from Chapter 3 is introduced as an variable in the LCA according to ISO 14040 and 14044 standards.

By comparing the results from Chapters 3 and Chapter 4, a discrepancy of the CO_2 footprint of both presented methods is revealed and discussed. The fifth chapter offers a solution to eliminate this discrepancy by merging the methodology of energy system modeling with the concept of conducting a LCA. First, the difference between the two methodologies of integrating direct and indirect emissions of electricity producing technologies is explained. Second, the developed method is used in a future energy system by modeling a dynamic manufacturing process of multi-crystalline silicon-based photovoltaic cells. Hydrogen, as an innovative reduction agent for SiO_2, is used to show the full potential for a profound sector-coupling which satisfies the needs of a PtX concept.

Chapter 6 addresses the influence of a chosen time horizon regarding the modeling results, when indirect emissions are considered. This is done by broadening the view from optimizing several single snapshots over the time horizon, implemented as an annual modeling approach towards considering the whole time horizon as one intertemporal optimization problem. In the latter, a CO_2 budget for the whole modeling period is defined from 2030 towards 2050, and later expanded to 2100. Results show significant differences regarding CO_2 abatement costs, and thus the time when technologies are installed by the energy system model.

Finally, in the last chapter (Chapter 7) the several results of each part of this work are summarized, and a conclusion is provided on the importance of using the PtX method in a decarbonized future energy system. In addition the improvement of integrating indirect emissions dynamically into existing energy system models is emphasized. In an outlook, further research aspects are sketched to show the full potential of hydrogen in combination with the PtX method in future energy systems.

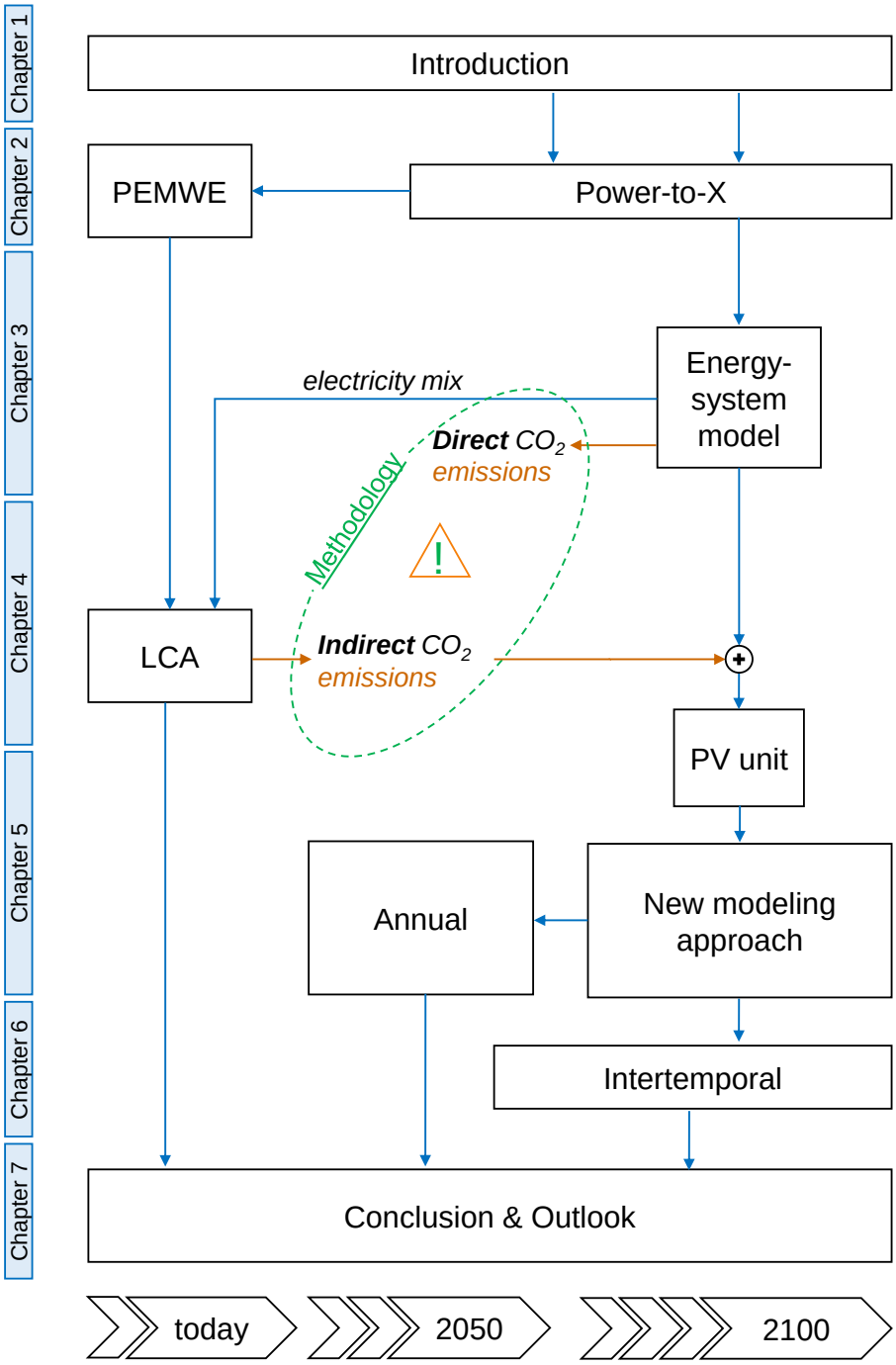

Figure 1.4: The structure of the dissertation sketched as a flowchart. On the vertical different chapters are listed which are including the corresponding items next to them. The green circle represents the different methodologies which are used by the two different models used. On the horizontal the years represent the time horizon, model results are valid for.

2 Power-to-X

There is no general definition of the term Power-to-X [35]. However, in the context of climate change mitigation, this is usually understood as the conversion of electricity from renewable sources into other applications or products such as gases, liquids or heat [36]. Sternberg answers the question of the "X" in the context of surplus power. In his work different storage technologies are presented. He distinguishes between the direct storage of electric current and the transfer of energy to another medium. Using an assumed annual electricity surplus of 1 MWh from renewable electricity sources, he evaluates different technologies [37]. Following definitions are given by Sternberg:

- **Power-to-Power** describes storage systems which convert electricity to chemical or mechanical energy. The most familiar example, used today, is pumped hydro storage with efficiencies up to 80% [38] but which are limited to geographical constraints [37]. Another technology of storing large amount of energy is the compression of air. Efficiencies of these adiabatic Compressed Air Energy Storage (CAES) vary between 55% and 75% [39]. Batteries, as representatives of electrochemical storage, are typically used for smaller applications, ranging from a few ampere hours (Ah) in a smartphone to several kWh in battery electric vehicles or stationary storage. The lifetime of the battery cells depend on various factors such as temperature, depth of discharge and material. In addition to the lead-acid battery, which also is used as a starter battery in vehicles, lithium-ion batteries are a well-known representative. The efficiency of lithium-ion batteries is around 95%, based on the amount of energy stored (Wh) [40].

- **Power-to-Mobility** temporarily stores electricity in lithium-ion batteries, for example, and converts this later into kinetic energy via the electric engine of a vehicle. A further term for this is grid-to-vehicle, if the vehicle is connected to the power grid. Another possibility is vehicle-to-grid, which means that electricity that has previously been temporarily stored in a vehicle is fed into the grid. The electricity consumption per km of driving distance of a medium class vehicle is given between 0.12-0.2 kWh/km [41], [42], [38].

- Similar to Power-to-Mobility, **Power-to-Fuel** (PtF) is another option for reducing the amount of fossil fuels in the transportation sector. In this case, electricity is used to create an energy carrier suitable for the refuel vehicles. E-fuels (or syn-fuels) are one possibility to supply existing internal combustion engine (ICE) with diesel and benzene [43]. This is done by using a carbon source to produce a CHx compound similar to the fossil fuel. Another opportunity is the conversion water into hydrogen and oxygen by using electrolyzer. In this case, fuel cell vehicle (FCV) are the preferable solution due to the high efficiency of fuel cells compare with ICE. Beside the mobility sector, hydrogen can also be used as chemical feedstock. To increase the low energy density, hydrogen is converted to hydrocarbons by different processes [44].

- **Power-to-Heat** technologies convert electrical power directly into heat. A distinction is made between the two types i) electric heaters, whose theoretical maximum Coefficient of performance (COP) is limited to 1, and ii) heat pumps, whose COPs are typically between 2.1 and 4.9. The COP is the ratio between the heat flow ($\dot{Q}$) that can be extracted from the heat pump and the electrical power P_{el} needed calculated as [45]:

$$COP = \frac{\dot{Q}}{P_{el}} \tag{2.1}$$

In this thesis the term Power-to-X, also called PtX, is understood as transforming electricity directly into another form of energy or converting it (under the use of further resources) into a new product. It aligns with Power-to-Heat (PtH) and power-to-gas (PtG) but is meant in a more general context. Thus, PtX enables coupling different energy sectors which is already done every day in small scale for example by using electric water jugs in households to heat up water. Power-to-fuel (PtF) is another application which stays in contrast to the direct use of electricity for the purpose of transportation (Power-to-mobility). Today, this is the source of intense media discussion which focuses on evaluating two technologies, namely BEVs and FCV.
BEVs, more commonly on streets today, herald a new age of private transportation converting electricity into mileage. However this is not an innovative technology as BEVs experience a relaunch after almost 100 years when the city of Berlin ordered 57 electric three-wheelers for the Post office [46]. Beside, electricity is also used already for some high temperature processes e.g. to power arc furnaces in aluminum production or for welding in construction. Using PtF, as a further option, comes along with significant losses due to individual process efficiencies of the value chain from energy to the product.

Electricity is versatile in its use and thus rightfully considered as the most valuable form of energy as the generation mainly relies on finite fossil fuels. This will however change in a carbon-neutral world which would be based solely on emissions-free renewable energy. Renewable energy is provided by the sun as solar irradiation, wind in exposed locations and in some regions by water bodies. The theoretically potential exceeds global energy demand. A small examples shows, that covering 1% of the Sahara with PV panels would be, theoretically sufficient to cover the world's electricity demand [47]. The implementation however comes along with problems, which are versatile and caused by the energy harvesting itself, distribution and social or economic aspects. The availability of renewable energy sources fluctuates and is not constant but is highly depending on the weather. Consequently, the discrepancy between energy demand and renewable energy supply is the main problem as society is used to daily rhythm. In Germany, this results in high peak electricity demand during noon in private households or higher traffic density in early and evening hours. Actually, electricity from renewable energy sources is limited especially when used to decarbonize energy demanding sectors.
Germany's total final energy consumption in 2017 was about 3,700 TWh, of which half was used to supply heat demand. Only about 14% of final energy consumption was covered by renewable sources [48]. In order to cover this final energy demand sustainably, a very ambitious expansion of wind and solar power plants would first have to take place.

However, the government of Bavaria, for example, recently announced that it will pass a new regulation regarding the distances between wind turbines and settlements. This "10H" rule limits the construction of new wind turbines to a minimum distance of 10 times the height of the wind turbine to the nearest village. As a result, the addition of wind turbines is strongly reduced and came to a virtual standstill in 2018 with only 50 MW of additional wind turbine capacity compared to 2014 (600 MW) [49]. Solar power plants, on the other hand, have no such distance regulation and can also be more easy integrated e.g. as photovoltaic roofs. However, due to the day/night cycle, solar irradiation, produces power peaks which adds up to a small number annually and are seasonally distributed over the year. Due to this fact, it is difficult to use the surplus power that is generated during these peak times. On the one hand the storage system must be designed for the maximum power value, and on the other hand the storage size must be dimensioned accordingly to store the energy temporarily. PtX systems such as hydrogen-generating electrolysers are currently still very cost-intensive and must have high capacity utilization to ensure cost-effective production. Thus, the substitution of entire sectors with surplus power from renewable electricity is limited, due to the low technical potential.
The current final energy demand in the overall German transportation sector, for example, amounted to about 750 TWh in 2017 [15], which would have to be generated by PtX technologies with corresponding conversion losses. With an optimistic assumption of an efficiency of 75%, this corresponds to a power demand of 1,000 TWh, which then would have to be provided by power generating technologies from renewable sources. If this electricity were to be covered by offshore windparks, a capacity of 250 GW would be needed (4,000 full load hours assumed). In 2018, the EU had 18 GW of offshore wind capacity installed, with an assumed quadrupled by 2030 [50].

2.1 Surplus power

Surplus power is the electricity from intermittent renewable energy sources which can not be integrated in the energy system. That is mainly caused by transmission grid limitations or an unbalance between energy supply and demand [51], [52]. The main idea behind today's PtX technologies is the efficient utilization of this surplus power from renewable like PV or windturbines which is otherwise curtailed and lost [37]. Such energy curtailments occur in Germany especially during summer in the south of Germany or at the North- and the Baltic-Sea during periods with strong wind. 5.5 TWh electricity from these sources were curtailed in one year, with the main proportion coming from offshore-wind (Table 2.1) [53]. On the first view this number seems to be big. However even with a 100% efficiency of a given PtX technology for producing synthetic fuel, it will only cover 1% of the energy demand coming from private transportation sector. This already shows that focusing solely on curtailed energy will not have a sufficient impact in the clean energy context. The energy system is facing a new demand which needs to be covered by additional renewable capacities. Also besides the technical solutions, citizen acceptance is needed for a transformation of the energy infrastructure.

Table 2.1: Curtailed energy in Germany in 2017

Technology	Curtailed energy (GWh)
Windenergy (offshore)	4,461
Windenergy (onshore)	826
Solarenergy	163
Total	**5,450**

The main four primary energy consuming states of Germany are Bavaria (1.9 EJ), Baden-Wuerttemberg (1.4 EJ), North Rhine-Westphalia (4.2 EJ) and lower-saxony (1.3 EJ) [54]. Two of the four states with the highest energy demand are located in the southern part of Germany (Bavaria, Baden-Wuertemberg). Since 80 % of the electricity was curtailed in the northern part from offshore wind farms in the North-sea and the Baltic region, it already shows the imbalance between renewable energy supply and demand. Latest discussions in the years 2014 till 2018 showed the difficulty of constructing high-voltage direct current (HVDC) transmissions lines from the north of Germany to the south with a capacity of 4 GW [55].

2.2 Power-to-Heat

Power-to-Heat (PtH) is the cheapest solution among the PtX technologies which uses electric energy and converts it to heat [56]. Either electric heaters are used to for the conversion process. Those combine the advantage of low investment costs and high efficiencies. A more expensive solution are heat pumps which uses heat from an ambiance medium to increase their COP above 1. The estimated potential for PtH in Germany is high between 23 TWh [41] and 561 TWh [57] for low temperature heat which can be used for domestic heating. Heat is a regional good as it can not be transported easily over longer distances. Thus, to prevent building infrastructure, PtH needs to be used at the location where surplus power as well as the heat demand is located.
A unique case where both requirements are fulfilled is the municipality of Greifswald which is located on the Baltic-Sea. Greifswald has a lot of domestic heat demand and some of these buildings have a moderate to poor insulation. It has a large potential for reducing heat by insolation but the low rent makes costly renovation a social issue. Greifswald is close to Lubmin which had a 2.2 GW nuclear power plant in the past and is equipped with robust transmission grid infrastructure. The offshore wind farms Baltic 1 and Baltic 2 are also connected to the Lubmin hub in the 50Hertz transmission grid. Thus, using PtH is a potential alternative which was investigated during a case-study for Greifswald.

2.2.1 Electric heaters

Electric heaters are already used in combination with heat storage for district heating e.g. in Nuremberg [58]. The principal is common in private households for heating up water. Electric heaters combined with heat storage are controlled bivalent (on/off) or step-wise [59].

2.2.2 Heat pump

Two different types of heat pumps are used today to cover heat in private households. Air heat pumps, are more easy to be integrated due to their simple and compact installation. However, their annual COP is quite low, given with 2.1 - 3.4 [60] due to cold air temperatures during heating periods. Groundwater heat pumps, on the other hand, do not use the air as a source of heat, but the groundwater from which they extract heat. The groundwater temperature is much more constant than that of air and even higher during heating periods, so that more heat can be extracted [61], [62]. The COP of groundwater heat pumps varies between 2.4 and 4.9. Due to the low temperature level, the energy is used for heating rooms and is also expanded with heat storage tanks.

2.3 Power-to-Hydrogen

Hydrogen is a chemical element with the symbol H which originates for the Latin word hydrogenium. With an ordinal number of 1, it is located in first period and first group of the periodic table. With a density of 0.0899 kg/Nm³ hydrogen is the lightest known chemical element. It has a lower heating value (LHV) of 33.33 kWh/kg (120 MJ/kg) and a boiling temperature of 20.39 K (Table 2.2) [25]. Hydrogen is also one of the most common element found in the universe. 73% of the sun consists out of hydrogen which burns via fusion reaction to helium. On earth, molecular hydrogen is rarely found but is present in a compound form in water (H_2O).

Table 2.2: Properties of hydrogen (at 1 bar)

property	value	unit
lower heating value (LHV)	3.00	kWh/Nm³
higher heating value (HHV)	3.54	kWh/Nm³
density	0.089	kg/Nm³
boiling temperature	20.39	K

Hydrogen is produced via three different methods: electrolysis, bio-chemical conversion or thermal conversion [63]. The latter is used today for supplying industrial hydrogen demand. As is is based on fossil fuels, the use is automatically connected to additional CO_2 emissions as shown in the next chapter. To overcome this problem, hydrogen can be produced in electrolyzers via splitting water (by applying a voltage). However, the energy source used, determines the level of environmental friendliness of the product. Using hydrogen from these innovative technologies poses the questions for the profitability and efficiencies [64]. As surplus power is a limited energy source, conversion losses through different process steps should be kept to a minimum [65].

2.3.1 Conventional hydrogen production

Worldwide around 65 million tonnes of hydrogen (∼2200 TWh) are produced commercially in one year [66]. With efficiencies between 66 % and 73 % [67, 25], steam methane reformers (SMR) are the standard technology in today's hydrogen manufacturing industry. By source, 68 % of hydrogen is produced from natural gas, 16 % from oil and

11 % from coal [63]. The main conventional hydrogen production methods prevalent in current industry are:

- hydrocarbon pyrolysis
- hydrocarbon reforming
- biomass processing

Pyrolysis is defined by a reaction in an inert environment at high-temperature. It was already used in ancient time to convert wood into charcoal under an anaerobic environment. There are versatile designs of reactor types and difference in quality requirements of the feed which can range from biomass to methane to crude oil. In pyrolysis, the feed is heated up to its decomposition temperature which then breaks chemical bonds. In contrast to the reformation, this process does not need catalysts. However for hydrogen production, hydrocarbon pyrolysis is mostly used for smaller applications such as in laboratories. For industrial sized production of hydrogen SMR are still the first choice [68]. Pyrolysis is mainly used for the petrochemical production of ethylene (C_2H_4) a precursor of polythene but also for creating aroma [69] which then lends the process the name "cracking". The physical design of the coil where the cracking of the feed (mostly naphtha) occurs is complicated, as for example a non-optimal dimension of the coils could lead to coking in the coils that needs to be burned out for further operation [70].

SMR is the most common representatives among the hydrogen hydrocarbon reforming technologies. The endothermic reaction ($\Delta\ G^0_{298} = +165$ kJ/mol) process takes place under high temperature and pressure (3.5 MPa) and is described by following equations:

$$CH_4 + H_2O \longrightarrow CO + 3\,H_2 \quad (\Delta H^0_{298} = +206\,\mathrm{kJ/mol}) \tag{2.2}$$

Eq. 2.2 is the basic reaction by using methane as feed. Hydrogen output is enhanced by a second process the water-gas-shift reaction (2.3):

$$CO + H_2O \longrightarrow CO_2 + H_2 \quad (\Delta H^0_{298} = -41\,\mathrm{kJ/mol}) \tag{2.3}$$

The net reaction of the SMR process is the sum of equation 2.2 and 2.3:

$$CH_4 + 2\,H_2O \longrightarrow CO_2 + 4\,H_2 \quad (\Delta H^0_{298} = +165\,\mathrm{kJ/mol}) \tag{2.4}$$

As a fuel, natural gas is used for heating as well as a feed for the process. Energy losses occur mainly from the surplus steam production [71]. The efficiency η of a SMR can be defined by eq. 2.5 where the power-flux p is described by the mass flow $\dot{m}$ times the LHV of the feed versus the product.

$$\eta_{SMR} = \frac{p_{H_2}}{p_{fuel}} = \frac{\dot{m}_{H_2} \cdot LHV_{H_2}}{\dot{m}_{CH_4} \cdot LHV_{CH_4}} \tag{2.5}$$

As conventional hydrogen production is linked to fossil fuels, a certain amount of green-house gases are emitted by this process. In total between 8.8 kg and 9.8 kg CO_2 are emitted per 1 kg H_2 depending on the efficiency (eq. 2.2 - 2.4). Facing the

threat of global warming, the goal is set to reduce CO_2 emissions which can be done by alternative and more efficient technologies such as electrolyzers or by using biomass.

Biomass can be mentioned as an environment friendly source to produce hydrogen in a sustainable way. Processes used are either thermochemical or biochemical. Latter is done under the an isolated environment with microorganisms with the added advantage that most of the processes needed for hydrogen production can operate using sunlight (photofermentation, biophototlytical spliting). However efficiency and throughput of these processes are not competitive and are only used on a laboratory scale. The thermochemical process is based mainly on wood, as straw or stems engender undesirable ash formation. Beside using wood from forest, scrap can be used with the risk that contamination of the material (stones, nails) can lead to damaging the pressurized tanks. Thus, unpressurized designs are common leading to a reduced efficiency [72]. Müller [73] presents a dual fluidized steam gasification system using wood chips as feedstock which is gasified and further distributed to a steam reformer at temperatures between 580 °C and 750 °C. After the hot gas stream passes several system components such as cooler, filter and CO-shift reactor the concentration of hydrogen in the gas stream increases continuously. System efficiency is stated to be 60% for hydrogen production from biomass including a 5% energy loss due to electrical demand for passing a gas permeation membrane in simulation. Coupling the system to a heat demand could make use of 17.5 MWh waste-heat coming from the process which further increases the overall efficiency. Beside gasification hydrogen can also be gathered from fast-pyrolyzing biomass which will lead to hydrogen as well as byproducts such as CO and CH_4 [74].

$$Biomass + Energy \longrightarrow H_2 + CO + CH_4 + \text{Byproducts} \tag{2.6}$$

Another possibility to produce clean hydrogen, so to say with electricity from renewable energy sources are the water splitting technologies. Three different types of electrolyzers are used commonly:

- alkaline
- solid oxide
- proton-exchange-membrane

2.3.2 Alkaline electrolyzer

Alkaline electrolyzers are the oldest and most mature type of electrolyzer [75]. They are already used in industry scale with up to 3 tonnes of hydrogen production per hour [76]. This type of electrolyzer has a diaphragm between anode and cathode in a liquid electrolyte of 20-40% potassium hydroxide (KOH) at a temperature of 70-90°C. Water is split at the cathode into hydrogen and OH^- when a voltage above decomposition potential is applied. The hydrogen gas bubbles created from this process, rise up from the bottom to the top of the cell on the cathode side (eq. 2.7). The diaphragm allows an exchange of OH^- ions from the cathode to the anode. On the anode side, ions form to water and oxygen which then gets collected similar to the hydrogen extraction. In

total, twice the amount of hydrogen is produced than oxygen (eq. 2.8). Nickel, cobalt and iron are used as catalysts in these processes.

$$\text{Cathode} : 2\,H_2O + 2\,e^- \longrightarrow H_2 + 2\,OH^- \tag{2.7}$$

$$\text{Anode} : 2\,OH^- \longrightarrow 0.5\,O_2 + H_2O + 2\,e^- \tag{2.8}$$

With an energy demand of 4.3 kWh per 1 m^3 H_2 (at 273 K, 0.1 MPa) the overall efficiency of such a system is 70% of the lower heating value of hydrogen. The electrolyzer can operate in part-load operation until 10-40% of its nominal load and can do a cold start in 60 seconds. These conditions are limited by danger of hydrogen diffusion from cathode to the oxygen side (anode) when the voltage is decreased which could result in a highly explosive mixture. Lifetime of alkaline electrolyzer can reach around 90.000 hours [77], however the replacement of degrading electrolyte is much simpler as compared to e.g. PEM electrolyzer. System prices are stated around 2000 € per kWh, with the goal of a reduction to 500 € per kWh in future by increasing power density and reducing material costs. These systems are used when industry grade hydrogen 5.0 (99.999%) is needed in a medium amount, which would be too small to justify a SMR [78].

2.3.3 Solid oxide electrolyzer cell

SOECs (solid oxide electrolyzer cell) is the least developed electrolysis technology and works with a high temperature between 700 and 1000 °C. The benefit of this system is that the free enthalpy (ΔG), also known as the Gibbs free energy, for this reaction is reduced with higher temperatures as the difference in reaction enthalpy is delivered by the heat [79]. Thus, the production of 1m^3 (3 kWh) of hydrogen only needs 2.6 kWh electricity at this temperature level. It has the advantage of a high electrical performance while having low material costs and the option of a reverse operation mode. Due to the high temperatures, stack lifetime is limited currently to around 10,000 hours. Research is working on operation at a lower temperature to prevent fast material degradation. Prices are still around 2000 €/kW with a cost reduction potential of 30% only by scaling up the process [78]. Due to the high operating temperature SOEC is not the first choice for a flexible operation schedule. Similar to the alkaline electrolyzer start-up time are in the range of minutes, with the minimum part-load hydrogen production of 30% compared to nominal capacity. In contrast to the alkaline electrolyzer where the alkaline solutions enables the OH^- exchange, here the oxygen ions are created (eq. 2.9 - eq. 2.10) and travels through the ceramic membrane.

$$\text{Anode} : O^{2-} \longrightarrow 0.5\,O_2 + 2\,e^- \tag{2.9}$$

$$\text{Cathode} : H_2O + 2\,e^- \longrightarrow H_2 + O^{2-} \tag{2.10}$$

2.3.4 Proton exchange membrane water electrolyzer

Proton exchange membrane water electrolyzer work at temperatures comparable to alkaline electrolyzer but instead of using a liquid electrolyte they use a thin solid polymer electrolyte membrane (PEM). This membrane is typically 60 to 200 micrometer thick

and made out of Nafion. It is embedded in between two electrodes with a thickness of 10 micrometer. Platinium is used as catalyst on the cathode and iridium on the anode. Using the PEMWE offers many advantages versus existing electrolyzer systems such as:

- high efficiency
- fast and dynamic load changes
- compressed hydrogen at high purity.

A summarized overview of the different hydrogen producing technologies is given in Table 2.3.

Table 2.3: Overview of the different typical types of hydrogen production

	SMR	**ALEL**	**SOEC**	**PEMWE**
system efficiency	66 - 73	70	high[1]	50 - 70
response time	n/a	sec - min	min	sec
load range (%)	n/a	20 - 150 [80]	30 - 100	0 - 200[2][80]
Investment costs (€/kW_{H2})	200 - 400 [81]	1000	2000	2000
operation temperature [78]	600 - 900 [82]	60 - 80	650 - 1000	50 - 80

[1] Voltage efficiency is given in literature with <110% [78], however beside electricity, energy is taken from heat and thus not comparable with the efficiencies of the other technologies.
[2] PEMWE can be operated for a short time above nominal load.

De-ionized water is used in these systems and it enters from the anode side of the cell. The assembly of membrane and electrode (MEA) is inserted in between two porous transport layers and the bipolar plates. The bipolar plates, usually titanium, are structured in a way that a constant water flow is enabled towards and the gas flows away from the MEA. Usually, carbon paper is used as porous transport layer on the cathode side and sintered titanium foam on the anode side with thickness of 280 micrometer each [34].

Applying a voltage of ≤ 1.23 V to the cell will start the water splitting by supplying the Gibbs free energy $\Delta\, G^0_{298} = 237$ kJ/mol. Considering the whole reaction enthalpy however a minimum voltage of 1.48 V is needed to provide the energy of $\Delta\, H^0_{298} = 286$ kJ/mol is needed according to:

$$\text{Anode} : \mathrm{H_2O} \longrightarrow \frac{1}{2}\,\mathrm{O_2} + 2\,\mathrm{e^-} + 2\,\mathrm{H^+} \tag{2.11}$$

$$\text{Cathode} : 2\,\mathrm{H^+} + 2\,\mathrm{e^-} \longrightarrow \mathrm{H_2} \tag{2.12}$$

$$\text{Sum} : \mathrm{H_2O} \longrightarrow \frac{1}{2}\,\mathrm{O_2} + \mathrm{H_2} \quad (\Delta \mathrm{H^0_{298}} = +286\,\mathrm{kJ/mol}) \tag{2.13}$$

Typical cell efficiencies lie between 62 % and 82 % based on the LHV of Hydrogen which is 242 kJ/mol. This corresponds to applied cell voltages between 1.5 V and 2 V [67] calculated from the cell voltage $\mathrm{E_{cell}}$ with following equation:

$$\eta_{\mathrm{cell,LHV}} = \frac{1.23\mathrm{V}}{\mathrm{E_{cell}}} \tag{2.14}$$

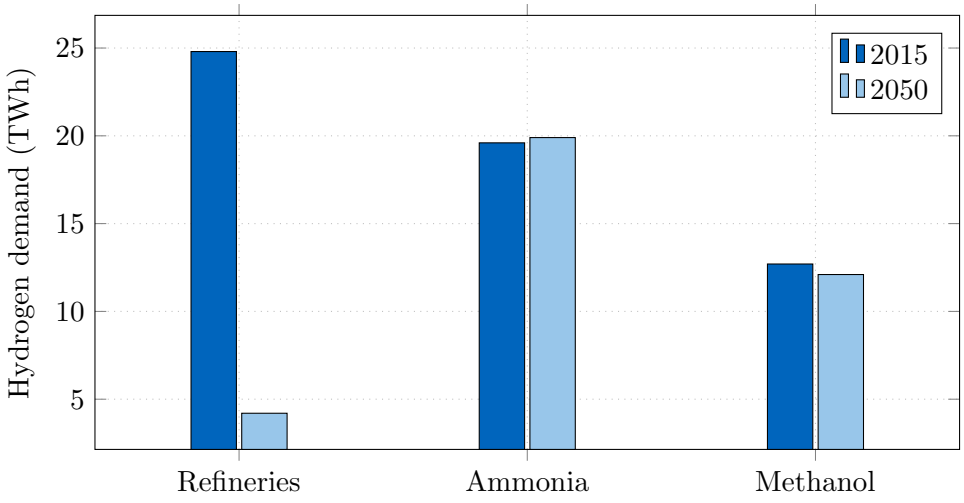

Figure 2.1: Hydrogen demand in Germany for the year 2015 and prognosticated for 2050

Due to several auxiliary and safety systems such as electronics, pumps and infrastructure as well as faradaic losses, system efficiency is lower than the cell itself and usually lies between 50 % and 70 % of the LHV. This corresponds to an hydrogen production rate between 170 and 230 m^3/h per installed MW of PEMWE. Hydrogen is delivered from the PEMWE at 30 bar pressure with at industry grade 5.0 (99.999%). As water is the only fuel beside electricity to provide energy, no direct emissions are created by this process.

2.4 Applications of hydrogen

Hydrogen is used nowadays mainly in refineries for the production of syn-fuel, oils, or lubricants. In the chemical sector, hydrogen is mainly used for the ammonia production, followed by the methanol synthesis. 80% of the ammonia production in Germany is used for the fertilizer industry. In the year 2015, a hydrogen demand of 57.1 TWh is stated in Germany. It is assumed, that hydrogen demand will stay constant for the production of ammonia and methanol production. Due to an assumed lower demand in mineral oils, a strong decrease of 83% is claimed for the hydrogen demand in refineries until the year 2050 [83]. These assumptions are plotted in Figure 2.1.

Besides using hydrogen in agriculture or in the petrol industry, further sectors can be addressed for future applications:

- Steel industry (reduction agent)
- Energy sector especially as a long-term energy storage
- As fuel in the transportation sector

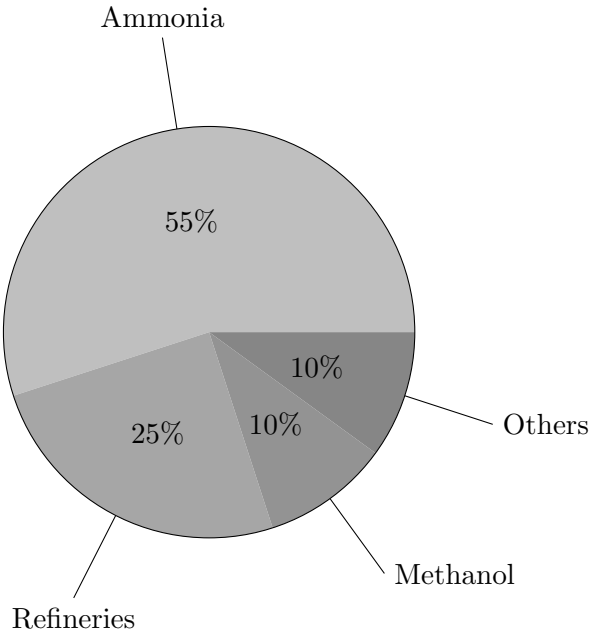

Figure 2.2: Share of worldwide hydrogen demand

2.4.1 Hydrogen in agriculture

Industrial produced fertilizers are essential to secure survival of world's population. In 1996 almost half of world's nourishment based on the use of fertilizers which led to a demand of 25 million tonnes (Mt) of nitrogen [84] (or 30 Mt NH_3).
Nitrogen, phosphorus and potassium are the three most important plant nutrients. Nitrogen is an essential constituent of amino acids found in vegetable, animal and human proteins. Especially high-energy crops such as peas, beans and soy are cultivated as an protein source for humans and animals but require a lot of nitrogen. Apart from amino acids, nitrogen is an important component of chlorophyll needed for photosynthesis of plants.

Due to the strong binding forces of the N_2 molecule, nitrogen, which is found in the atmosphere at a concentration of 78%-vol., can not be used directly by plants. There are two processes of how inert nitrogen is transferred from the atmosphere to biosphere.

- Spontaneous lightning strikes or photochemical reactions (about 10% of the nitrogen for plants).
- Microorganisms or bacteria in a symbiosis with roots of the plants.[85]

The price that had to be paid feeding a constant growing population results in environmental impact, such as the acidification of groundwater from over-fertilization. Today, 2-3% of global energy demand is accounted for fertilizer production [86]. About 97% of the nitrogen fertilizers are made from ammonia [87]. In contrast to the German hydrogen demand, the ammonia synthesis causes the highest hydrogen demand worldwide. Ammonia industry accounts for 55% of industrial hydrogen processes [88] as shown in Figure 2.2.

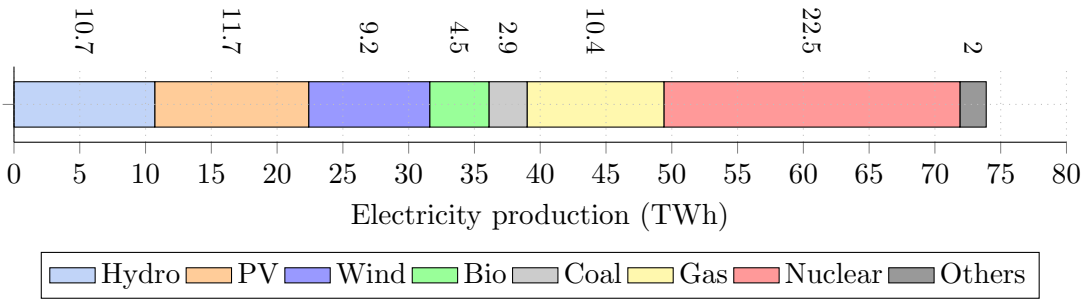

Figure 2.3: Gross electricity production of Bavaria in the year 2018. In total 73.9 TWh have been produced by renewable and conventional power plants

Currently, the Haber-Bosch process is used for the industrial production of ammonia. At temperatures between 350 and 500 °C, nitrogen and hydrogen reaction takes place:

$$N_2 + 3\,H_2 \longrightarrow 2\,NH_3 \tag{2.15}$$

In the industrial world, nitrogen can be extracted from air via air-separation units (ASU). In rectification columns, electric current is used to strongly cool the air and separate it into the components based on their different boiling temperatures. Most of the hydrogen needed comes from steam reforming, where natural gas and water are converted under high temperature and pressure into carbon dioxide and hydrogen. The production costs of 1 kg H_2 is stated in the range of 1 € to 3 € for central plants but is heavily dependent on the gas price [89]. To avoid direct CO_2 emissions, hydrogen extracted from water electrolysis can be used, which is powered by renewable electricity. When using wind power for hydrogen production, the costs according to recent studies are at 5 € to 11 €/kg H_2 [90]. In 2013, about 3 Mt of ammonia was produced in Germany [91], of which 83% was processed further in the fertilizer industry [92]. From the stoichiometry of eq. 2.15 it follows that about 500 kt H_2 are needed to fulfill this demand. Using hydrogen from renewable energy sources with electrolyzer will prevent the usage of SMR (∼8.8 kg CO_2/kg H_2) and thus result in a CO_2 avoidance potential of direct CO_2 emissions of 4.4 Mt_{CO_2} (eq. 2.16). To put this in context, in Germany alone 66 $Mt_{CO_2\text{-eq.}}$ are emitted yearly in the agricultural sector.

$$0.5 Mt_{H_2} \cdot \frac{8.8 t_{CO_2}}{1\ t_{H_2}} = 4.4 Mt_{CO_2} \tag{2.16}$$

The amount of electricity needed to produce the hydrogen via PEMWE sums up to 30 TWh which roughly corresponds to the electricity produced by renewable sources in Bavaria during one year [93]. The production of electricity for the year of 2018 is depicted in Figure 2.3.

The additional costs for food due to switching from conventionally produced hydrogen to renewables would be negligible. Assuming 1 kg of bread requires 850 g of flour and the yield of a wheat field is 800 g/m², it will results in a acreage occupation of 1 m² [94]. Around 170 kg Nitrogen per hectare per year is recommended for fertilizing winter-wheat [95, 96] which results to 17 g nitrogen per m². From eq. 2.15 follows that about 4 g hydrogen are needed for the production of 17 g Nitrogen.

2.4.2 Hydrogen in steel industry

In the year 2007 about 67 Mt of CO_2 were emitted in the steel sector in Germany. Crude steel and pig iron production account for two-thirds of these emissions. The latter is manufactured in a blast furnace with high temperatures up to 2000 °C. Traditional coke (pyrolyzed coal) is used for the exothermic reaction with injected air leading to heat and CO_2. Beside using coke as a fuel it is also needed as a reducing agent. Coke and carbon-monoxide react in a weak exothermic reaction to form pig iron eq. 2.17.

$$2\,Fe_2O_3 + 3\,C \longrightarrow 4\,Fe + 3\,CO_2 \quad (\Delta H^0_{298} = -22\,kJ/mol) \tag{2.17}$$

After the reduction process iron still contains 10% of other components such as phosphorous, sulphur, silicon and still 4% of carbon is present which leads to undesirable material property like brittleness and reduced hardness. Further process steps lead to different types of steel which fulfill individual use cases. Since 2007 steel production in Germany reduced by 13% from 48.5 to 42.1 Mt_{Steel} [97] and carbon dioxide emissions by 16% to 56 Mt_{CO_2} but still accounts for 6% of Germany's greenhouse gas emissions (GHG) [98] (95% of GHG are CO_2 [99]). Thus, 1.3 kg CO_2 are emitted per 1 kg of steel, which is twice the value resulting from the reaction (eq. 2.17). The substitution in the reduction process, with hydrogen from renewable sources, will therefore lead to a potential of 28 Mt of saved emissions (assumed 0.6 kg CO_2 per 1 kg Fe from eq. 2.17). As it holds true for most chemical processes a constant procedure is vital for efficiency and product quality. Disturbances or even interruption in the supply with reduction agents or energy will lead to product loss or time-intensive repairs in the facility (e.g. glass production).

2.4.3 Hydrogen as one element in security of energy supply

With the phase out of coal and nuclear power-plants, Germany risks giving up her independence in its energy supply. The new direct gas pipeline from Russia (Nordstream II) enables a natural gas supply without passing through other countries before it reaches Germany. For the transition phase from coal to natural gas this project is a feasible solution. Today underground gas storage with a capacity of 85 TWh [100] exists in Germany which are available to ensure energy supply.

With the decision of a fossilized energy supply and the plan of an expansion of renewable energy technology capacities, the question of energy storage arises. For daily shifts battery storages are a possible solution. Li-Ion batteries with prices between 200 € to 400 € per kW and kWh [101] and about 20.000 cycles in lifetime are expensive but feasible for small scale applications. Due to the fast response time of battery storage they can contribute to grid stability as the future energy system lacks inertia from rotating masses of conventional power-plants. This can lead to imbalances in grid frequency which is not compensated sufficiently anymore [102]. Existing battery storage range from capacities of some hundred kWh (EEBatt) [103] for frequency stability [104] and up to 50 MWh (Jardelund) [105] for a long-term storage.
The plan of increasing installation of renewable energy capacities is a right step to an independent. However, the electricity output is depending on the fluctuation of wind and the day-night shift of solar irradiation. This is different to the existing demand orientated energy supply where industry produces in base-load and electricity tariff-

structure are usually too flat for being incentive enough to change citizen's behavior. Smart-meter, smart-buildings and further smart implementations can help to overcome some of these problems in small scale time shifts.
Hydrogen as energy carrier for storing and later reconversion into electricity is a possibility especially for long-term energy storing. The cost intensive components are the electrolyzer for splitting water with energy into hydrogen and oxygen as described in detail in Chapter 2.3.4. This hydrogen can be burned similar to natural gas to meet heat demand. Existing gas-pipelines offer the possibility of holding up to roughly 10% concentration of hydrogen and further keep the function of distributing the energy. In case of covering electricity demand, a fuel-cell is needed to reverse the water-splitting process. As energy surplus from renewables will occur randomly, a flexible system is needed which sets PEMWE and PEMFC from the technical parameters as a first choice. With prices around 2000 €/kW they lie in and order of 10 compared to Li-Ion batteries. System costs are strongly defined by charging and discharging power. In contrast to Li-Ion batteries, energy content is relatively cheap, as this is defined by the hydrogen storage. Large amounts of energy can be stored in form of hydrogen in caverns which are available in the north of Germany [106] with a price around 200 €/MWh [107]. A recent study calculated the technical potential of Europe's hydrogen storage capacity in salt caverns to 84.8 PWh_{H_2}. Regarding this study, Germany has the highest potential with 9.4 PWh_{H_2} which corresponds to 70 defined standard caverns (500,000 m^3) each with a storage capacity of 133 GWh_{H_2} (onshore) [107]. Thus, Germany has an excellent access to long-term energy storage in form of hydrogen. Compared to this, existing pump storage in Germany reaches a capacity of about 40 GWh_{el} with a power of 7 GW [108].

2.4.4 Hydrogen in the transportation sector

Worldwide energy demand in transportation sector is stated with 33 PWh and predicted to exceed 44 PWh until 2040 [109]. In Germany as well as in the USA 30% of the total energy demand accounts for the transportation sector. The most popular alternative versus internal combustion engines (ICEs) are battery electric vehicle (BEV) as they are currently discussed in all public media [110], [111], [112]. BEV have the advantage of a very high overall efficiency including low losses in charging, discharging (including self-discharge rate) and excellent kwh per km ratio. Energy for propulsion is stored in batteries which are significantly determine the purchasing cost of BEVs [113]. The C-rate of batteries is limiting the charging progress of these vehicles and can make refueling a time-consuming process. Tesla is leading with the highest recharging rate of 120 kW from their supercharger stations [114], [115]. Charging 1/3 of the total range of Tesla's Model S (610 km) is taking only 15 min. Tesla already announced an update for some vehicles to further increase charging rate to 250 kW [116].
Besides, another promising alternative to use are vehicles with fuel cells which burn hydrogen to create electricity including the benefit of fast vehicle charging. Daimler currently announced their first electric vehicle combining fuel-cell and plug-in-hybrid-technology in the GLC F-CELL series. With a tank size of 4.4 kg hydrogen compressed at 700bar, 430 km distance can be driven from hydrogen without refueling. The 2100 kg heavy Mercedes demands 1 kg H_2 per 100 km in hydrogen mode and 0.27 kWh in battery mode which extends the total range by additional 50 km [117]. The hydrogen tanks weight roughly 100 kg and have a volume of 150 dm^3 at 700bar [118]. In com-

parison only the battery pack of the Tesla Model S edition with a size of 85 kWh, already weights about 540 kg. This corresponds to 25% of the total mass of the Model S with a range of roughly 420 km [119]. However for BEVs no additional weight will be added for a fuel cell which is the case for FCVs. In addition, Daimler announces, that the refueling process of the GLC F-CELL is finished within 3 minutes [120]. in the following chapters, the two technologies FCVs and BEVs are implemented in an energy system model (Chapter 3). In addition, especially for the FCVs their impacts during life-time is analyzed in Chapter 4. In the following, a few applications are mentioned which illustrate the importance of hydrogen in the transport system. One example of a possible hydrogen application for heavy duty vehicles was discussed during my research stay at the University of Texas in Austin at the Energy Department. Thus, Texas is mentioned in the following as an use case abroad. Then the focus is set to Germany. Applications in the field of passenger and freight transport as well as aviation are listed and compared based on the hydrogen demand.

Texas with its heavy petrol industry is currently increasing its share of renewable energy especially for wind, making hydrogen a promising alternative energy carrier. Especially the Texas triangle with the vertices in Houston, San Antonio and Dallas has a potential hydrogen demand for light duty vehicles of 3.9 billion kg per year. Including the other parts of Texas increases hydrogen demand up to 5.3 billion tonnes [121]. The study conducted by Nagasawa et al. uses sensitivity analysis of different marginal prices for hydrogen, to estimate the amount of environmental friendly hydrogen production. It revealed that having a marginal price of $ 4 per kg hydrogen will result into 0.84 billion kg of economical feasible hydrogen production which could cover 22% of the future hydrogen demand of the Texas triangle. During early morning hours cheap wind energy could be used to already cover 10% of the demand at a marginal costs of $ 1 with electrolyzer which are assumed to have 75% system-efficiency. Compressed hydrogen as fuel for light duty vehicles as well as for trucks below 10 t mass and close operation distance ranges is a feasible solution. For longer transportation distances, trucks with up to 40 t in mass and operating ranges up to 1000 km, compressed hydrogen would not be applicable but liquefied hydrogen could be feasible as energy density can be increased further. However, the cost difference and energy losses between compressed and liquefied hydrogen are significantly different [122].

Hesse, a state in Germany, just announced a plan to own the largest fuel-cell fleet in the world. 27 trains will be powered by fuels cells in the Rhein-Main area powered by hydrogen from the industry park in Höchst which is located in Taunus. As in many applications a hybridization of a battery next to the fuel-cell combines the benefits from recharging by recuperating of brake energy and power for acceleration. As in this case-study the hydrogen is a byproduct of the chemical plant it can be re-used now but still not be claimed as CO_2 free [123].

By 2050 worldwide, urban population will increase by 25% [124] which will lead to an increased demand for public transportation. Buses are one possibility for inner-city connection which are operated by diesel today. Beside biofuel, hydrogen will be an opportunity for less air pollution in cities. Compared to electrifying buses with overhead connection line, hydrogen based solutions require no new expensive infras-

tructure. The benefit of using FC buses instead of battery electric buses is revealed especially in winter. The passenger space is defined by big window areas and results in high heat losses due to the opening doors at every stop. During cold winter the energy consumption of a bus can easily double up to 2 kWh per km driving due to these additional heating requirements. Fuel-cells are beneficial in this environment as their waste heat (60-80 °C) is a suitable heat source for adapting passenger's ambient temperature [125]. Battery driven buses have problems due to the cold environment to provide the nominal capacity and power. As 400 km range is needed to cover the whole transportation spectrum of buses in cities a drop down to 150 km will already reduce the field of application by 70% [126].

With the high amount of energy needed for the propulsion of e.g. ferries, liquefied hydrogen and therefore cryogenic storage are needed in **marine** applications. With around 2 t of hydrogen used per day per vessel, cheap fuel costs are dominating the upfront capital investment decisions. In addition, vessels do have long lifetimes which further reduces the importance of capital costs. Aggravated by the fact that most vessels are manufactured to individual applications, a roll out of new propulsion systems might be hampered [122].

In the field of **aviation**, carbon-based fuel use is currently seen as the only alternative [33]. PtX technologies such as co-electrolysis can meet precisely these requirements and produce a synthetic fuel. In 2016, the energy requirement in Germany for aviation was about 390 PJ, which corresponds to about 9 million tonnes of kerosene. Another possibility, however, is the direct use of hydrogen as an energy carrier. Due to the high power density required for take-off operations, the use of fuel-cells is ruled out. However, hydrogen can also be burned directly in turbine engines with with some adjustments. Due to the low volumetric energy densities, it is liquefied at about -253 °C (LH_2). Although the gravimetric energy density is 2.8 times higher than that of kerosene, it still requires about 4 times the volume to provide an equivalent amount of fuel. A further hurdle is that fuel is usually stored in airplane wings, which will not be possible with cold liquefied hydrogen, due to the weight of the storage as well as an increasing chance that icing of the wings can occur due to (LH_2). One possibility is to store hydrogen in the fuselage, but this reduces capacity of passengers in a typical A380 from 555 to 211 [127]. To burn LH_2, it is first converted to a gaseous state, which can be achieved at a sufficient rate via a heat exchanger despite the low temperatures due to the lower air density and lower boiling temperature at heights. Already in 1975, NASA published a study together with Lockheed concerning the "Application of hydrogen fuel to long-range subsonic transport aircraft" [128]. A more recent research in this field is the Cryoplane project, which similarly focuses on the same requirements such as heating up hydrogen before combustion and decreasing weight of cryogenic storage. For the design of a passenger aircraft, the approach is to implement the fuel-tanks above the passenger's cabin into the roof structure, whereby less interior space is lost but the aircraft will significantly increase its heights. A comparison between hydrogen and kerosene is made in Figure 2.4 and shows that H_2 combustion is a cleaner process, as fewer amounts of greenhouse gases such as nitrogen and no carbon dioxide are emitted but therefore about 2.5 times more water vapor [129]. Depending on the altitude, greenhouse gases have a different global warming potential (GWP), which is for CO_2 very constant over a 100 years period, whereas the GWP of contrails at travel

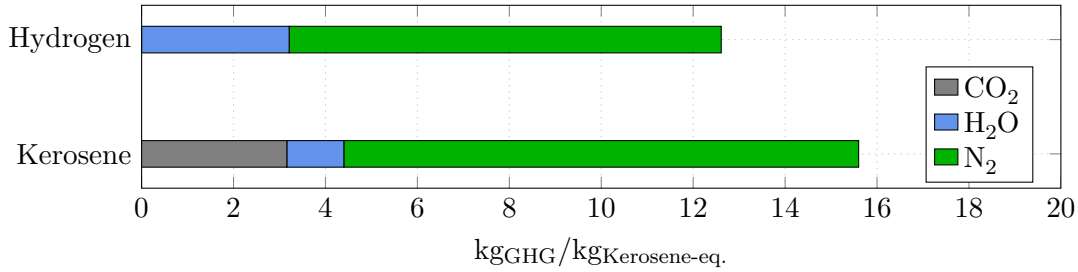

Figure 2.4: Exhaust components of 1 kg kerosene-eq. (0.36 kg H_2) with a gravimetric air to kerosene ratio of 316:1

altitudes between 10 and 12 km (33-38 thousand feet) is about twice as high [130], [131]. Since water or ice crystals are a component of contrails, an increased emission of water vapor at these altitudes can have negative consequences with regard to global warming [132, 133].

3 Modeling energy systems

As presented in the previous chapter, there are numerous use cases for PtX technologies. As this abbreviation already contains the word "power", the availability as well as the power source is a decisive factor to determine PtX potentials. electricity should be procured on the basis of renewable power generation in order to exploit its full potential in terms of climate protection. It is therefore an object of investigation to describe the electricity system in which future PtX technology will be placed. Thus, identifying the potential of the PtX technologies using energy system models is a suitable approach. The character of an energy system model is guided by its assumptions and is characterized by individual results. In order to model future energy systems, premises are used to build a pathway into a possible future which are characterized by various scenarios which are used for describing a certain point in time.

Energy system modeling began in the early 1970s for analyzing energy systems and especially for energy supply to better understand power subsystems. Mostly, these models address a specific problem and require beside skill and good data also computing power to solve the problems with mathematical algorithms. Energy balance in respect of accounting all energy flows is a common and useful way for representing energy systems. For a detailed depiction the reference energy system was introduced by Hoffman and Wood in 1976 [134] which adds the aspect of network description to the energy balance framework. Two different approaches of modeling are developed and used today: the top down approach which is mainly used from the macroeconomic view is based on the influence of price and market design and the bottom up approach which represents the technical characteristic of the energy sector [135]. Between these two extremes lie multiple hybrid solutions that are more inclined towards one of the mentioned approaches.

3.1 Literature review on energy system models

As several studies of applied energy system models are available [136] having different goal and scope. Some are focusing explicitly on the energy sector [137] and some trying to draw a full picture by including other relevant sectors [41].

Pfenninger describes an energy system "as the process chain (or a subset of it) from the extraction of primary energy to the use of final energy to supply services and goods" [138]. He divides the models into four different categories that are relevant for energy policy:

1. Optimization of energy systems: These models use methods of optimization to answer the question of the development of future scenarios.
2. Simulation of energy systems: In contrast to optimization methods, simulation uses the behaviour of a system to make predictions.

3. Power systems and electricity market models: These models focus exclusively on the electricity sector to develop scenarios and make predictions.

4. Mixed methods of scenario development: Based on qualitative or diverse methods, rather than strictly mathematical models.

Pfenninger further distinguishes the first two groups according to defined pairs of purpose: simulation/forecast, and optimization/scenarios". In this thesis, the method of the first category is used to answer the question about the provision of energy for the production of hydrogen via PEMWE. However, the boundaries between the first and second category are blurred, as for example the availability of wind and solar energy is simulated with the claim of perfect foresight.

The backbone of energy system models have been the optimization method mainly designed with a bottom-up approach. This has the advantage of a detailed description of physical parameters to describe technical components. However, these models must be simplified so that their results can be traced and interpreted. In the following a few representatives of existing energy system models and use cases are mentioned which are mainly from the categories one and two as presented [138].
Most of current studies claim to give an insight into the future and therefore involve predictions on the costs of fuels and batteries or limitations in renewable energy capacities and storage. Changing these parameters, also causes the results and conclusions of different models to change as the object function is usually minimizing costs. Beside these predictions, models simplify and abstract the reality. Some models allow the individual parameter settings and offer the user a higher degree of freedom while some are very limited. HOMER [139] is a model previously used for industrial purposes which comes with a comfortable GUI but lacks of limited insight into the model. It is a commercial tool which is due to the implemented functions being very limited in means of changing input parameters or giving more detailed insight into specific model functions. Another tool is TIMES [140] which might be one of the most known optimizations programs which enables the modeler to use it for a variety of applications. Beside the commercial solutions, over time a variety of different free open-source programs were developed such as urbs [141] or OSeMOSYS [142]. Most of energy system models are based on a cost-minimizing optimization problem but differ in regional or spatial resolution and scale. Also, some technical features are implemented differently such as using a total CO_2 budget over several years or a yearly constraint. Regional resolution lead to additional complexity as the question of granularity and energy transmission need to be answered. Pfenninger for example uses Calliope [143] for giving an answer to the share of different energy sources having in scope Great Britain [144]. Industry related models are also found as Edelenbosch [145] addresses this sector in a long-term run, setting his scope on energy demand and green house gas emissions until 2100. Rinkjob [146] reviewed a variety of existing models describing future energy systems with high shares of renewables and distinguished them in their methodology like linear programming (DIETER, urbs, EMMA), mixed integer programming (AURORAxmp, BALMOREL) or agent based modeling (GridLAB-D, EMLab-Generation) to mention few. Beside the mathematical methods employed, some of these models also differ in their implemented features. Some of these features are future possibilities while not common today, such as demand-side-management (DSM), but could be adapted to the

society (e.g. by using smart-meters).

All the reviewed models mentioned, have in common, that primary energy is converted into final energy by means of technologies. Thereby, the the solution space of the models is limited by certain constraints such as capacities. What is not taken into account is the energy which had to be expended for manufacturing of these energy-converting technologies. In fossil power plants this energy input and the associated CO_2 emissions are negligible compared to the output of electricity and CO_2. Therefore, for example, the emissions of a coal-fired power plant per kWh of electricity are determined by stoichiometric combustion and the efficiency of this technology. Wind power plants, on the other hand, do not emit any CO_2 according to this approach. This is a new problem in energy system modeling in general, which was noticed during the P2X project and which has to be considered especially for the ambitious climate protection goals. For this reason the missing sector, the manufacturing of electricity producing technologies, is taken into account for energy system modeling in the following. However, first of all an energy system model is conventionally developed and extended by the manufacturing sector for renewable energy technologies in the later chapters. The different stages of the conventional modeled energy system are shown below:

- Presentation of the model generator used
- Development of a scenario with focus on heat demand in municipals
- Development of a scenario with focus on hydrogen demand in Germany
- Modeling of an energy system with 16 nodes for Germany
- Reduction of the 16 node problem to a 1 node model

In later chapters, the results of the 1-node model is used to discuss the general methodological problem of energy system modeling under very limited CO_2 emissions.

3.2 Model-generator *urbs*

The linear programming tool urbs with a perfect foresight is exclusively used in this thesis for conducting the energy system modeling. urbs is programmed in the Python language and was published in the Ph.D. thesis of Dorfner in 2015 [147]. The basic method was presented first time by Richter who used a reference energy systems for representing the electricity and heat supply in Augsburg during his dissertation [148], as he named this method Urban Research Toolbox: Energy Systems (URBS). Dorfner used the opportunity to further develop this method and maintaining a new published version. It is a linear optimization model generator that calculates the minimum cost of expansion and dispatch of power-plants within a defined energy system, limited by the operating conditions and constraints such as CO_2 emissions or maximum capacity potential. The model allows the mapping of several sectors with their respective interactions such as energy transmission and coupling of different energy sectors. The complexity of each processes are simplified regarding the technical parameters, allowing the calculation of large systems. The code is published open source

on GitHub and extended the functionality of urbs is constantly developed. The interface is easy accessible via Excel sheets for feeding the model with input data. An extensively description is available (https://urbs.readthedocs.io/en/latest). Through ongoing maintenance, urbs receives updates and new features in periodical intervals. As easy it is to use the interface, as skillful modeling practice is required to describe a given problem efficiently by keeping problem size low. As the problems easily exceed memory (RAM) of personal computers specialized high-performance computers are used for complex problems when simplifications are not possible. The standard form of a linear optimization problems as used in urbs can be written as a minimization problem such as:

$$\begin{aligned} \min_x & c^T x \\ \text{s.t.} & Ax = b, \\ & Bx \leq d, \\ & x \geq 0, \end{aligned} \tag{3.1}$$

where c is the vector of cost coefficients and x the vector of variables. A and B are the coefficient matries for the vector x belonging to the equality and the inequality constraints respectively. The vector of variables is given with:

$$x^T = (\zeta, \rho_{ct}, \kappa_p, \hat{\kappa}_p, \tau_{pt}, \epsilon^{in}_{cpt}, \epsilon^{out}_{cpt}) \tag{3.2}$$

Where ρ are the amount of stock commodities (c) used by different existing or new process (p) capacities (κ, $\hat{\kappa}$). τ describes the process throughput and ϵ the total inputs and outputs of the commodities.
urbs uses a set of equations for its method, which are given in the following. The parameters and variables used are listed in Table 3.1.

As the objective is to minimize total system costs, the total annualized system costs can be written as:

$$\zeta = \zeta_{inv} + \zeta_{fix} + \zeta_{var} + \zeta_{fuel} + \zeta_{env} \tag{3.3}$$

These costs are separated between ones which are related to the capacities of processes (p) such as annualized investment, annual fixed costs and ones related to energy flows such as fuel and variable costs. Environmental weighting such as CO_2 taxes are not used. This also holds true for purchase processes which allow a power exchange with other regions. Variable costs are extended to a year while investment costs are once paid and are depreciated over a period of time (n). To do so urbs uses the annuity method by calculating an annuity factor (eq. 3.4). This factor is multiplied with the newly build capacity ($\hat{\kappa}$) and specific investment (J) of the corresponding extended process (p) by taking into account a weighted average cost of capital (i), which was set

Table 3.1: List of variables and parameters used in urbs [147]

Name	**description**
ζ	systems costs
ρ	stock commodities
K	existing capacity
$\hat{\kappa}$	new installed capacities
κ	total capacities
π	Transmission capacities
ϵ	commodity flow
k	cost factor
p	process
s	storage
$\underline{K}$	minimum allowed capacity
$\overline{K}$	maximum allowed capacity
CB	commodity balance function
t	modeling time step
a	arc (start/end of a transmission device)
$\bar{l}$	maximum stock per time step
$\overline{L}$	total available stock
e	efficiency factor
w	weighting (if less than a year is modeled)
v	region
$\overline{M}$	global limit of CO_2 emissions
r	input/output ratio of a process
d	commodity demand
τ	process throughput
z	time series
I	state of charge

to 5%:

$$\zeta_{inv} = \underbrace{\frac{i \cdot (1+i)^n}{(1+i)^n - 1}}_{\text{annuity factor}} \cdot \left(\sum_{p \in P} k_p^{inv} \hat{\kappa}_p + \sum_{f \in F} \sum_{a \in A} k_{af}^{inv} \hat{\kappa}_{af} + \sum_{s \in S} (k_s^{c,inv} \hat{\kappa}^c{}_s + k_s^{p,inv} \hat{\kappa}_s^p) \right). \tag{3.4}$$

Annual fixed costs describe specific costs (k_p) for maintenance and staff per installed capacity and is given by:

$$\zeta_{fix} = \sum_{p \in P} k_p^{fix} \kappa_p . \sum_{p \in P} k_p^{fix} \kappa_p + \sum_{f \in F} \sum_{a \in A} k_{af}^{fix} \kappa_{af} + \sum_{s \in S} (k_s^{c,fix} \kappa_s^c + k_s^{p,fix} \kappa_s^p) \tag{3.5}$$

Variable costs are added when processes and scale with the utilization and thus related to energy throughput. The variable costs are describe by k_{pt}^{var} per time step and etrapolated over a whole modeling horizon of one year with the weighting factors w and Δt:

$$\zeta_{var} = w \cdot \Delta t \sum_{t \in T} \left(\sum_{p \in P} k_p^{var} \tau_{pt} \sum_{a \in A} \sum_{f \in F} k_p^{var} \tau_{aft}^{in} + \sum_{s \in S} \left(k_s^{c,var} \epsilon_{st}^{con} + k_s^{p,var} (\epsilon_{st}^{in} + \epsilon_{st}^{out}) \right) \right). \tag{3.6}$$

Fuel costs represent the fuel needed for a specific process to convert energy, adding up over time. The costs are depended on the specific costs per fuel (k^{fuel}) and usage of the total fuel available on the stock market (C):

$$\zeta_{fuel} = w \cdot \Delta t \sum_{t \in T} \sum_{c \in C} k_c^{fuel} \cdot \rho_{pt}. \tag{3.7}$$

Independent of the model time, expansion constraints are defined for the individual processes. The installed capacity is described by the existing K_p and new capacity $\widehat{\kappa}_p$:

$$\begin{aligned} &\forall p \in P : \\ &\kappa_p = K_p + \widehat{\kappa}_p, \end{aligned} \tag{3.8}$$

and restricted to the minimum ($\underline{K}_p$) maximum ($\overline{K}_p$) allowed capacity, given as parameter:

$$\begin{aligned} &\forall p \in P : \\ &\underline{K}_p \leq \kappa_p \leq \overline{K}_p. \end{aligned} \tag{3.9}$$

The central rule for the urbs model is the vertex rule that express the commodity balance (CB) for every process at time ("Kirchhoffs current law") as shown for one

region:

$$\forall c \in C_{st},\ t \in T,\ f \in F:$$

$$\mathrm{CB}(c,t) = \sum_{c,p \in C_p^{\mathrm{out}}} \epsilon_{cpt}^{\mathrm{out}} - \sum_{c,p \in C_p^{\mathrm{in}}} \epsilon_{cpt}^{\mathrm{in}} + \sum_{s \in S_c} \epsilon_{st}^{\mathrm{out}} - \sum_{s \in S_c} \epsilon_{st}^{\mathrm{in}} + \sum_{a \in A} \sum_{f \in F} \pi_{at}^{\mathrm{out}} - \sum_{a \in A} \sum_{f \in F} \pi_{at}^{\mathrm{in}}. \tag{3.10}$$

The helper function describes, the difference between energy demand and supply from commodities. This contains losses due to process efficiencies and effects from energy storage (s) and transmission lines (π). Where f describes a transmission of energy between arcs (a). Thus, any consumption ($CB > 0$) must be covered by a source term ($\rho > 0$) and any commodity surplus ($CB < 0$) leads to an additional demand ($d > 0$) that must be supplied by:

$$d_{ct} + CB(c,t) - \rho_{ct} \geq 0 \tag{3.11}$$

The limitation of stock commodities is given by a maximum amount per time ($\bar{l}_c$) step as well as the total amount ($\overline{L}_c$) during modeling horizon given in 3.12:

$$\begin{aligned} &\forall c \in C_{\mathrm{st}}: \\ &w \sum_{t \in T} \rho_{ct} \leq \overline{L}_c \\ \\ &\forall c \in C_{\mathrm{st}},\ t \in T: \\ &\rho_c t \leq \bar{l}_c. \end{aligned} \tag{3.12}$$

Transmitted energy output is limited by the transmission line efficiency (e_{af})

$$\begin{aligned} &\forall a \in A,\ t \in T,\ f \in F: \\ &\pi_{aft}^{\mathrm{out}} = \pi_{aft}^{\mathrm{in}} \cdot e_{af}, \end{aligned} \tag{3.13}$$

where the maximum transmitted energy flow input is restricted by its capacity (κ_{af})

$$\begin{aligned} &\forall a \in A,\ t \in T,\ f \in F: \\ &\pi_{aft}^{\mathrm{in}} = \kappa_{af}. \end{aligned} \tag{3.14}$$

The range of minimum $\underline{K}$ and maximum expandable $\overline{K}$ transmission capacity is limited by given parameters

$$\begin{aligned} &\forall a \in A,\ t \in T,\ f \in F: \\ &\underline{K}_{af} \leq \kappa_{af} \geq \overline{K}_{af}. \end{aligned} \tag{3.15}$$

The actual installed capacity κ is calculated by the existing and newly installed capacity

$$\begin{aligned} &\forall a \in A,\ t \in T,\ f \in F: \\ &\kappa_{af} = K_{af} + \hat{K}_{af}. \end{aligned} \tag{3.16}$$

The maximum amount of emitted carbon dioxide ($\overline{M}_{\mathrm{CO}_2}$) is set as a parameter and restricted by

$$w \sum_{t \in T} \sum_{v \in V} CB(v, \mathrm{CO}_2, t) \leq \overline{M}_{\mathrm{CO}_2}, \tag{3.17}$$

where v represents one site out of all regions (V) for which the total CO_2 emissions are limited. In order to enable multiplie input multiple output (MIMO) functionality, where more than one products are taken as an input and/or produced by a process, eq. 3.18 is introduced. The throughput (τ) is defined by the process flow ϵ, for the input and output, multiplied by an constant factor (r).

$$\begin{aligned} &\forall p \in P,\ c \in C,\ t \in T: \\ &\epsilon^{\mathrm{in}}_{pct} = r^{\mathrm{in}}_{pc} \tau_{pt} \\ &\epsilon^{\mathrm{out}}_{pct} = r^{\mathrm{out}}_{pc} \tau_{pt}, \end{aligned} \tag{3.18}$$

With the throughput which is also used to calculate the variable costs (eq. 3.6), a process such as Combined Heat and Power (CHP) unit can be described which has the two commodities heat and power as output. The overall efficiency (η) of a process (p) to convert an input commodity (c_1) into an output (c_2) is given by:

$$\eta = \frac{r^{\mathrm{out}}_{pc_2}}{r^{\mathrm{in}}_{pc_1}} \tag{3.19}$$

and limited by the capacity of that process

$$\begin{aligned} &\forall p \in P: \\ &\tau_{pt} \leq \kappa_p. \end{aligned} \tag{3.20}$$

The storage capacity is defined by its storage capacity (κ^c) and storage power (κ^p) which are defined (in case of capacity) by the new installed capacity ($\hat{\kappa}^c$) and the already installed capacity (K^c).

$$\begin{aligned} &\forall s \in S: \\ &\kappa^c_s = K^c_s + \hat{\kappa}^c_s \\ &\kappa^p_s = K^p_s + \hat{\kappa}^p_s. \end{aligned} \tag{3.21}$$

The total installed capacity and power are in the range of the defined boarders, ‘$\overline{K^c}$ describe maximum content and $\underline{K^c}$ the minimum, as given in:

$$\begin{aligned} &\forall s \in S: \\ &\underline{K}^c_s \leq \kappa^c_s \leq \overline{K}^c_s \\ &\underline{K}^p_s \leq \kappa^p_s \leq \overline{K}^p_s. \end{aligned} \tag{3.22}$$

The storage state is calculated by the equilibrium of every outflow, inflow of every timestep and added to the content defined by the previous timestep

$$\begin{aligned} &\forall s \in S: \\ &\epsilon^{c}_{s,t} = \epsilon^{con}_{s,(t-1)} + \epsilon^{con}_{s,t} + \epsilon^{in}_{s,t} \cdot e^{in}_{s,t} - \epsilon^{out}_{s,t} \cdot e^{out}_{s,t}, \end{aligned} \tag{3.23}$$

where the final storage ($\epsilon_{t=end}$) state must meet (or exceed) the initial content of the modeling period ($\epsilon_{t=0}$) which is defined by the state of charge (I_s.) at the beginning.

$$\begin{aligned} &\forall s \in S: \\ &\epsilon^{con}_{s,(t=0)} = \epsilon^{con}_{s,(t=end)} \\ &\epsilon^{con}_{s,(t=0)} = \kappa^{c}_{s} \cdot I_s. \\ &\epsilon^{con}_{s,(t=end)} \geq \kappa^{c}_{s} \cdot I_s \\ &0 \leq I_s \leq 1. \end{aligned} \tag{3.24}$$

Another type of commodities others than "stock" are intermittent (im). There availability is given by time related constraints, as time series (z), and define a process (ϵ) output as

$$\begin{aligned} &\forall p \in P,\ c \in C_{\mathrm{im}},\ t \in T: \\ &\epsilon^{\mathrm{in}}_{cpt} = z_{ct} \cdot \kappa_p. \end{aligned} \tag{3.25}$$

Typically they are used for renewable energy systems such as PV, where the installed capacity (κ) is stated in the unit $\mathrm{MW_p}$. This equation (eq. 3.25) makes clear, that working with intermittent variable will require a curtailment process to dissipate surplus on commodity outflow to meet the commodity balance (eq. 3.10). Otherwise, artifacts will occur such as an increased use of storage or transmission due to their efficiencies. By changing the "=" sign into "$\leq$" in eq. 3.25 will solve this issues. However thereby, surplus power is less traceable which might be important in the field of energy economy.

After this model is set up and filled with parameters, the problem is reformulated into a Pyomo model and solved with a mathematical solver (glpk, gurobi). For a better data handling input and output values are stored in a dictionary format and are combined in a HDF5 file for further evaluation.

In the following of this chapter two models are built and solved by using the urbs method. The first is focusing on the heat sector on municipality level by using surplus power for sector coupling. The later describes the electricity sector of Germany and couples with the private transportation sector. This is done by introducing hydrogen as an new energy carrier (commodity) to the model. The geographical granularity is first chosen to model all 16 states of Germany and in a second step condensed to one node.

3.3 Development of an energy system model focusing on Power-to-Heat

PtH is a very efficient conversion method compared to other PtX technologies such as PtF. Additionally, the heating sector accounts for nearly half of the energy demand in Germany and thus has a very high potential for decarbonization. Hot spots for concentrated heat demand are, for example, in cities where the infrastructure for distributed space heating is already present in some of them in Germany. Commonly, CHP is used as an efficient technology to prevent individual decentralized heating solutions. Sacrificing a slight efficiency in electricity generation, the utilized heat from combustion brings a lot of benefit.However, it should be taken into account that this currently efficient solution, will soon lose this status. The reason for this lays in the fact, that CHP usually runs on natural gas, thus emissions are still linked to a fossil source which needs to be prevented in future to reach climate goals. To estimate the year from which electricity from natural gas powered CHP will be inefficient, specific emissions of electricity are calculated and plotted. Figure 3.1 sketches the projected governmental climate policy targets from Germany [10], projected emissions of electricity from the grid and the generated power from CHP calculated by different methods [149]. As VDI 4661 does not specify one true allocation method, emissions of CHP in this study were calculated by using the *Finnish method*. Coefficients (efficiency parameters and specific CO_2 emissions per kWh_{gas} ($\hat{c}_{gas}$) are taken from literature [149]. The presented methods enable the calculation pf specific (eq. 3.27) specific CO_2 emissions ($\hat{c}_{el}$) by using the efficiency of reference systems for a separate heat ($\eta_{th,ref}$) and electricity ($\eta_{el,ref}$) production. These results are then compared with the typical CHP efficiencies for combined heat (η_{th}) and power (η_{el}). The PES number (eq. 3.26) represents the primary energy saving from separate heat and electricity production.

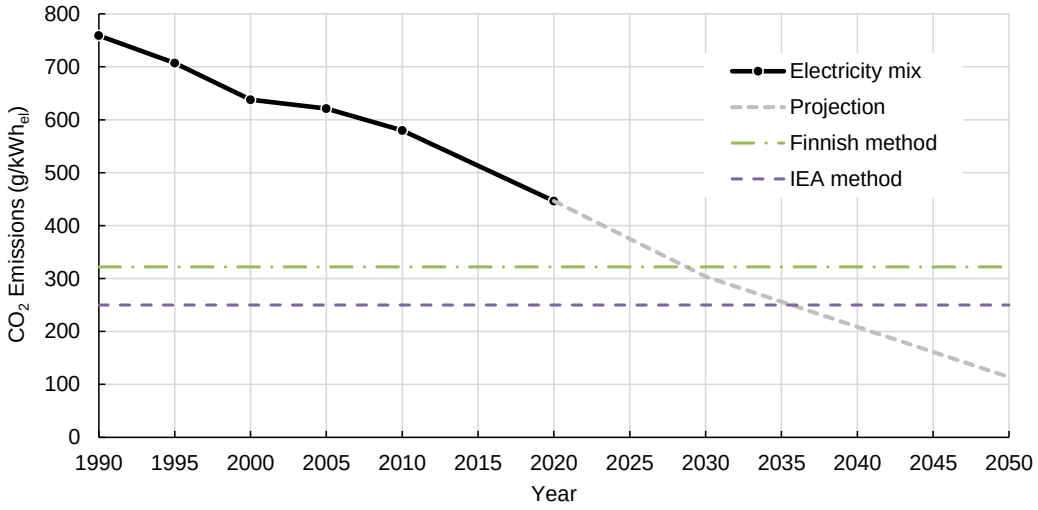

Figure 3.1: Predicted specific CO_2 emissions of the German electricity mix (black line) compared to the Finnish (green, dotted) and IEA (purple, dashed) allocation method. The intersection indicates the year when CHP will lose the status of an efficient technology as additional emissions will occur compared to using electricity for heating.

Table 3.2: Installed capacity of renewable energy technologies in Mecklenburg-Western Pomerania

Technology	2015	2030	2050
Offshore (MW)	336	3,800	8,100
Onshore (MW)	2,884	7,866	14,755
PV (MW_p)	1,373	2,515	4,000

$$\mathrm{PES} = 1 - \left(\frac{\eta_{\mathrm{th}}}{\eta_{\mathrm{th,Ref}}} + \frac{\eta_{\mathrm{el}}}{\eta_{\mathrm{el,Ref}}} \right)^{-1} \tag{3.26}$$

$$\hat{c}_{\mathrm{el}} = \frac{1 - \mathrm{PES}}{\eta_{\mathrm{el,Ref}}} \cdot \hat{c}_{\mathrm{gas}} \tag{3.27}$$

A case study is presented below to propose a method of solving the problem of inefficient CHP utilization. This is done by using surplus power from the state to enable a PtH supply for a coastal city in the northern part of Germany.

In this study, conducted for Greifswald [150, 151, 152], an energy optimization problem is solved to meet the heat demand of the city. From the results it can be stated that using heat from surplus power combined with heat storage systems is a low-tech solution to cost-efficiently reduce CO_2 emissions in that sector. It is shown that a reduction of 40%-80% of CO_2 emissions in the heating sector can be achieved by using PtH in the year 2030 and 2050. This methodology is cheaper compared to an ambitious renovation of the outdated building insulation in Greifswald. A heat storage of 900 MWh (2030) and 1500 MWh (2050) is needed, which is not more than 19 kWh per citizen in average. Furthermore the specific heating costs will be raised by just 11% from 2017 to 2030 and another 6% until 2050 by implementing this solution.

3.3.1 Method of the Greifswald study

The method determining the potential of available power surplus (β) is calculate by eq. 3.28

$$\beta_t = \sum_{r \in RES} \epsilon_{r,t} - \left(d_t + \sum_{l \in Lines} \cdot SIL_l \cdot \xi_l \right). \tag{3.28}$$

where (ϵ) is electricity production in (MWh/h) from source (r), where (r) is part of (R) technologies considered (on-, offshore wind, and solar power respectively) as stated in Table 3.2. The electricity demand is depicted by the letter (d) (MWh/h), (ξ) is the load factor according to the St. Clair curve which is shown in Figure 3.2, and SIL is given by equation 3.29.

For the year 2030 and 2050 the predicted installed capacities of renewable energy sources (RES) in the federal state Mecklenburg-Western Pomerania are taken from several studies [153, 154, 155, 156] and stated in Table 3.2.

Typical wind and solar potential is taken as a time-series to provide hourly (t) energy supply. The premise is set, that the difference between the electricity (ϵ) from renewable sources (r) and the electricity demand (d) of the region, which exceeds transmission grid's capacity ($SIL \cdot \xi$), is defined as surplus power. Furthermore, it is assumed that this surplus is a time related energy pool from which only PtH devices can drain. The transmission line (l) capacity is approximated by using the St. Claire curve Figure 3.2 together with the calculation of the surge impedance loading (eq. 3.29) of a specific transmission line. It is a simple method to describe the capability of power line transmission. It comprises three different influences whose domination depends on the line length and results in a hyperbolic shape [157]:

- thermal limit (0-80 km)
- voltage drop (80-320 km)
- angular stability (320-960 km)

The load factor (ξ) given by the St. Clair curve is stated on the y-axes in Figure 3.2. It can be interpreted as a multiplicator by which the transmission line's power limit is changed. As seen in the figure, for line lengths greater than 480 km, the load factor of the transmission line falls under 1. The nominal transmission capacity of a power line is defined by the surge impedance loading (SIL) which depends on the voltage level (V), the line inductance (L) and the capacitance (C). For a 230 kV transmission line, an inductance of 0.5 mH and a capacitance of $6.33 \cdot 10^{-6}$ mF is taken. The 380 kV transmission line is described with 0.3 mH and $4.61 \cdot 10^{-6}$ mF [158], [159], [160]. The length of the main transmission lines are measured using ArcGIS. Shape files including power level of the lines are used as input for the software. Since the shape files are not always accurately labeled, additional information is taken from the 50hertz grid operator [161]. Only transmission lines interconnecting Mecklenburg-Western Pomerania with other states are used for representing the surplus power of this particular state as this is the energy which would be lost due to the lack of power transmission capacity. The connection between Mecklenburg-Western Pomerania and its western neighbor Schleswig-Holstein was not taken into account as it is assumed that Schleswig-Holstein will have the same situation of a surplus power generation. This is due to the large amount of offshore wind turbines which are installed in the North-sea which is close to the Baltic-Sea. Therefore it can be assumed with reasonable confidence that the timeseries of wind in Schleswig-Holstein will not change significantly to that of Mecklenburg-Western Pomerania and an energy exchange between these two regions is not likely. The overall calculated transmission lines are stated in Table 3.3. A plausibility check was done as a follow-up with the corresponding grid operator.

$$SIL_l = V_l^2 \cdot \sqrt{\frac{C_l}{L_l}} \tag{3.29}$$

3.3.2 Model description

To solve the optimization problem, an energy system is modeled to find the optimal power mix for the investigated scenarios defined by their minimum costs. The model determines the optimal combination of investment and variable costs for a given set

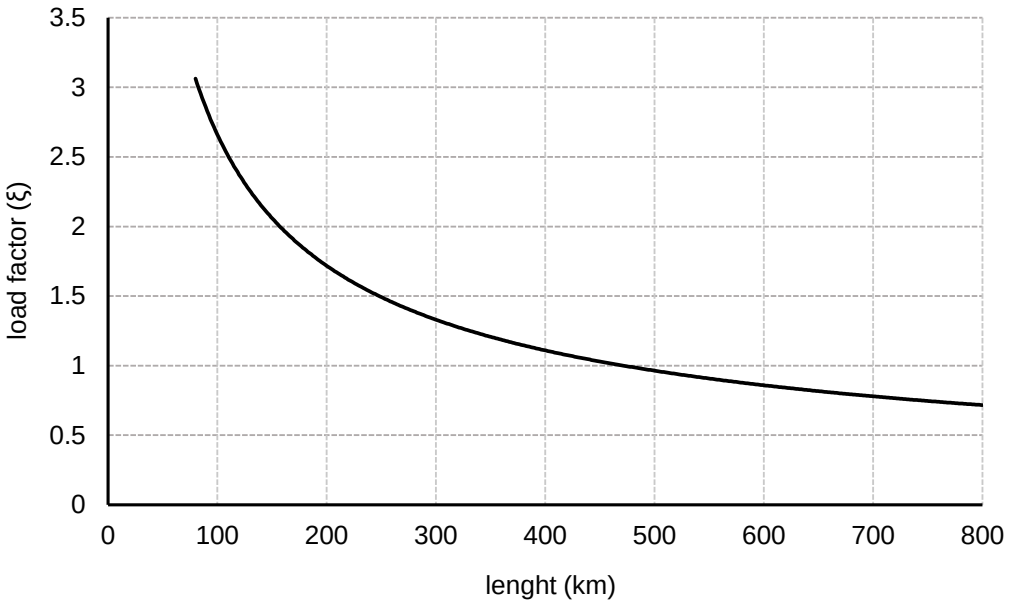

Figure 3.2: St. Clair curve

Table 3.3: Main transmission lines taken into account for energy exchange between Mecklenburg-Western Pomerania and neighboring federal states except Schleswig-Holstein

Name	**Voltage (kV)**	**Length (km)**	**Load factor** (ξ)	**Capacity (MW)**
L518	380	175	1.85	1,047
L517		175	1.85	1,047
L513		170	1.95	1,103
L514		170	1.95	1,103
L331	230	214	1.73	357
L332		180	1.9	352
L305		30	3.7	696
L306		30	3.7	696
Total				6,401

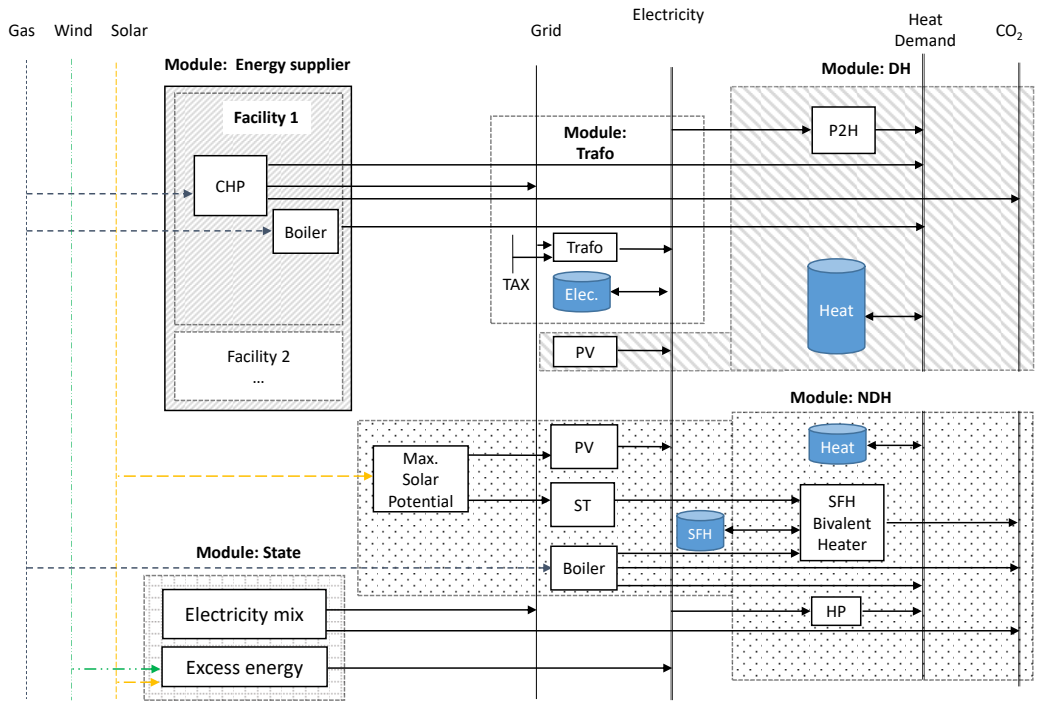

Figure 3.3: Model structure: The units "energy supplier" and "state region" supply the demand of the unit "district heating (DH)" and "non-district heating (NDH)". The "transformer" module (called "Trafo" by its German name in figures) is optional to add taxes to electricity production costs which are not coming from the excess energy process or "DH/NDH" photovoltaic (PV) systems. In the NDH area, heat can also be supplied by solar-thermal (ST) systems.

of conventional as well as PtH technologies. It differentiates between energy carriers, technologies for energy conversion, transmission infrastructure and storage options. All model components are represented through linear constraints, parameterized by technology properties such as costs, energy conversion or emissions. Fluctuating intermittent renewable sources are represented through normalized time series of their availability in each of the simulation time steps. The actual energy output of installed peak capacities (MW_p) of wind farms and photovoltaic systems per hour are limited by the normalized time-series between 0 and 1 every hour. This implies perfect foresight for both, capacity planning and operational scheduling.

An overview of the model structure is given in Figure 3.3 which describes the power flow from left to right. The vertical lines represent the energy carrier, horizontal lines connection input and output flows with technologies, depicted as boxes. The model is separated into five modules which represent different characteristics of the system:

- The surplus power which is calculated in the **state** module (by using eq. 3.29) represents the state region including installed wind capacities from on- and offshore as well as transmission line capacities.
- The part of the city which is connected to the district heating grid, is represented by the **DH** module. Here, the energy for spacial heating is generated in case of using PtH technologies with electric heaters in combination with large heat storage.

- The decentralized heat supply is represented by the **NDH** (non-district heating) module, where individual heating solutions are provided. One option is to use natural gas as a fossil energy carrier or solarthermal panels for direct heat production. Photovoltaic paired with heat-pumps or small electric heater is another option.
- Within the **energy supplier** module, energy for spatial heating is generated by central units from the municipal utility with CHP fed via natural gas.
- Finally, the **trafo** module represents the point where the transmission grid ends and distribution grid begins.

Heat is provided by centralized or decentralized technologies as well as using electricity from different energy sources. The municipal energy supplier is modeled by the CHP capacities, efficiencies and fuel costs. Detailed information regarding the assumed costs and emissions per technology are given in the Appendix A in the Table A.1. The ratio between heat and electricity production of the CHP is fixed at the beginning of the optimization and will stay constant. Electricity from the power grid is modeled unlimited as a slack term the costs of per kWh used. Surplus power is limited by the installed capacity of wind and solar power which is restricted to suitable regions in the state module.

3.3.3 Scenarios

Following scenarios are developed for the optimization problem. The reference scenario starts with today's situation of the city with 55 thousand inhabitants. The city is divided into two heating sectors: The district heating sector (DH) which supplies roughly half of the households with heat and the non district heating sector (NDH) which is characterized by individual heating solutions. The starting point for the determination of the local heat demand is the heat cadastre provided by the city of Greifswald. This cadastre is an extension of the existing database and offers, among other things, building-specific information on heat requirements, supply providers, building age classes and properties under renovation. A detailed description of the data analysis is given in a technical report [150]. Following scenarios are defined to achieve a CO_2 reduction of 80% until the year 2050 in the heating sector of the city.

1. the current situation is represented in the reference scenario by mapping heat demand by energy sources. In the NDH module, this is done by calculating energy demand for heating from an existing building database of the city. The installed heat technology of each building results in CO_2 emissions in this sector. In case of the DH module, heat demand is taken from the energy supplier and emissions are calculated by applying the already presented *Finnish method*. A heat requirement of 265 GWh is covered by the district heating region by emitting 53 kt of CO_2. 208 GWh of heat is generated by decentralized heating technologies resulting in 57 kt CO_2.
2. For the year 2030 a moderate partial renovation is assumed for the entire building stock. This potential is already available in the corresponding building database and will result in a reduced total heat demand of 18% but also entail renovation costs. However the climate goal of CO_2 reduction is assumed to be 40% of the

reference case. Therefor, PtH abilities are introduced to the model and their needed capacities are calculated by the optimization. The NDH module has the ability to use ground water heat pumps fed by electricity from the grid. It must be stated, that specific emissions from the grid are modeled with 300 g/kWh as shown in Figure 3.1. In addition, heat storage is allowed to be built, whose power and capacity is a further result of the optimization. It is assumed that the expansion of renewable energy technologies by 2030 in the state module reach 2 GW_p for PV, 4 GW_p for offshore and 8 GW_p for onshore. The total transmission line capacity is calculated to 6.4 GW. Generated power from wind and PV exceeding this value is seen as available surplus power for PtH.

3. In the year 2050, all buildings will be fully renovated, leading to a 28% reduction in heat total demand. In this scenario, 80% of overall CO_2 emissions must be reduced in the heating sector. Further it is also assumed, that additional expansion of renewable capacities reaches 4 GW_p for PV, 15 GW_p in onshore and 8 GW_p in case of offshore. Existing 230 kV transmission lines are expected to be upgraded to 380 kV level which increases, the maximum capacity to 10.2 GW. SFH (single family households) have the option to follow a bivalent heating strategy of solar thermal panels paired with small heat storage and gas boilers to cover peaks in heat demand. Based on available Geo-Information-System (GIS) data, 1650 SFH units are estimated which are suitable for this strategy. The storage size per SFH is limited to 500 l at a temperature of 60°C each. Specific CO_2 emissions of electricity from the grid is assumed to be 100g/kWh. Another way of achieving a reduction in CO_2 emissions of 80% in the year 2050 is an ambitious renovation which will reduce the heat demand by the same amount. The advantage of this path is that no change in heating supply technology is needed but utilization will be reduced and naturally additional renovation costs will occur. A benchmark value of 1500 €/m^2 is assumed for later calculation through all building of the city during this ambitious renovation.

A brief summary of the different scenarios are listed in Table 3.4. In contrast to the centralized heating supply, the decentralized heating sector must be modeled differently. In case of different participants of a pool (municipality), which decide individually for their heating technology, an approach of linking processes in a fixed ratio is chosen. As every individual of that pool has usually only one predominant heating technology available, heat generation of a pool must be used proportionally over time. Otherwise, optimization results would show a base-load and peak-load behavior, which would mean that individual households have multiple heating technologies available, instead of one, which is not realistic. Figure 3.4 sketches this behavior in an example where no fixed ratio is set and each participant can choose every hour from a variety of heating technologies. Between the hour 4 and 5, for example, the heat demand of the pool is only covered by gas- and oil-heaters but not by electricity. This would imply that "participant3" has at least one further heating technology to cover heat demand when electricity is unfavorable to use. In contrast, Figure 3.5 represents a fixed ratio between heating technologies, where each participant is able to cover his own demand with one individual technology. This adds a realistic aspect to the model, as not only the sum of the energy of the pool but also that of each participant is modeled correctly.

Table 3.4: Summary of the different scenarios modeled for the PtH case-study

Scenario	Description	Heat demand	
		Total (GWh_{th})	Peak (GWh_{th})
2015 reference	The reference scenario based on existing building database.	DH: 265 NDH: 208	91 79
2030 PtH	Partial renovation giving 18% reduced heat demand on average. CO2 emissions reduced with 40% by introducing P2H and storage.	DH: 217 NDH: 171	76 65
2050 PtH	Medium renovation giving 28% reduced heat demand on average. All transmission lines are upgraded to 380 kV. CO2 emissions reduced with 80% by introducing P2H and storage. SFH are introduced with bivalent heating options.	DH: 190 NDH: 151	66 57
2050 renovation	Extensive renovations giving 80% reduced heat demand on average. The reference scenarios energy system is used.	DH: 53 NDH: 41	18 16

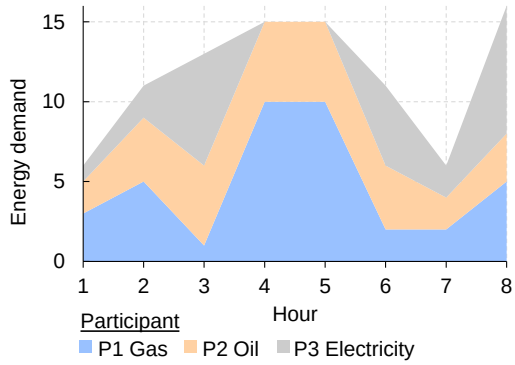

Figure 3.4: The heat demand of a pool of participants covered by single technologies which are not in a fixed ratio. This does not reflect a realistic behavior of each participant as only one technology will be predominant for each.

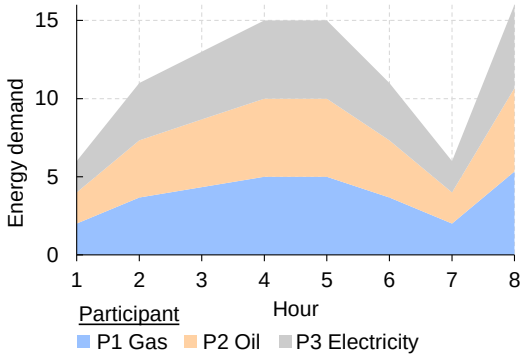

Figure 3.5: In contrast to the graph alongside, this heating pool follows a fixed ratio of heating technologies for each participant. For every hour, the share of heat supplied per technology stays same.

This functionality is not default, and is optionally available in urbs [162]. This feature was implemented as:

$$\begin{aligned} &\forall p \in P_{prop}, c \in C, t \in T: \\ &\epsilon^{\text{out}}_{p,c,t} = d_{c,t} \cdot \delta_{p,c}, \end{aligned} \tag{3.30}$$

where δ is a constant factor (ratio), for a process belonging to a set of proportional processes, (P_{prop}) to cover a demand (d). This ratio must hold true for every timestep and set of processes.

Total system costs of the modeling results are taken to calculate the averaged specific heating costs (K'_{ph}) for producing heat of the different measures. The calculation of specific system costs for heating is shown for the reference case in eq. 3.31 in the year 2015, where the system costs (K) are divided by the overall heat demand (Q) which results in 0.073 € per kWh heat.

$$K'_{ph,Ref} = \frac{K_{Ref}}{Q_{Ref}} = \frac{34,528,254€}{47,000MWh} = 0.073\frac{€}{kWh} \tag{3.31}$$

In addition to the specific heating costs, costs for saving CO_2 are calculated. Here, these costs are determined by the additional costs compared to the existing system (reference scenario) and the amount of greenhouse gas not emitted. In case of renovation this makes sense, as these costs are not covered by the system costs given by urbs.

Renovation costs (K_{ren}) are calculated for each building existing in the building database of Greifswald and added to the system costs (K) of the corresponding scenario and subtracted from the reference costs of the original scenario. These total costs are divided by the reduction of CO_2 emission (e) in the corresponding scenario (x) in order to calculate CO_2 avoidance costs (K'_{CO_2}). In that study an annuity of 7% (a) is taken

to calculate the yearly share as:

$$K'_{\mathrm{CO}_2,x} = \frac{K_{ren,x} \cdot a + K_x - K_{ref}}{e_x}. \tag{3.32}$$

Renovation costs for each building type is stated in the appendix, while for the "renovation scenario" 1,500 € per m³ are taken as stated in Schmees [163]. The specific annual costs for saved heat are calculated by dividing the total renovation costs by the avoided amount of heat and multiplied by the annuity factor.

$$K'_{sh,x} = \frac{K_{ren} \cdot a}{Q_{Ref} - Q_x} \tag{3.33}$$

3.3.4 Model results of the Greifswald study

The results of the year 2030 are included in the Appendix to avoid repetitions. However, the results of the year 2050 for the ND and NDH sector are more important. With the ambitious CO_2 reduction of 80% and a small assumed reduction in heat demand by renovation (28%), following technologies are installed as decided by the model, stated in Table 3.5 and Table 3.6. By using P2H, emissions are kept low in the DH region. the CHP-units of the energy supplier become redundant due to their fossil energy source. The high amount of excess power and reduced heat demand, made the P2H in combination with storage able to cover the entire heat demand in the modeled year. The storage is built up to its maximum allowed capacity of 1.5 GWh. In addition nearly one third of electricity from the grid is used for P2H due to its low specific CO_2 emissions. In the non-district heating region, single family houses (SFH) use

Table 3.5: DH technologies installed in 2050

Technology	Power (MW)	Energy (MWh)	CO_2 (tonne)
electric heater	134	190,453	7,992
Grid	—	(79,922)	(7,992)
Excess energy	—	110,530	0
Storage	(100) max	(1,500) max	—
Total	134	190,453	7,992

a bivalent strategy of solar thermal technology (ST) and thermal storage. To cover peak loads, additional gas boilers are installed which corresponds, together with the solar-thermal technology to a bivalent heating system. 18 MWh of thermal storage are installed in private households, which corresponds to 500 single family households with a 500 liter storage at a temperature spread of 60 K. Expensive biomass heating is built up to the maximum allowed capacity as they are considered to be emission free sources. A moderate part of electric heaters is an element of the cost minimal solution. Combined with heat pumps, this strategy is chosen to use the low-emission household electricity from the grid. The excess power, which cannot be transmitted to other states, increases and is available for P2H. Thus, no extra PV needs to be built in the DH or NDH modules. Therefore, it is more beneficial to install solar-thermal collectors for single family houses as another flexibility option.

Table 3.6: NDH technologies installed in 2050

Technology	Power (MW)	Energy (MWh)	CO_2 (tonne)
Heat pump	13.6	39,571	989
Electric heaters	22.6	58,410	5,841
Solar thermal (bivalent))	12.4	9,936	0
Gas boiler (bivalent)	11.4	30,709	7,370
Storage (bivalent)	(4)	(18)	-
Biomass	5.0	13,118	210
Total	65	151,744	14,410

Table 3.7: specific costs of all scenarios in the PtH model

Scenario	**heating** (K'_{ph}) (€/kWh_{th})	**renovation**[1](K'_{sh}) (€/kWh_{th})	**CO_2 saving** (K'_{CO_2}) (€/t)
2015 reference	0.073	0	-
2030 PtH	0.081	0.086	26
2050 PtH	0.086	0.012	290
2050 renovation	0.073	1.48	$6{\cdot}10^3$

[1] the category renovation represents the energy costs saved by renovation

The costs for each scenario conducted in this study are listed in Table 3.7, starting with the reference scenario, were no CO_2 costs for saving occurs. While specific heating costs are just slightly different for the scenarios, the costs for implementing a measure for saving CO_2 behaves in the opposite way. From this result, is can be clearly stated, that renovation is the most expensive measure to save CO_2 emission in the heating sector.

3.3.5 Discussion of the Greifswald study results

In the **2030 PtH** scenario, the goal of reducing CO_2 emissions by 40% is set as a constraint. Due to the moderate renovation, heat demand is decreased by 18% to 388 GWh_{th}. In the NDH region, the dominant heat supplier are gas heaters with 133 GWh. The maximum allowed capacity of 13.6 MW_{th} of ground-water heat pumps (COP 4) is installed. Only 1.5 MW_p PV, a small part of the total capacity (45 MW_p), is installed to provide some part of emission free power for the heat pumps. 18% of that electricity from PV is shifted to the DH region via grid. In the district heating region, heat is covered up to one third from PtH technologies using excess power. 944 MWh of heat storage is built to make the variable excess power usable for a longer period of time. The charging and discharging rate is limited to 100 MW.

A further renovation wave reduced heat demand by 28% in total in the **2050 PtH** scenario. PtH in the district heating region covers the total heating demand of 190 GWh_{th}. Three quarter of the used energy comes from excess power and the rest is taken from the grid with the low specific emissions of 100g/kWh. A storage of the maximum allowed dimensions of 1,500 MWh in capacity and 100 MW in power is

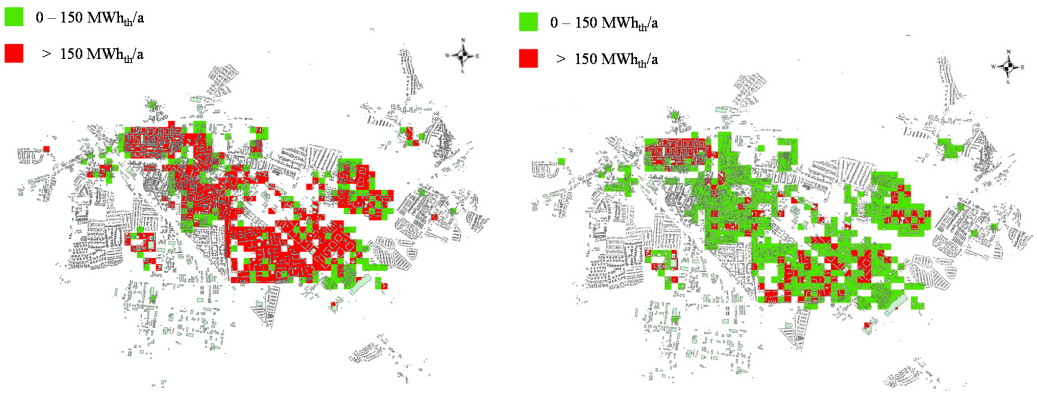

Figure 3.6: Heat demand of a moderate renovation scenario in the year 2030 (left) and an ambitious renovation scenario in the year 2050 (right). Green squares shows heat demands with less than 150 MWh per year which will not be profitable for a district heating network. Red squares indicate heat demand above 150 MWh_{th}

installed. In the NDH region, the bivalent heating system is built by a capacity of 12.4 MW_p paired with gas boiler to cover peaks of the same capacity. A total storage size of 18 MWh_p and power of 4 MW is installed. Ground water heat pumps are still reaching the maximum installed capacity of 13.6 MW_p. In contrast to the previous scenario, no PV panels are built. This can be explained by the increased amount as well as the availability of surplus power. Thus, no PV panels are built neither in the NDH module.

In contrast to using surplus power for heat supply, an ambitious renovation scenario would also lead to the same CO_2 reduction, but at costs of a disintegration of the wide existing district heating network. GIS is used to illustrate this effect in Figure 3.6. The yearly heat demand of the sketched buildings are summed up and represented in squares of 1 hectare in size. Green squares illustrate low heat demand between 0 and 150 MWh/a whereas red squares symbolize higher heat demand above 150 MWh/a. It is obvious that an ambitious renovation scenario leaves only the city center to be profitable under the constraint, and that 150 MWh heat acceptance is the limit to make district heating profitable [164]. In addition, the specific costs listed in Table 3.7 shows that it is not the cheapest solution.

3.4 Development of an energy system model focusing on hydrogen demand

As described in previous section, various different tools for modeling energy systems already exists, each with specific strengths derived from the requirements of the scenarios for which it is used. Identifying the potential of the PtX technologies using energy system models is such a requirement. The character of an energy system model is guided by its assumptions and is characterized by individual results. In order to model future energy systems, scenarios or premises are set to build a pathway into a possible future which are characterized by various scenarios and used for describing a certain

point in time. In existing energy system models, hydrogen is not the main aspect in modeling purpose. Some models do include hydrogen in form of PtG or power-to-liquid (PtL) which corresponds to the (current) PtX aspect but do not have a given demand which needs to be satisfied. Rather, the energy quantities of the hydrogen produced are defined by the surplus power and chosen as the last option. From an economic point of view, this makes sense, but prevents the presentation of a possible future in which hydrogen plays a significant role. Three available studies [41, 165, 166] have a very comprehensive approach and mostly use similar central scenarios such as decarbonization targets, final energy consumption, available storage technologies or sector coupling but distinguish by nuances. The scenarios are different, assumptions are made which, as in [41], assume an import of electricity in Germany of 63 TWh in 2050 and backup power-plants of up to 70 GW. PtH is used as another flexibility option of 23 TWh for Germany in 2050 with the goal of a 80% in reduction of CO_2. PtG or PtL are not used until a 95% CO_2 reduction scenario which means, that hydrogen does not play a role before that reduction goal.

The study from Dena [166], for instance, classifies imported PtX (synfuels and hydrogen) as energy carrier with a zero CO_2 footprint [167]. There, PtX is also used to cover parts of Germany's primary energy demand in 2050 with a 95% CO_2 reduction in a mainly electrified scenario (EL95). This corresponds to 533 TWh from which 74% are imported and thus defined as CO_2-neutral. In a scenario which emphasizes a mix of a broad technology mix (TM95), an even higher PtX demand of 908 TWh (630 TWh CH_4, 169 TWh H_2, 108 TW synfuel) is needed from which 82% are imported. On the one hand it makes sense, that imported PtX fuels have to have a very low carbon footprint in a 95% scenario. On the other hand, with these unlimited amounts of imported CO_2 free energy carriers, the validity of the results might blur. However, both mentioned studies have in common that the BEVs experience significantly earlier penetration than the fuel-cell vehicles (FCVs). It has to be noted, that the FCVs are more expensive than the BEVs, which is especially in the Dena study the factor that prevents the penetration of this technology, aside from their lower efficiencies compared to the BEVs. In general, PtH is one of the first sector coupling technology emerging in the system due to his high efficiency and low investment costs. Since the heat sector is a very large reservoir that can generate and store heat from electricity efficiently, this is the preferred technology in all scenarios. Power-to-gas (PtG) or PtL is one of the last options used in the sector interconnection due to its high investment costs and high efficiency losses due to transformation.
The mentioned study [41] uses in a nearly completely decarbonized system huge backup capacities with only few full-load hours as a consequence, this allows short-term electricity import with high peaks which are carbon-free [166]. This methodology will prevent the over-expansion of storage capacities which are only used for few hours over the year. It is worth a discussion if these assumptions (backup power-plant capacity & CO_2 free energy imports) are an adequate solution beside most of the models are having a full foresight.
For the reasons set out above, a **specific new energy system is developed** which assumes a hydrogen demand due to a set assumption of a future fuel cell vehicle fleet, as presented in Figure 3.7. This assumption reflects current research in the field of vehicle development, which is not limited to BEVs.

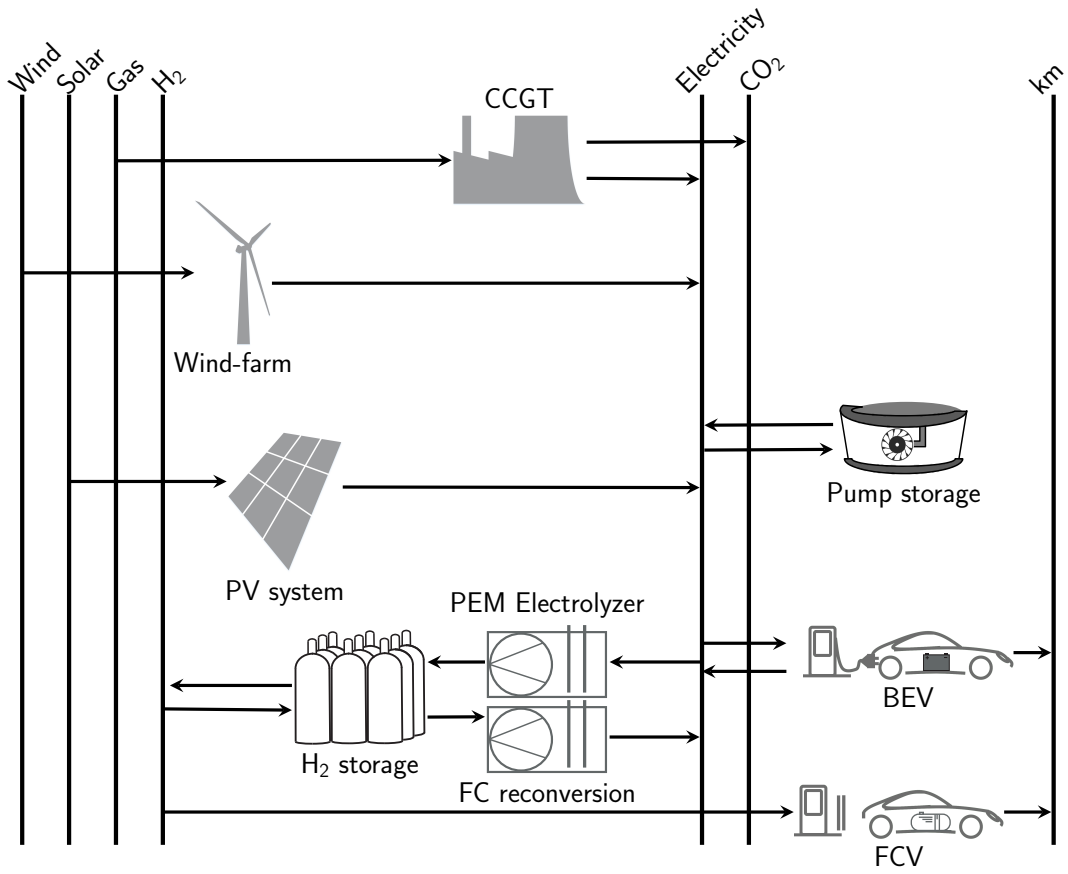

Figure 3.7: Reference energy system for the different scenarios in the year 2050. On the left side timeseries for intermittent supply such as wind or solar and the stock commodities Gas are located. Different processes transform this input with an efficiency factor to cover a given demand which could lead to CO_2 emissions. For scenarios with share of other fossil fuel than CCGT (years before 2050), the further conventional power-plants are included in the same family. Hydrogen as an energy carrier can be used in the same way as electricity stored in batteries by reconversion via fuel-cells.

Considering the supply of a constant hydrogen demand from transportation sector, several question will be answered by the model such as:

- The amount of full-load hours a PtX technology can operate exclusively on otherwise curtailed energy.
- Amount of hydrogen produced for demand and reconversion.
- PtX storage capacity.

The term *full-load hour* here corresponds to one hour operation of a technology with 100% of its installed capacity. Storages can help to shift energy from a time with very low costs to a time with a higher value. It can also help keeping the capacities of the generation technologies small by exploiting their base-load capability. Thereby storages need to have a sufficient size to have significant impact in the energy system. PtX products can be stored as energy carrier in liquid form such as Fischer-Tropsch (FT) diesel, OME-synfuel and liquefied hydrogen.

A first model was initially divided into 18 nodes as one per federal state, the North-Sea and Baltic-Sea and presented at the 8th Energy Colloquium of the Munich School of Engineering (MSE) at TUM [168]. Figure 3.8 was presented during a poster session at the colloquium to show the electricity demand of the federal stated of Germany, the installed renewable energy capacities as well as the hydrogen production. However, this fine granularity, in modeling each federal state extensively by their electricity and private mobility demand, is unrewarding in this particular case. However it can be stated, that renewable technologies are installed especially in the regions where the offer of irradiation and wind is favorable. In addition, it seemed that PEMWE installations match to the expansion of wind capacities in particular. This might be due to the higher full-load hours of wind compared to solar (see Appendix Figure A.2 and Figure A.3). As the focus of the P2X project lies on the total amount of hydrogen produced in Germany in different scenarios, the additional computational time required for solving a 18 node problem is not reasonable in this case. Thus, regions have been combined into one node for further research.

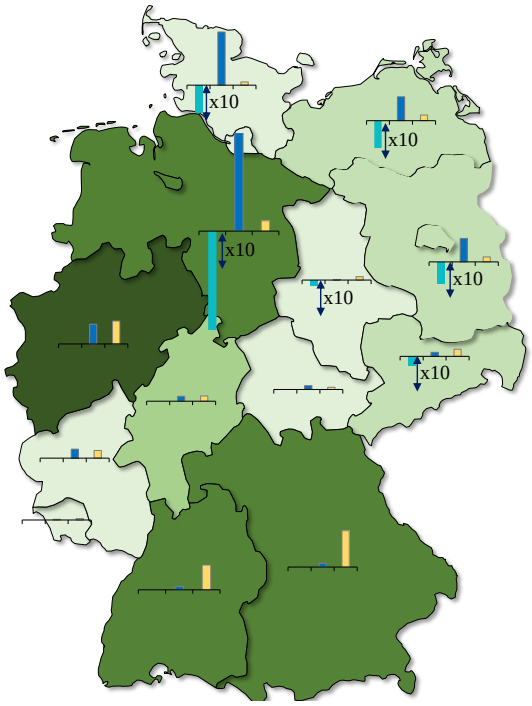

Figure 3.8: Energy production from wind (dark blue) and solar PV (yellow) and the hydrogen production by local electrolyzers (teal). The latter is magnified by a factor of 10 for a better visibility. The electricity demand is visualized in green, where high demands are shown in darker shades

3.4.1 Main assumptions

It is assumed that in the future only combined cycle gas-turbines (CCGT) will be used as fossil-based power-plant with a overall efficiency of 50% (60% in KSZ95). Since PEMWE is still a very young technology, its future cost depends strongly on several factors. On the one hand, the increasing demand of electrolyzers could lead to lower production costs. However, the increasing demand for noble metals which are severely

mined, such as iridium and platinum, could have a converse effect. With an increased demand of these materials, this could lead to a shortage in the stock market and lead to higher prices. Currently, the cost estimates of a PEMWE system vary between 1860 € and 6000 € per kW_{el} [169]; with view to the future application, the lower value is used for the reconversion of H_2 via fuel-cell (FC) as well. Today, stacks of the PEMWE have a lifetime of 60,000 hours which corresponds to almost 7 years neglecting stress due to fast change in load of the electrolyzers, a future lifetime of 10 years is assumed. Costs for the renewable energy technologies are taken from literature [170] for the year 2050 and stated in Table 3.8. Natural gas price for CCGT was set to 45 € per MWh in 2050. The amount of FCVs and BEVs was calculated and set as already installed in the model, so that no extra costs occur. Hydrogen storage has a large variance in price. Hydrogen storage systems can be available in different versions (tanks, gas cylinders, caverns) and therefore also have different costs. For hydrogen caverns 13 €/kWh are stated by Dechema [79] but a pipeline infrastructure may also have to be set up. The same study estimated that a H_2 pipeline network would cost about 23 billion euros for delivering approximately 10,000 gas stations with hydrogen. In addition hydrogen would also have to be compressed beforehand, resulting in further costs. For this model, the cost structure were simplified and storage costs of 10 €/kWh capacity as well as additional costs for the charging and discharging infrastructure of 20 €/kW are assumed.

Table 3.8: Capacity costs and efficiency (η) of different technologies used in the energy system model

Technology	invest (10^3 €)	η (%)	maintenance (10^3 €/a)	depreciation (a)
CCGT (MW)	450	50-60	6	30
PEMWE (MW)	1,860	70	93	10
FC (MW)	1,860	70	93	10
Photovoltaic (MW_p)	640	time-series	13	25
Onshore (MW_p)	1,167	time-series	40	25
Offshore (MW_p)	2,000	time-series	40	25
BEV (MW)		already installed		
FCV (MW)		already installed		
H_2 storage (MW)	20	100	0	50
H_2 storage (MWh)	10	100	0	50

The tolerated **CO_2 emission** budget is limited by the energy economy and private traffic sector in 2050. Depending on the scenario total emission which are allowed to be emitted are restricted by the modeled scenario with the aims of the German government [171]. The model is run without any emission constraints for the year 2018 with the corresponding installed capacities from that study. The resulting amount of emissions are then taken as reference value for further scenarios. The KSZ80 is modeled with an 80% CO_2 reduction for the year 2050 in the energy sector which correspond in the model to 43 mega tonnes (Mt) for the energy sector. In addition the total CO_2 budget is increased by additional 20 Mt for the private transportation sector which applies the same reduction goals for the use of cars. In total a limit of 63 Mt is set as a constraint for the KSZ80 which is adapted to the different KSZ**x** scenarios by the

factor (100-**x**)/100 which represents the emission savings compared to the reference year.
The **maximum capacity** of wind turbines is calculated by the share of the non-occupied area excluding e.g. settlements, rivers or road, in Germany which is calculated from a tool [172] developed at TUM-ENS. From this, an occupancy of 5% of the suitable space in Germany is assumed as not all useful space will be allocated to wind farms. By assuming 5 MW_p turbines in 250 m distance each, a potential of 20 MW/m^2 is available which corresponds to 198 GW onshore capacity. To verify this approach, the results are checked with literature. This calculated number is slightly higher than the 178 GW_p stated in [173] (Scenario: Energiewende-Referenz) but much lower than the 930 GW_p from [174] as a higher share of Germany's landmass for wind farming is assumed. As a premise one-fourth of the capacity is assigned to very good wind locations (the best third of each region). This is later used to assign the correct wind load profile to the installed windturbines which will result into a certain electricity generation. As a simplification, the remaining 3/4 are assigned to the second best third of wind locations. This should show that not all locations have the same quality and sweet spots are occupied at some time. The quality of a wind location is characterized by the amount of full load hours of their corresponding wind time series [175]. The maximum capacity of photovoltaic systems is not limited. The use of conventional power plants is determined by the model.

3.4.2 Modeling private transportation sector

Electrifying the private transportation sector has a huge potential in matching the goal of a wide decarbonization. Two different types of vehicles are modeled in the presented energy-system. BEVs are predestined to operate journey distances shorter than 250 km as no time intensive charging (> 30 min) of the vehicles are needed within these ranges. Hydrogen vehicles, however, are more suitable for longer journeys as stated by Felgenhauer [89], and therefore the remaining mileage is satisfied by FCV. The basic assumptions for implementing the private transportation sector in the reference energy system are stated in a previous work published as a working paper [176] which was conducted during the P2X project [33]. Electrified private mobility to match the goal of a decarbonization in the private transportation sector. An analysis of the average distance in kilometers traveled per trip was performed with reference to [177]. In 2017, 730 billion vehicle kilometers were recorded in Germany of which about 86% of the mileage are driven by passenger cars (630 billion km) [178]. The average distances for private transport in Germany are distributed according to Table 3.9 with reference to their occurrence. Trips with a length of over 100 km account for 1.7% of the total mileage with an average of 251 km [177]. Depending on the type of vehicle used and the driving speed, the fuel required and thus also the energy requirement may vary. From the analysis it is stated that 71% of the mileage is provided by BEV and accordingly remaining mileage demand is covered by FCV as BEV has an overall higher rate of efficiency (0.57 MJ/km) compared to FCV (0.73 MJ/km) [41]. For simplification the final energy demand from transportation sector equally divided per km. The final energy demand for BEV accounts to 70 TWh while FCV will increase final energy demand by another 50 TWh which needs to be covered by PEMWE, renewable energy technologies and power-plants.

Table 3.9: Distribution of private vehicle journeys by distance (0.2% not relatable)

∅ distance (km)	<0.4	0.4-0.6	0.6-1	1-2	2-5	5-10	10-25	25-100	251
distribution (%)	1	2	6.9	12.4	23.9	19.9	21.2	10.7	1.7

3.4.3 Hydrogen transportation

Compared to electricity transmission, hydrogen distribution has an underrepresented infrastructure in Germany at the moment. On the one hand, a wide pipeline network for natural gas exists but due to regulations limited to 10% for hydrogen, as higher concentrations of hydrogen in metallic pipeline could lead to brittleness of the steel which results into a reduction of the cracking resistance [179]. A study from the same source two years later in 2016, however, states that even a share of 30% hydrogen in the natural gas network will not be an issue and strongly suggests a revision of these regulations [180]. Thus, the transportation of hydrogen is not covered by the scope of this model. However transporting H_2 with LOHC (Liquid Organic Hydrogen Carrier) is one feasible possibility similar to the transportation of petrol. LOHC is a technology which provides logistic options such as an ease of transportation with ordinary fuel trucks by bounding H_2 chemically to the organic carrier. From the chemical formula of dibenzyltoluol (DBT) $C_{21}H_{20}$ which is used as carrier, it is obvious that LOHC can be loaded with 1/12 of its mass with hydrogen. The carrier's mass weights 92% of the total, which can be charged currently up to some hundred times with an overall efficiency of 70%. If the heat loss, which occurs during charging LOHC with hydrogen, could be used in a smart way with other applications the overall efficiency would further improve. However this is neglected in the model and additional energy for transporting LOHC to its destination is also not taken into account yet but in Chapter 4 for environmental purpose. With a price of 4 €/kg, the medium for storing energy is very cheap (2.1 kWh/kg) [181]. Compared to fossil energy carriers such as petrol, LOHC is inflammable but critics highlight the fact that the gravimetric energy density is about 5-6 times lower compared to diesel or petroleum (∼12 kWh/kg). In addition, the heavy carrier itself needs to be returned after the discharging process back to the hydrogen producing facility, which is energy demanding. In contrast to diesel, LOHC is not carcinogen and therefore does not have to be labeled as hazardous material but still is harmful to water organisms [182]. A further possibility for the distribution of hydrogen is the liquefaction through strong cooling down to about - 253 °C. The advantage of a higher energy density of 2.34 kWh/l LH_2 is currently opposed by an energy consumption of 11-15 kWh/kg H_2. According to the current study, it is assumed that the energy consumption can be reduced to 6 kWh/kg H2. At a weight of around 71 g/l LH_2, the volumetric energy density increases from 3 kWh/m³ to 2.3 kWh/l, but is still 5 times smaller than that of conventional fuels. Another alternative offers the compression of hydrogen up to 900 bar, for which only 3-5 kWh/kg H_2 of electric current has to be used for the compression [122].

3.4.4 Charging behavior of BEVs

Compared to FCVs the behavior of BEVs are modeled completely differently. Here, data of the vehicle traffic on the the German roads were taken in an hourly resolution. In a first step, the data of automatic counting stations on the German roads per federal

state are evaluated with a MATLAB script. These data capture the hourly events of passing vehicles. As an approximation, these are used and added up to the total kilometers traveled per federal state (b) [178]. Subsequently, the share of each driven hour (t) to the annual peak (k) demand is formed. In order to calculate the traction current (d_{BEV}) which needs to be charged, the proportion of the vehicle fleet (v), which is not on the road must be used for calculation, which is represented by the last summation in eq. 3.34. Figure 3.9 represents such a possible fleet driving behavior and also the inverse exemplary. Because BEVs are not charged during a journey due to the long charging time, but rather tends to be charged when parked over a longer period of time, the charging behavior was plotted as an inverse versus the actual traction current and implemented as demand for electricity in the energy-model. Thus, the BEV are modeled as an electricity storage from which electricity is taken to cover the given time series of energy demand to cover mileage. In addition a flexibility option for BEVs is implemented in means of vehicle-to-grid with a 1-C charge-discharge rate. Thus, the charged batteries can be used to provide electricity to the grid in time of low vehicle density on the streets. An availability of the full battery (22 kWh) capacities of 20% of the fleet for vehicle-to-grid is assumed.

$$d_{BEV} = \sum_{b=1}^{16} k \cdot \sum_{t=1}^{8760} (1 - v_{t,b}) \tag{3.34}$$

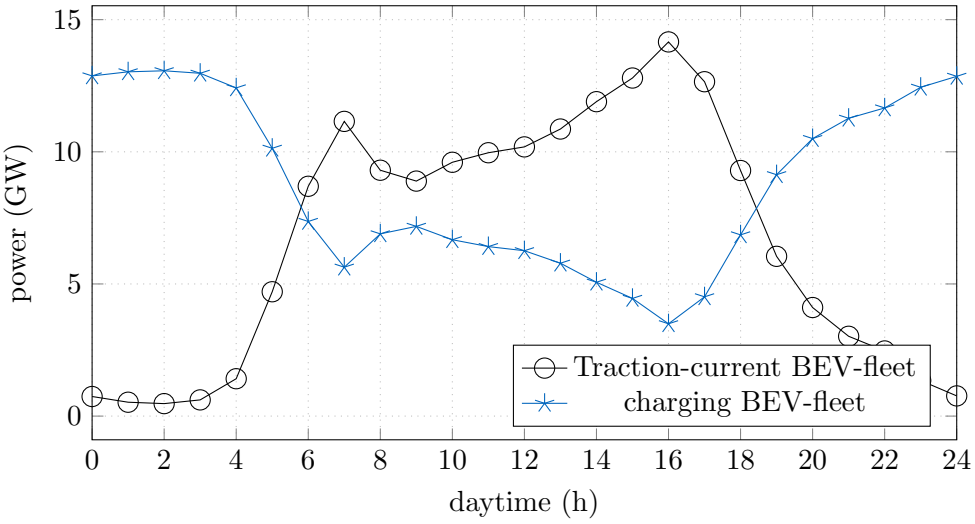

Figure 3.9: Load profile (charging) of BEV fleet and the traction current.

.

3.5 Result of the hydrogen model

The model is run for the years 2030 and 2050 distinguished by their individual CO_2 goals. These are taken in percentage point reduction compared to the reference year, from [41]. For 2050, two emission goals are set. One is the scenario with the goal of reducing 80% of the CO_2 emissions and the other one with an even more ambitious aim of 95%. Year 2030 is used to show the path but is not related to the other years by an

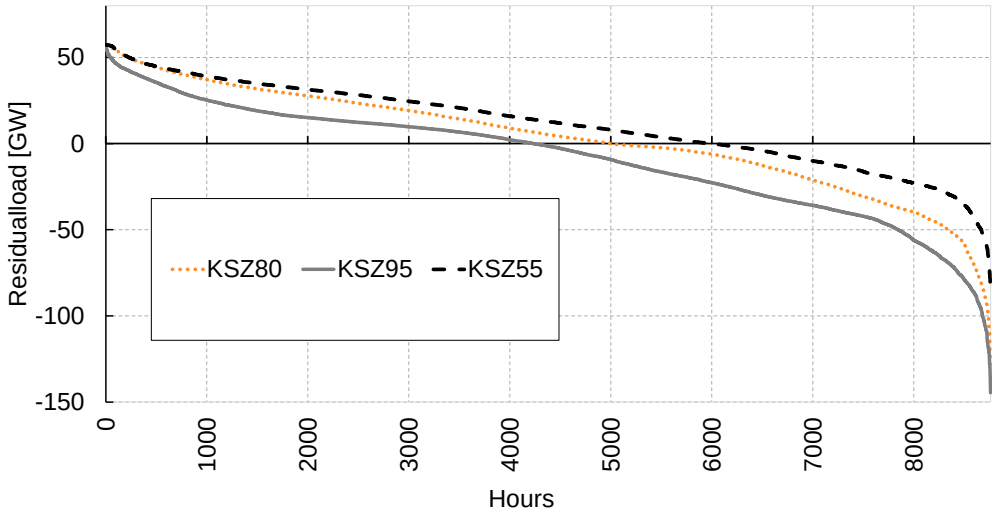

Figure 3.10: Residual load of electricity from the model under CO_2 reduction constraints of 55% (black dashed), 80% (orange dotted) and 95% (grey line).

inter-temporal coupling. This means, it is a green-field approach, where in every scenario the capacities of technologies are built independently of the other scenarios/years. The residual-load curve (Figure 3.10) is calculated by subtracting, for each hour, the electricity produced via renewable energy sources from the energy demand and sorting the resulting time-series in descending oder, starting with the highest value. The maximum power demand from fossil power plants is in all cases 60 GW. In year 2030, a hydrogen storage of 480 GWh capacity is installed with almost 50 GW charging/discharging power. The same amount of hydrogen storage is built in the KSZ80 scenario for the year 2050. A closer look reveals, that the installed PV capacity increases from 130 GW_p to 180 GW_p and wind from 90 to 120 GW_p.
The KSZ95 scenario however leads to further increase of the PV installation to 240 GW_p. In this scenario, the reconversion of hydrogen appears for the first time with almost the 13 GW installed fuel-cells which is slightly less compared to 17 GW PEMWE. Additional 160 GW_p of wind turbines are installed which is an increase of 30% compared to KSZ80. Due to this increase of the renewable energies in the system curtailment of surplus power occurs way more often which is visible by the increasing area between the KSZ90 curve and below the x-axis.

The result of each scenario is evaluated by its annual duration load curve of electricity and specific CO_2 emissions. To do so, the specific emissions connected to 1 kWh of electricity are plotted for every hour of the year descending in Figure 3.11. It is obvious that the specific CO_2 emissions per 1 kWh electricity are different for each scenario as the share of electricity generating technologies are different. The extremes are found on the top left side (the highest number) when electricity is produced conventional and the situation when no fossil fuel is used (intersection with the x-axis). In 2030, also few coal power plants are used beside CCGT and therefore the emissions are slightly higher. As KSZ80 is still an ambitious scenario but not as strict as the KSZ95 and more likely achievable until 2050, this scenario is taken for further investigation. In many discussions, surplus power is seen as a costless good which can be used for PtX

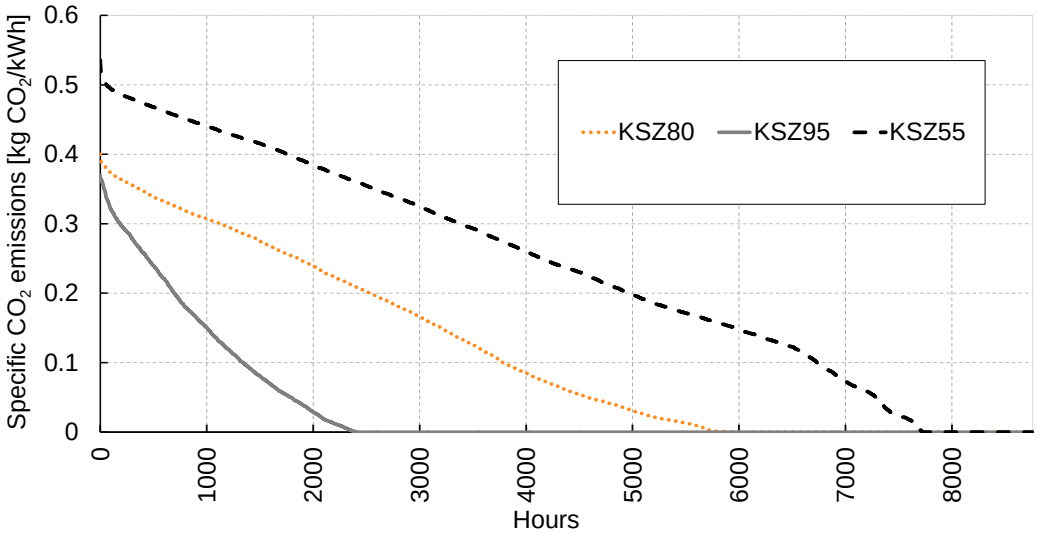

Figure 3.11: The annual duration load curve representing the specific CO_2 emission per kWh electricity during a year (sorted descending)

technologies. For this reason, even some project proposals suggest operating the PtX plants purely on surplus power to make innovative technologies feasible.

In Figure 3.12 the duration curve of the electricity mix with 80% CO_2 reduction is presented. Hydrogen production based on emission-free, renewable electricity is thus limited to 3000 hours per year. If, for example, the capacity utilization of the plant is to be increased by another 2000 hours, emissions of around 50 g/kWh$_{el}$ must be expected for this period of electricity consumption. With a higher capacity utilization, the emissions increase on average to 25 g/kWh$_{el}$ over the entire time, which is allocated to the product. A further 2000 hours lead to an increase in average emissions of 80 g/kWh$_{el}$ for the production during the best 7000 hours of the year. It must be mentioned that the depiction the load curve is presented, does not reflect a real facility operation as the operating time period does not have to be continuous but will be separate hours over the year depending on the availability of renewable energy. It is thus a best-case estimation of the balance between plant utilization and electricity emissions in an energy system that is strongly but not yet fully decarbonized. Rather, the approach can also be pursued to distinguish between a grid-conducive operation and a continuous base-load operation. The latter is represented over the whole year with 8760 full-load hours whereas the grid-conducive operation represents the 3000 hours in which the plant conduces to utilize energy surplus or offers operating reserve. This type of operation management would have to be considered separately when it comes to competitiveness. An assessment will have to be made with regard to the eligibility for governmental subsidies or the possibility of reacting to price signals on the electricity market which is excluded from the scope of this work. Besides, this representation cannot be scaled arbitrarily and is therefore limited in its statement as, for example, the surplus power may not be sufficient to supply a large pool of PtX plants with electricity in the same hour. However, emissions from electricity are not solely responsible for emissions from a PtX product or hydrogen production from PEM electrolysis. The entire value chain of hydrogen production involves input in

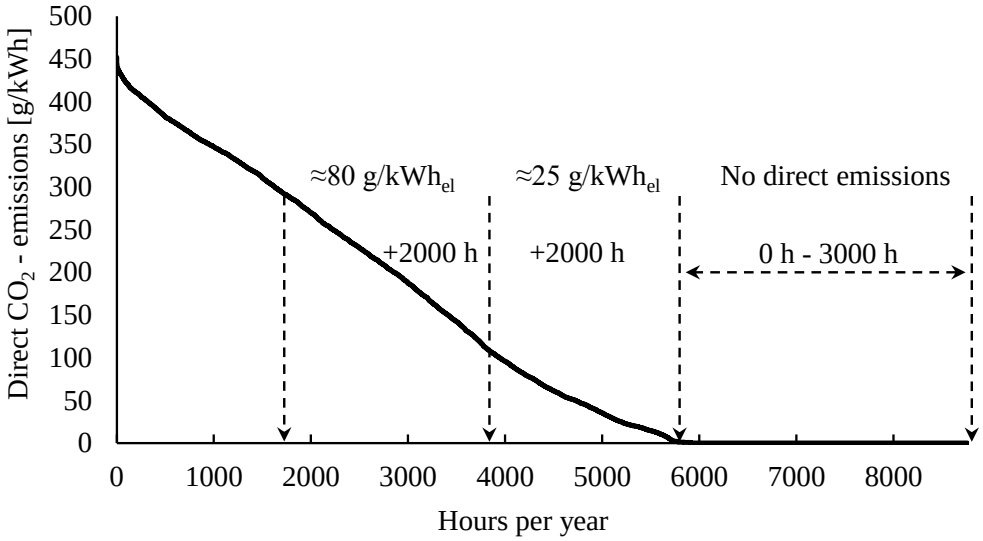

Figure 3.12: Ordered CO_2 curve of the electricity mix in the year 2050 with a 80% CO_2 reduction goal versus the year 1990. Arrows mark the amount of hours a facility can operate a year, by using electricity with certain greenhouse gas emission mix.

form of energy and material. For example, steel is required for the piping in the plant, which has to be mined beforehand and processed into steel in blast furnaces and then transported over long distances. In order to evaluate this effect of the upstream process chain, a life cycle analysis is carried out in the following Chapter 4.

4 Life-cycle assessment of PEMWE

The first LCA was conducted by the Coca-Cola Company in 1969 to determine which beverage container was most efficient and was less resource and energy demanding. It was investigated the depletion of natural resources, the release of environmentally harmful substances and the fuel demand for transportation [183]. Several events triggered the demand on studies to minimize the environmental impact of products and industrial processes. Concerns of an increased growth of population came up [184] which strongly connects to resource depletion and developed a new sense for sustainability [185]. The oil crisis in 1973 and 1979 shocked the world with an increase in oil prices between 100% and 400%. and the first time solid waste was announced to become an urgent issue in 1988 [183]. In 1990 a workshop was held by the Society of Environmental Toxicology and Chemistry (SETAC), and as an outcome the term **life-cycle assessment** (LCA) was defined, which led to the first peer reviewed journal article about LCA methodology in 1992 [186]. This finally led to a standardization of LCA methods in the International Standards Organization (ISO) 14000 series [187] in 1997. With updates in 2006, the method of conducting a life-cycle assessment (LCA) was regulated as stated in the ISO 14040 and 14044 standards today. The content of the following sections rely on the research results gained during project work in P2X, in particular the system analysis of PEMWE, that was published by Bareiß et al.[34]

4.1 Methodology

LCA is an approach to allocate all aspects of resources and energy in a value chain of a product stage which is the subject of investigation. It covers all important production steps beginning by raw material extraction, followed by refining processes, transportation, assembly and usage phase until waste management. The study includes phases depending on the defined system boundaries. LCA can be a tool to analyze one product but also for comparison between different technologies. In this case, an appropriate **functional unit** is be chosen to which all impacts are related to. Unusual for engineers, a functional unit need not be defined necessarily by a SI unit. Rather, a functional unit represents a reference value for once concrete application. This approach strengthens specific properties of investigated technologies in trade of general validity. Since an LCA is performed over the entire lifetime of a product, it is essential to consider the LCA a time frame of the use case. Impacts of the technology or product of interest are then shared among the whole time frame. Potential impacts can be measured by using different methods such as the Intergovernmental Panel on Climate Changes (IPCC) method for global warming potential (GWP) within the next 100 years or the cumulative energy demand (CED) which distinguishes between renewable and non-renewable energy. A complete LCA consists out of 4 stages [188]:

- goal and scope

- inventory of inputs and outputs
- impact assessment
- interpretation of results

4.2 Goal and Scope

The main objective of the LCA in this chapter is the **assessment of hydrogen in a modeled energy system** for the years 2017, 2030 and 2050 in Germany. This is done by defining the functional unit of 1 kg H_2 at 30 bar pressure under 5.0 quality, produced by PEMWE at 60 °C temperature. To estimate the environmental impact of hydrogen, electricity as one input source is derived from the presented energy system model of Chapter 3. The system boundary defines the input and output as well as all relevant system components which are included in Figure 4.1. Some of them are modeled on an inventory base and some with a considerable higher level of detail (LOD) as stated concisely in Table 4.1.

Table 4.1: Level of detail of modeling the PEMWE system components

Components	**level of detail**
stack	high (detailed Inventory list)
foundation	assessment of constructional engineering (TUM)
design	container 20 ft. standard
BOP	estimation
assembly	not taken into account[1]

[1] Information about the process in particular, for assemble the components are confidential and not shared by companies (email correspondence).

4.2.1 Electricity & scenarios

The LCA will be conducted for different scenarios stated in Table 4.2. As input data for the electricity mix, the share of energy sources is taken from the energy system model (Chapter 3). The reference case is the year 2017, with a corresponding power-plant mix. The year 2030 and 2050 are modeled with a reduction of 55% in CO_2 emissions and for 2050 with a 80% (KSZ80) as well as a 95% (KSZ95) reduction. As the electricity mix of the corresponding year is taken as input, the results can be interpreted as an assessment of hydrogen production in the corresponding year. The same methodology from Chapter 3 is used to differentiate between a constant production in base-load through the year, with 8760h full-load hours and a production based on the availability of renewable energy. For the latter, hydrogen from PEMWE is only produced when no fossil fuel is used for generating electricity. Consequently the specific CO_2 emissions of the electricity mix will be zero (See Figure 3.12), in case of the KSZ80 scenario. Here, a PEMWE could operate 3000h in the year 2050 on full-load capacity. Of course, the amount of full-load hours are calculated (similar to wind time-series) for every hour over the year as the utilization of the nominal capacity. This amount of hours result from the energy model for every scenario and is stated in Table 4.2. Since two different

Table 4.2: Share of electricity producing technologies in the corresponding scenarios. For every year, except 2017, it is split between operation in baseload and one only with electricity from renewable energy sources. This affects the hours of utilization

Scenario	Hours	Wind	PV	Gas	Coal	Lignite	Rest
baseload							
2017 (Reference)	8760	0.17	0.06	0.13	0.14	0.24	0.26[1]
2030 (KSZ55%)	2030	0.43	0.24	0.17	0.06	0.10	-
2050 (KSZ80%)	8760	0.39	0.21	0.40	-	-	-
2050 (KSZ95%)	8760	0.66	0.29	0.05	-	-	-
only renewables							
2030 (KSZ55%)	1000	0.65	0.35	-	-	-	-
2050 (KSZ80%)	3000	0.65	0.35	-	-	-	-
2050 (KSZ95%)	6500	0.70	0.30	-	-	-	-

[1] 7.2% biomass, 14.3% nuclear, 3.2% hydro-power, 1.3% waste

methods, energy system modeling and LCA, are combined in this chapter, there is a methodological question which has to be answered. This is especially important for the transition from the two extremes, fossil power generation to purely renewable power generation. The question is how the surplus power is to be rated. As shown previously in showed in Figure 3.11, each scenario has a decent amount of unused surplus power (negative area). In the following a method will be developed how to deal with this fact: It is assumed that every PV panel or wind turbine that is manufactured and installed, demanded for a certain amount of energy and material. Furthermore, the lifetime of PV and wind turbines will be handled in the was same as it was done for PEMWE. It is assumed, that power plants are designed for a certain lifetime, independent of their real operating time. With this approach, an installed solar system, even if not producing electricity has an impact on the life cycle analysis, but does not supply electricity to the PEMWE. In contrast, in case only the electricity that is used for the PEMWE would be considered, the impact of the solar system in the overall view would be omitted. For this reason, i) the whole energy system is considered to determine an electricity mix which is used for hydrogen production. ii) The ratio of the amount of electricity produced (regardless whether it is curtailed) by the different power plants is used in the following (as shown in Table 4.2). This procedure serves as a detailed explanation at this point to create the basis for correctly classifying later results of this chapter.

4.2.2 Impact categories

Two LCA methods are available to measure the effect of a technology: the endpoint and the midpoint. The difference is the length of the causal chain caused by a technology. The endpoint results shows the effect resulting from changes in e.g. ecosystem, human health or resource depletion but afflicted with uncertainty. So the endpoint tries to give an overall view where the midpoint method already had stopped before. In case of the midpoint method, specific impact categories are evaluated targeting a certain sector of interest. For instance "freshwater ecotoxicity" is such a impact category which is an indicator for the water quality. In the endpoint method, the impact of damaging the water ecosystem then leads to a decrease in population of animals and

finally might extinct an species. Whereas the midpoint method comes along with more specific impact categories to show the direct results of a technology to a specific sector such the depletion of water or metal. In case of this analysis, the midpoint method is used for comparing the impact of hydrogen from PEMWE with the SMR, which is today's standard for producing H_2. As the the dataset for SMR is not available in the Ecoinvent database 3.3, values of the different impact categories are taken from GaBi in that case. The following two impact categories will be discussed in detail: i) GWP and ii) metal depletion (MDP), as the former is focused on in recent debates and thus central aspect of this work. In contrast to conventional power-plants, renewable energy technologies often uses resource intensive materials (e.g. rare earth material, noble metals) which is covered by the MDP impact category. This is already an urgent topic, which is recently discussed for the technology of Li-ion batteries as the depletion of lithium has a big impact on rolling out BEVs [189], [190] and is also associated with additional environmental impacts [191]. A short description of these two impact categories is given below. In addition, a complete table of impact categories is stated in the Appendix in Table A.4.

- The impact category **global warming potential** (GWP) quantifies the effect of a product towards global warming. In the IPCC report [192], factors are determined, estimating the amount of heat, a greenhouse gas traps compared to an equivalent amount of CO_2 within a certain period of time. The absorption coefficient for infrared heat radiation and the duration of the gases which stay in the atmosphere are taken into account by this impact category. The potential for CO_2 is set as the reference value with a coefficient of 1, whereas methane has 25-times the effect as a greenhouse gas compared to CO_2. Typical time horizons are 20, 100 or 500 years and are indicated by an index. A time horizon of 100 is assumed for this LCA, which corresponds to the standard value if no index is given.

- **Metal depletion** (MD) as impact category for the midpoint method is normalized to the unit Fe-eq. measured in kg which describes the value of material which is used in reference to iron. With 163.000 $kg/kg_{Fe\text{-}eq.}$, platinum has the highest factor compared to iron with a factor of 1. But also beside the direct use of metals for construction purposes, some technologies such as nuclear-power-plants need uranium as fuel which is typically accounted as MDP [193]. Taking into account the recycling processes for some materials could significantly influence results regarding the metal depletion from extraction. However in this case, no recycling rate is considered as it lies out of the scope of this work.

4.3 Life-cycle inventory

Figure 4.1 gives an overview of the relevant system parts of a PEMWE which describes the boundary of this LCA. As a first step, purified water is fed into the system at the anode side with a conductivity below 0.1µSi/cm and pumped towards the cell stack. An additional purification unit is used to further reduce impurities of the water which would lead to a degradation of the stack. There, water is split into O_2 at the anode side and H_2 on the cathode side by applying a voltage. At the anode side water together with produced oxygen is led to a water-gas separator where the separated oxygen is

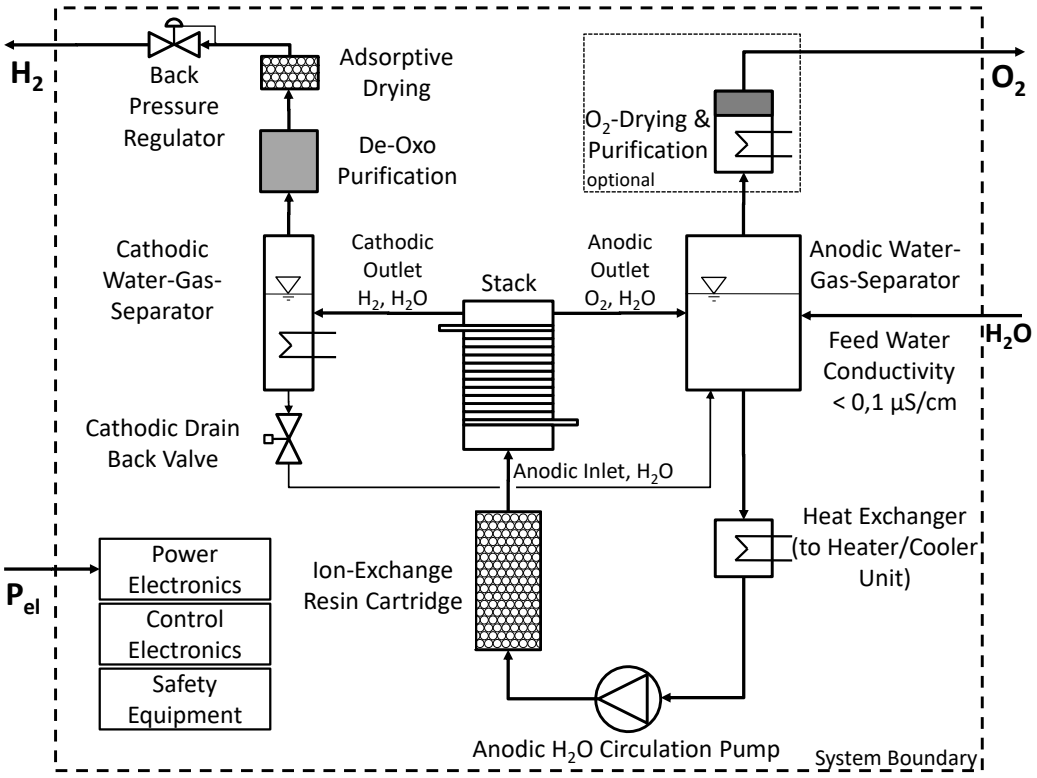

Figure 4.1: System boundary of the assumed PEMWE with all obligatory components used for the LCA [34].

blown off. In case of a business model[1] for oxygen it would be purified and dried in an additional process. As side effect, the decision of venting oxygen prevents an allocation problem as the product of interest will be solely hydrogen. The remaining water is added to the feed to minimize water loss and cooled down in a heat-exchanger. On the cathodic side hydrogen with water content is cooled down after leaving the stack and separated from water. Water loss is kept to a minimum by returning the separated water from anode and cathode back to the feed.

4.3.1 Hydrogen purification

After hydrogen passes the water-gas separator on the cathodic side, hydrogen is still saturated with water vapor as expected for the vapor pressure, defined by the temperature of the water-gas separation unit. The purity of hydrogen needs to meet industry grade, as described in Chapter 2.3.4. Thus, additional expenditure has to undertaken to guarantee purity. In the following, the amount of water remains is calculated to estimate the energy needed for removing the oxygen part in the H_2O. The absolute humidity which remains in the mixture is calculated by the gas-law in eq. 4.1 as proportion of vapor in the produced hydrogen at 30 bar. An ambient temperature of 20 °C is assumed which leads to a water-pressure of 23 mbar [194]. Thus the share of water

[1] The question of a business case was discussed during project meetings. According to process engineers, producing concentrated oxygen would lead to safety issue which does not meet an economic business in this particular case

which remains in hydrogen still amounts to 770 ppm or 7 g water per 1 kg of hydrogen. Corresponding to the water vapor pressure, the hydrogen is treated by a purification system which reduces the oxygen content to less than 5 ppm to fit the 5.0 standard.

$$\frac{m_{\mathrm{H_2O}}}{m_{\mathrm{H_2}}} = \frac{\frac{p_{\mathrm{H_2O}} \cdot V \cdot M_{\mathrm{H_2O}}}{R \cdot T}}{\frac{p_{\mathrm{H_2}} \cdot V \cdot M_{\mathrm{H_2}}}{R \cdot T}} = \frac{23\mathrm{mbar} \cdot 18\mathrm{g/mol}}{30,000\mathrm{mbar} \cdot 2\mathrm{g/mol}} = 6.9 \cdot 10^{-3} \tag{4.1}$$

Besides the water content, some oxygen impurity will remain in the gas, which is removed by a de-oxo purification unit. According to Trinke et al. [195] the oxygen impurity is stated with 800 ppm which is approximated by the water vapor pressure of roughly 24 mbar at 20 °C ambient temperature. A de-oxo unit removes the oxygen by forming water in a catalytic recombination. The volume of 1 kg H_2 at 30 bar pressure is calculated by eq. 4.2 to 0.4m³.

$$V_{\mathrm{H_2}} = \frac{n_{\mathrm{H_2}} \cdot R \cdot T}{p_{\mathrm{H_2}}}$$
$$0.4\mathrm{m}^3_{\mathrm{H_2}} = \frac{\frac{10^3\mathrm{g}}{2\mathrm{g/mol}} \cdot 8.31\frac{\mathrm{J}}{\mathrm{mol \cdot K}} \cdot 293\mathrm{K}}{3 \cdot 10^6\mathrm{Pa}^2} \tag{4.2}$$

The content of oxygen in 1 kg H_2 is calculated by eq. 4.3 to 0.4 mol. As 2 mol of H_2O is formed by 1 mol of O_2 during the catalytic recombination in the de-oxo unit (eq. 4.4), roughly 15 g of water is formed due to the water content (0.4 mol of O_2 leads to 0.8 mol of H_2O per 1 kg of H_2). Thus approximately 14 g H_2O, calculated in eq. 4.5, has to be added to the 7 g water from the gas-water separator. This will happen in a following adsorption process.

$$n_{\mathrm{O_2}} = \frac{p_{\mathrm{O_2}} \cdot V_{\mathrm{H_2}}}{R \cdot T}$$
$$0.4\mathrm{mol}_{\mathrm{O_2}} = \frac{24\mathrm{mbar} \cdot 0.4\mathrm{m}^3_{\mathrm{H_2}}}{8.31\frac{\mathrm{J}}{\mathrm{mol \cdot K}} \cdot 293\mathrm{K}} \tag{4.3}$$

$$\overbrace{2\,\mathrm{H_2O}}^{2\text{ mol}} + \overbrace{\mathrm{O_2}}^{1\text{ mol}} \longrightarrow \overbrace{2\,\mathrm{H_2O}}^{2\text{ mol}} \tag{4.4}$$

$$m_{\mathrm{H_2O}} = n \cdot M = 0.8mol \cdot 18\frac{g}{mol} = 14.4g \tag{4.5}$$

Usually, de-oxo units are a combination of the catalytic recombination process and a device for subsequently drying the water. This unit works typically with silica gel as an adsorbent. As silica gel is not included in the Ecoinvent database, material and energy input is taken from literature [196] and modeled. Typically two separated tanks

[2] 1 bar ≙ 10^5 Pa

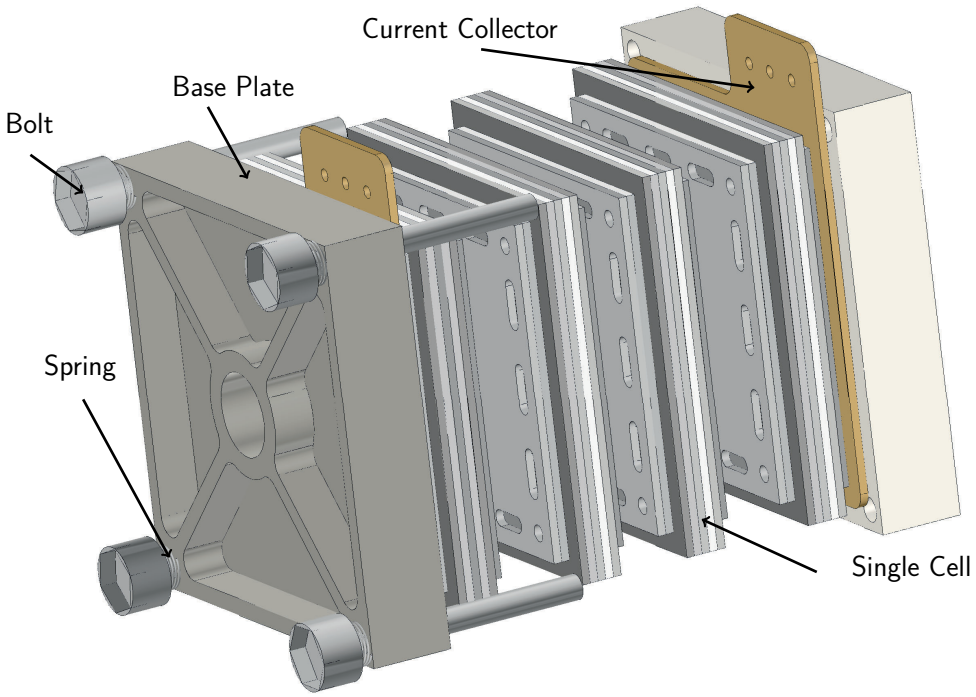

Figure 4.2: Sketch of a PEM stack with several single cells connected in series.

of silica gel are used for a de-oxo purification unit. When the silica gel in the first tank is saturated with water, the gas-stream is switched to the second tank, meanwhile the first tank is dried by baking. Between 7,100 and 8,400 kJ are needed to evaporate 1 kg of H_2O from silica gel [197] which results in an energy demand of 0.05 kWh per 1 kg of dried H_2.

4.3.2 PEMWE stack

The stack, shown in Figure 4.2, is the core part of an electrolyzer and is modeled in detail for this LCA. Typically a system in a GW range is a combination of multiple single cells in series which than builds up a stack, as shown in Figure 4.2. In the middle of each cell the membrane electrode assembly (MEA) is located which consists of the gas diffusion layer, the catalyst layer and the polymer electrolyte membrane which allows only the H^+ ions to pass through. The MEA is embedded in between the two electrodes (anode, cathode) with current collectors, mainly made out of copper or aluminum [198]. Endplates made of steel or aluminum are designed relatively thick, unlike the other cell components, and hold the single cells tight together. The compression over a typical lifetime of 40.000-60.000 hours is ensured by several bolts and flat springs [78]. Future lifetime of PEM-stacks is assumed to extent up to 90.000 hours as new materials will substitute the PtL and MEA which are prone to degradation [199]. Cell efficiencies are stated with 70% at 1.79 V cell voltage and 1.5 A/cm² current density today [67]. The overall system efficiency is reduced due to further utilities by 10 percentage points to 60% [67]. A comprehensive overview of all current and estimated system parameters for the future are listed in 4.3. A reduction of catalyst loading for the next years is assumed

Table 4.3: Current and estimated near future PEMWE system parameters

parameter	**2017**	**2030+**
cell voltage level (V)	1.79	1.79
current density (A/m²)	1.5	3
power density (W/m²)	2.7	5.4
η_{cell} (LHV)	0.7	0.7
η_{system} (LHV)	0.6	0.6
Anode Ir. loading (mg/m²)	2	0.2
Cathode Pt. loading (mg/m²)	0.2	0.05
Ti. bipolar plate thickness (mm)	3	0.3
Membrane thickness (µm)	200	50
Single cell format (m²)	500	1000
Stack lifetime (years)	7	10
BOP lifetime (years)	20	20

as similar to today's stack efficiencies. Potential of improvement on the cathode side is taken from literature [200], showing that platinum loading could be reduced from 0.2 mg_{Pt}/m^2 today down to 0.025 mg_{Pt}/m^2 without significant losses in performance. For the future this reduction is modeled by using a security factor of 2 as this reduction potential is not validated so far. From the view of rolling out this technologies and scaling capacities up to GW scale, the reduction of used materials from Pt-groups is crucial as these noble metals are very rare. The amount of mined Iridium, that is used at the anode, is directly linked to the platinum mining as a byproduct. The availability of Iridium was stated in 2017 with approximately 4 t/a [201] on the market. Bernt [200] shows that a reduction of 90% iridium in the stack is possible without any losses in performance. The amount of cell material and the number of cells in the stack were calculated in the current P2X project and are stated in Table 4.4. The total active cell area is assumed with 37 m² for a state of the art 1 MW electrolyzer and 18.5 m² for a future design as current density is assumed to be doubled. The active area[3] for a single cell, as sketched in Figure 4.3, is expected to increase from 500 cm² to 1000 cm² per cell in future. Beside the reduction of cost intensive materials such as titanium, iridium, platinum and Nafion®, the amount of copper and aluminum will increase due to the higher cell area [34].

4.3.3 Further facility components

Literature on the amount of material used for the facility and auxiliary devices is very limited. Inquiries to companies turn out to be difficult as most of these information are confidential and therefore not shared by them. Hence most materials need to be estimated, as only some parts, such as the de-oxo unit are available as blueprints. Further parts are needed for an operation of the PEMWE such as power electronics (rectifiers, transformers), safety equipment and control devices. It is assumed that the whole system fits into a standard 40-ft container, that is primary made out of steel and is based on a foundation shaped in 4 concrete blocks with a 1m² size, 0.25m depth

[3] the active are describes the part which is actually used e.g. for reactions, not taking into account additional space which is needed for mounting

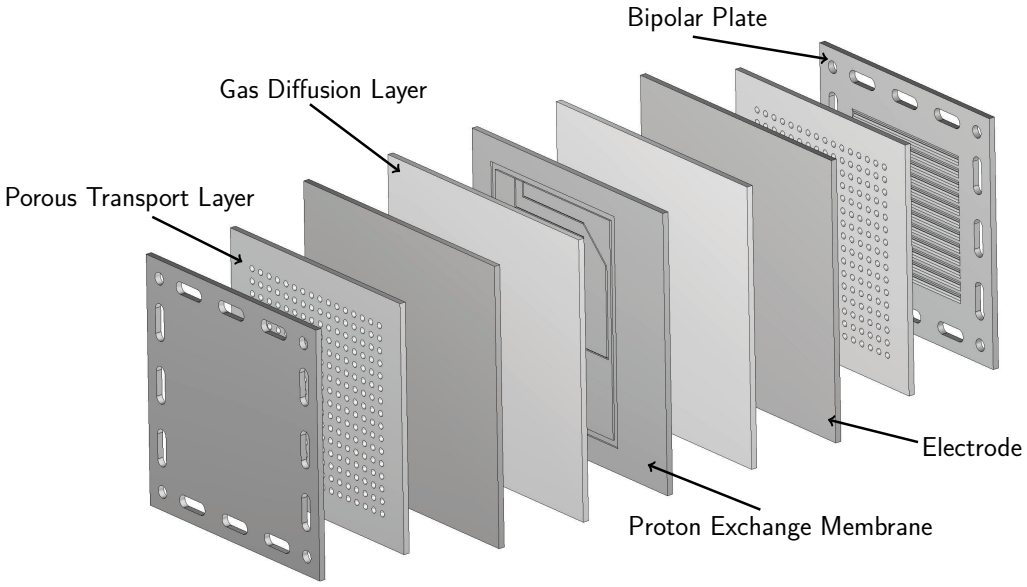

Figure 4.3: A single cell of a PEM-stack drawn as exploded view with the different layers.

Table 4.4: Materials for a 1 MW PEMWE stack, state-of-the-art and near future

Material (kg)	**2017**	**2030+**
Titanium	528	37
Aluminum	27	54
Stainless steel	100	40
Copper	4.5	9
Nafion®	16	2
Activated carbon	9	4.5
Iridium	0.75	0.037
Platinum	0.075	0.010

and a total mass of 5.6 t. The lifetime of the system is set to 20 years. However the stack is set to 7 years lifetime and improves to 10 years for 2050. A summary of the aggregated materials of the BOP is stated in Table 4.5.

4.4 Life cycle impact assessment

When performing a LCA, the ecological evaluation of a modeled product compared to its alternative manufacturing processes is of particular interest. In order to perform this assessment, the life-cycle-impact assessment (LCIA)defines impact categories by which the material flows with their upstream process chains are converted into potential environmental impact on the basis of the inventory list. Typical evaluation criteria are the GWP or the CED, but these categories are strongly dependent on the subject of interest. The LCIA helps to interpret the results of a modeled system by evaluating in a standardized way. Thus it also enables the comparison of a product, regarding the impact categories, with a reference system. Consequently LCAs are, beside energy

Table 4.5: Additional materials for a 1 MW_{el} PEMWE

Material	**Mass (t)**
Low alloyed steel	4.8
High alloyed steel	1.9
Aluminum	< 0.1
Copper	< 0.1
Plastic	0.3
Electronic material (power, control)	1.1
Process material (adsorbent, lubricant)	0.2
Concrete	5.6

system modeling, another tool that can help politicians in making decisions. Already by describing these two impact categories, it is obvious that the electricity mix is essentially influencing the results of this LCIA. Thus the electricity mix for all scenarios are based on the energy model from previous chapter 3. The LCA model is run seven times with different CO_2 constraints, referring to the climate goals of Germany [41], as explained previously. In the following, the scenarios stated in Table 4.2 are taken to evaluate the impact categories. As lifetime is measured in years, it is assumed, that a reduced amount of full-load hours per year will not afflict the lifetime. Thus reduced full-load hours will lead to a higher influence of the PEM-stack and BOP per kg of produced H_2, as less hydrogen is produced over lifetime. This effect can be observed in the Figure 4.4 and is depicted more precisely for 1000 full-load hours, with renewable energy, in the scenario for the year 2030. But still with this approach, the impact of the BOP and PEM-stack for the category of GWP is negligible compared to the used electricity. The GWP is plotted on the y-axis in the unit of kg CO_2-equivalent (CO_2-eq.) per FU (1 kg H_2). On the x-axis the amount of full-load hours per scenario, as well as the corresponding year, are stated. It is clearly visible, that electricity has the main impact in respect to the global warming potential of 1 kg hydrogen from PEMWE, which makes sense as per 1 kg hydrogen at least 55.5 kWh electricity are required. The GWP in the year 2017 got the highest value with 29.5 kg CO_2-eq. per 1 kg H_2, as still significant amounts of fossil fuels such as coal, gas and lignite are used for electricity production. It is obvious that with the phase-out of coal until 2038 the carbon footprint of the electricity mix is improving and that this impact category, which is here related to electricity, strongly abates over the years. For hydrogen production, based purely on renewable electricity, the GWP lies between 3 and 4 kg CO_2-eq. per 1 kg H_2 at the cost of a drastic reduction in full-load hours. However this scenarios is three times more environmental friendly than that of the reference process (SMR). As marginal costs of the produced hydrogen decreases with an increased utilization of the PEMWE, a realistic industrial use cases of PEMWE is a base-load operation in the year 2050, either with a 80% or 95% CO_2 reduction. When carbon emissions are reduced by 80% in the energy sector, the GWP of the PEMWE is equal to that of reference process. A 95% CO_2 reduction will even lead to one-third of that of the reference case due to the rare use of CCGT in the electricity mix.
In Figure 4.5 the MD for individual scenarios according to BOP and Electricity for PEMWE is shown as they are calculated by SimaPro. An increased MD value for

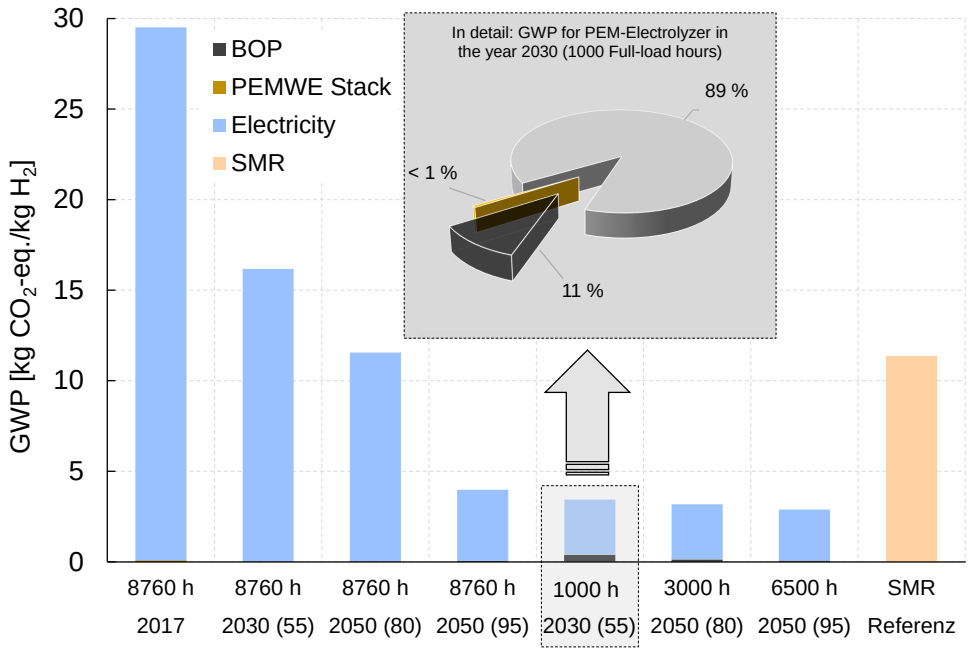

Figure 4.4: Global warming potential (GWP) of producing 1 kg H_2 with PEMWE in different scenarios

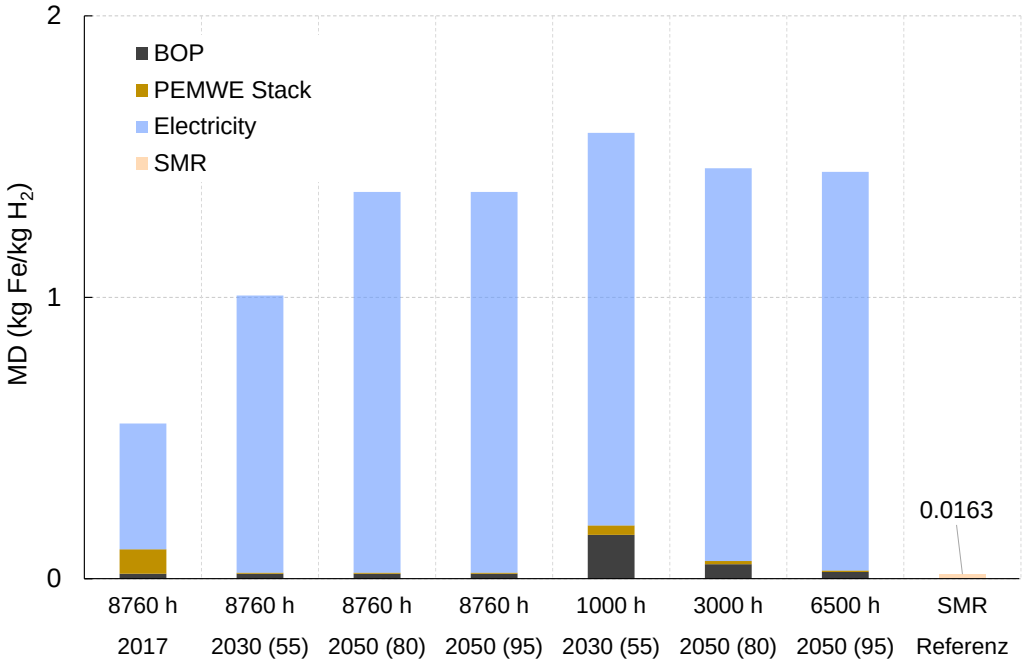

Figure 4.5: Metal depletion (MD) of producing 1 kg H_2 with PEMWE in different scenarios

the BOP and the Stack can be clearly observed for the year 2017, which results from the high demand for platinum, iridium and titanium. These materials will be greatly reduced in the future years by improvements of the stack. The reference value for the SMR is stated with 0.02 kg Fe/kg_{H_2} from GaBi database, which is a comparable low value. For the year 2030 with 1000 hours the impact of MD is again significantly higher for the BOP and the stack. However it is not expected that the total MD increases over the years, as this behavior is converse to that of the GWP. A analysis of the cause of the increase in MD revealed, that electricity is a main driver. This observation leads to a further investigation of the electricity mix used in the different scenarios.

Figure 4.6 visualizes on the x-axes the impact categories for a representative selection of all scenarios used in this chapter. On the y-axis the share a power plants contributes to this impact category is given. Following impact categories[4] are included in the Figure - Global warming potential (GWP), Ozone depletion (OD), Terrestrial acidification (TA), Human toxicity (HT), photochemical oxidant formation (POF), Particular matter (PM), Metal depletion (MD) - which are typically subject of interest in available LCAs [203]. Results are very different for each electricity mix, as Lignite for example contributes with half of the total GWP of the electricity mix in the year 2017. Whereas in the year 2050 under baseload condition nearly 90% of the ozone depletion (OD) cause by CCGT. Another often discussed category in context with traffic, is the particular matter (PM), as it directly afflicts humans health, especially in inner cities [204].
Regarding the MD, a uniformity is observed for the different scenarios, as wind contributes with the highest share and PV as the second. This is surprising since wind only contributes with a share of 17% on the total electricity mix, used in the model for the year 2017 (see Table 4.2). As this depiction only shows the share a power plant contributes to one 1 kWh, the absolute numbers are plotted in Figure 4.7. It is obvious, that in scenarios with less renewable technologies, the absolute value for MD is noticeable smaller. It can be stated, that Wind an PV are the main drivers for metal depletion in scenarios with a high share of installed capacities of renewable energy technologies. The highest value can be observed in this case for the KSZ80(3000h) scenario, as the energy system contains a share of 65% from wind an 35% from PV. The value for the reference case in the year 2017 is the lowest, as only few renewable energy technologies are available in this system. This coincides with the observation made regarding the impact of 1 kg of hydrogen in Figure 4.5.
According to Chen [205], the production of solar cells need conductive paste which is made out of silver (Ag-paste), gold contacts, iron, zinc and energy which are the main drivers of MD. In the case of wind turbines, copper is mainly used for the generators, aluminum, iron and nickel are used for the tower and nacelle and mainly iron for the rotor blades [206], [207]. Thus, the strong increase in metal consumption for the scenarios with high proportions of energy from PV and wind turbines is justified.

4.5 Interpretation of LCA results

The used electricity is the biggest driver for almost all impact categories, stated in the Appendix in Table A.4, of the PEMWE. While life cycle-related greenhouse gas emissions (kg CO_2-eq.) strongly decrease with an increasing amount of renewable elec-

[4]Further information about the method of each impact category is available online [202]

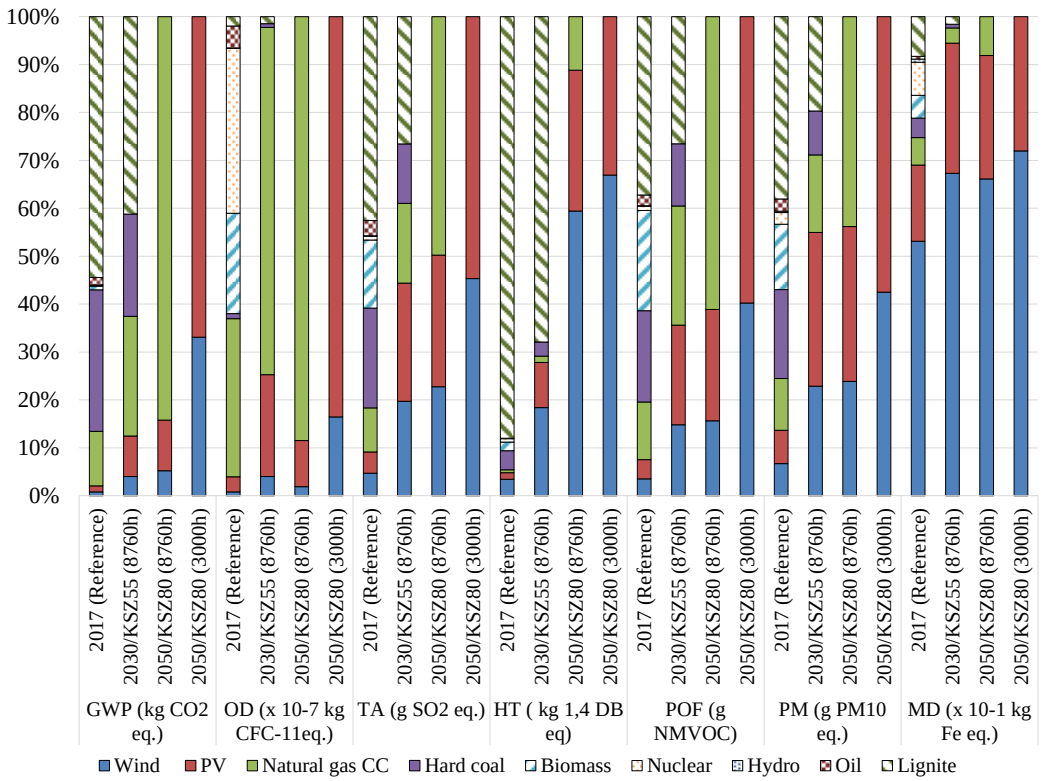

Figure 4.6: Composition in percentage of the different power plants onto the investigated impact categories for 1 kWh electricity of a selection of scenarios.

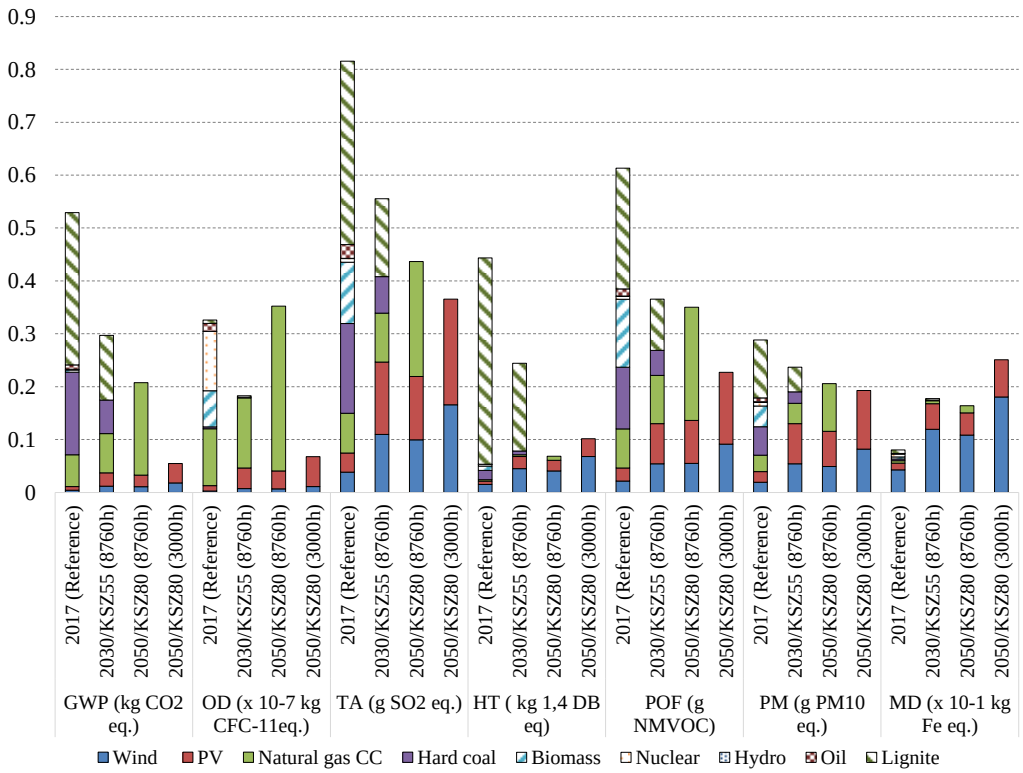

Figure 4.7: Absolute values of power pants contributing to the impact categories, for 1 kWh electricity, in selected scenarios.

tricity, this correlation is reversed for the indicator metal depletion (MD) and the use of critical raw materials such as iridium. The reason lies in both, the construction phase of the PtX technology "PEMWE" itself as well as the use phase. In PtX technologies, catalysts are typically more often used than in their reference processes [30]. These catalysts are based on rare materials such as iridium, platinum which have a very high metal depletion potential, represented by a high factor in Fe-eq. This is an important topic concerning today's innovative technologies, that needs to be addressed. Bernt [200] estimated, that a yearly PEMWE installation of 150 GW would be needed to play an role in worldwide fossil energy demand in the transportation sector. Currently, this energy demand is stated in the order of 100 EJ (1 10^{20} J). With an average life of 10 years, an average installed capacity of 1.5 TW of PEMWE is feasible. Assuming a production on full capacity at 60% system efficiency 8 PWh (30 EJ) hydrogen will be produced, which is roughly 1/3 of the global energy needed for transportation. In combination with other technologies such as BEVs this might be a possibility to substitute worlds fossil fuel demand in transportation.
However, this is only achievable with a drastic reduction in the use of rare materials. The same problem is already been faced with the use of batteries for battery electric vehicles. Different studies complain of the increasing demand in lithium as well its associated impact from mining [189]. With a reduction in the use of noble materials, the impact of BOP and the stack decreases, as platinum group materials and titanium are the main driver. Both of them are reduced by 90% until 2030 (see Table 4.4).
Regarding the use phase, wind and solar energy do not have any direct CO_2 emissions,

so that any GHG emissions here can be attributed to the construction of the plants and thus the upstream chains. In contrast, energy supply based on fossil fuel from conventional power-plants is consumption-based, as for every kWh of produced energy a certain amount of CO_2 is emitted from the combustion. Thus GWP decreases for the different scenarios in future, especially for those which purely run on renewable-energy. However in this case the metal depletion rises, as wind and solar power plants are more complex and uses more metal per kWh electricity output over lifetime, compared to fossil power-plants. Of course this is also related to on utilization far below base-load, as the availability of wind and solar irradiation define the utilization. As a consequence, the impact categories of electricity from wind farms and PV would decrease, for locations with more full-load hours than those in Germany. In addition, the electricity mix which is used for manufacturing renewable energy technologies, determines their CO_2 footprint. This will then influence directly the GWP for hydrogen produced by PEMWE.
As the datasets of Ecoinvent are very detailed and complex, changes of whole value-chains are very limited and can only be conducted on the top level, such as the assembly part of a process in a reasonable amount of time. The structure of the database is a tree and pulls information from several thousands of different data-blocks, each with a very small share of its overall impact. However, these small shares sum up to a significant value (see Figure 5.1) especially for renewable energy technologies. With the course towards a sustainable and renewable energy system, the electricity mix will change significantly over time as this is the implied goal. This is a very important fact as data which are valid for today's applications might change in future. Thus it can be inferred, that conducting a LCA, in they it is currently done, may not be the right method to estimate impacts of technologies in future, as they are mainly defined by their electricity consumption. However it can be said beyond controversy, a radical change in the energy system will affect the production of energy-intensive materials and thus the indirect emissions of renewable energy technologies. The following Chapter 5 investigates this issue for further discussion in depth with a **novel approach**.

5 Integrating LCA to energy system modeling for PV production

The importance of energy system modeling tools was described in the previous Chapter 3. The purpose of such a tool is to point towards a feasible direction for how the "Energiewende" can be successfully accomplished while keeping costs and CO_2 emissions low. In energy system modeling usually only **direct emissions** from burning fossil fuels are considered as CO_2 emitting source. Therefor, renewable energy alternatives such as photovoltaic-systems and wind parks are not classified as climate damaging technologies. The approach of conducting a LCA, in contrast, is different to a energy system modeling tool, as material and energy expense of the whole life-cycle is assessed.

Few studies on energy system modeling tools identify the output of **indirect emissions** which are emitted during the upstream process, such as the manufacturing, refining or even the energy supply phases which contribute to the overall CO_2 emissions. MCDowall's study [208] however, integrates indirect CO_2 emissions into his European energy model for wind turbines in the tool TIMES, as a fixed value, per kWh electricity. Consequently he identified, that the optimal power plant mix of the model result is changing as energy from renewable technology is less attractive. Although his study has taken into consideration the entire life-cycle of CO_2 emissions, fixed values were applied for these emissions which limits the significance of this important approach. It can be argued, that with the development of more efficient electric supply, the life cycle process would also become more CO_2 efficient. Therefore these values should not be modeled fixed, but rather as variables. Dufo-López [209] uses a multi-objective function approach to minimize levelized costs of electricity (LCOE) as well as CO_2 emissions resulting into a Pareto front. Here renewable technologies are introduced as having CO_2 emissions also set as a constant parameter, and not as variable, which was also carried out by You [210]. Pehl [211] further develops this point and changes indirect emissions of different technologies in a separate model and introduces them into an optimization model as constant values for different years.
In this chapter a novel approach is presented which allows the model, introduced in Chapter 3, to reduce the environmental impact of renewable energy technologies by improving the endogenous electricity-mix. This was modeled using photovoltaics systems as an example identifying emission output mainly from silicon treatment.

5.1 Direct and indirect emissions

The Ecoinvent database used for the LCA in Chapter 4 includes information such as manufacturing processes, material and energy demand for different technologies. Bases on the origin of these emissions it can be distinguished between two fundamentally different types:

- indirect emissions: These emissions are related but not limited to upstream-processes during manufacturing such as e.g. mining, distributing or construction phase. Basically, emission occur over the whole value chain of an entity. In the case of producing steel, iron ore needs to be mined, for which heavy duty vehicle as well as a refinery and workshop for tools are needed.

- direct emissions: These emissions occur during the final conversion step of an given input to a functional unit. In the case of power-plants the functional unit will be calculated in kWh electricity. In this case the emissions are based on the combustion of fossil fuels, from which emissions occur based on the stoichiometry and the efficiency of the plant.

In case of the conventional power-plants only the emissions from burning fossil fuels are plotted in Figure 5.1 as they are included in the energy system model and are responsible for the majority of GWP. As e.g. coal mainly consist out of carbon, its is not surprising that 96% of GHG emissions derive from the combustion process in a coal-fired power plant [212]. In contrast to conventional power plants, the direct CO_2-eq. of renewable energy technologies are zero as no burning of fossil fuels takes place. However the figure leads to the conclusion, that renewable energy has a significant CO_2 footprint that originates from their whole life-cycle. This is specially evident in the production of PV systems as it is a very energy-intensive process and therefore results are highly susceptible to changes in electricity supply. taking into consideration the points that were discussed, modeling future energy systems without indirect emissions, but with the expectation of a significant change in that modeled energy system, is worth a discussion. The energy system model which was already presented in chapter 3, is extended by a dynamic process for **photovoltaic solar cells** based on multicrystalline silicon (mc-Si) wafer by modeling parts of the manufacturing process. The specific CO_2 emissions for electricity from PV-systems in Germany is stated in the ecoinvent database with 0.1 kg_{CO_2}/kWh. In advance, a short analysis of the exported data revealed that this value is cut in half, when all emissions with the keyword: "electricity" are neglected. However this is a rough estimation, as some processes involving electricity demand are embedded within subcategories which are untraceable and therefore cannot be extracted.

5.2 State of the art multi-crystalline PV manufacturing

The process of producing solar grade silicon (SG-Si) from silicon-dioxide is a well-established technology which is done in industrial scale. As facilities for this mature process are planed for decades, no conceptual changes are done in manufacturing. [213, 214]. An overview of the necessary processing steps is given in figure. 5.2 where the pathway from raw material SiO_2 to the final product, the silicon wafer is, depicted.

5.2.1 Carbothermic reduction

The initial process step silica undergoes, is the carbothermic reduction. In this step the feedstock is purified to metallurgical grade silicon (MG-Si) [215]. This is carried out by treating silica with coal mixed in a large crucible to reduce oxide from silica

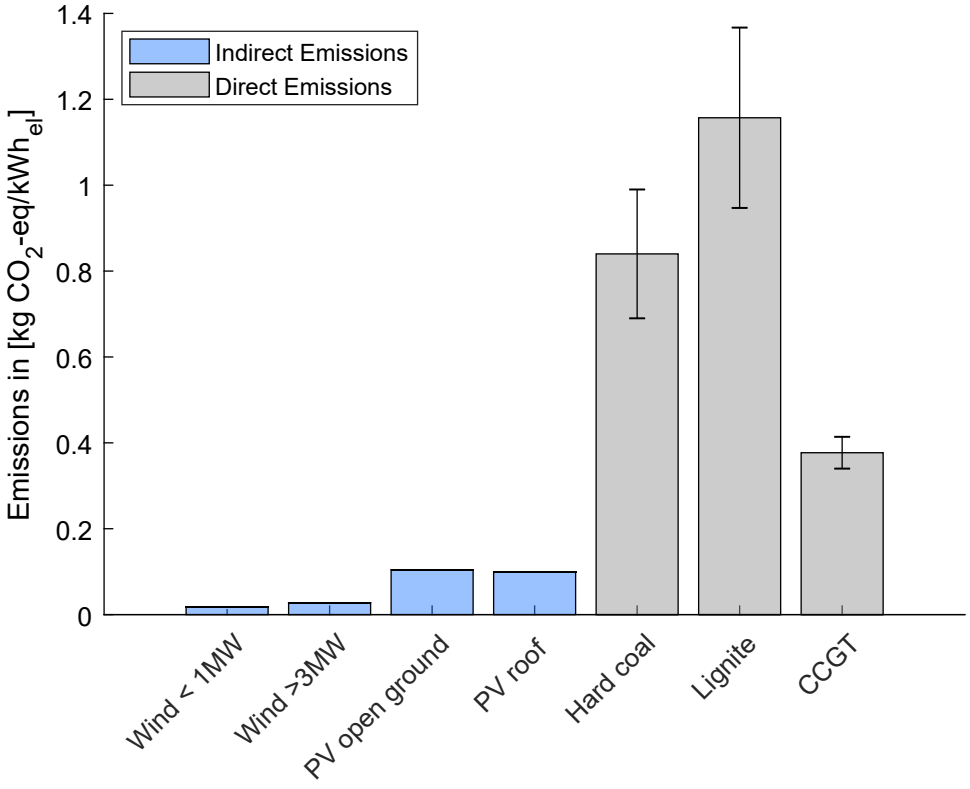

Figure 5.1: Green-house-gas emissions per kWh electricity produced by different technologies in Germany. Indirect emissions for renewable technologies are taken from ecoinvent database 3.3 using Recipe method. Direct emissions for conventional power-plants are calculated from combustion only with a range of their efficiency

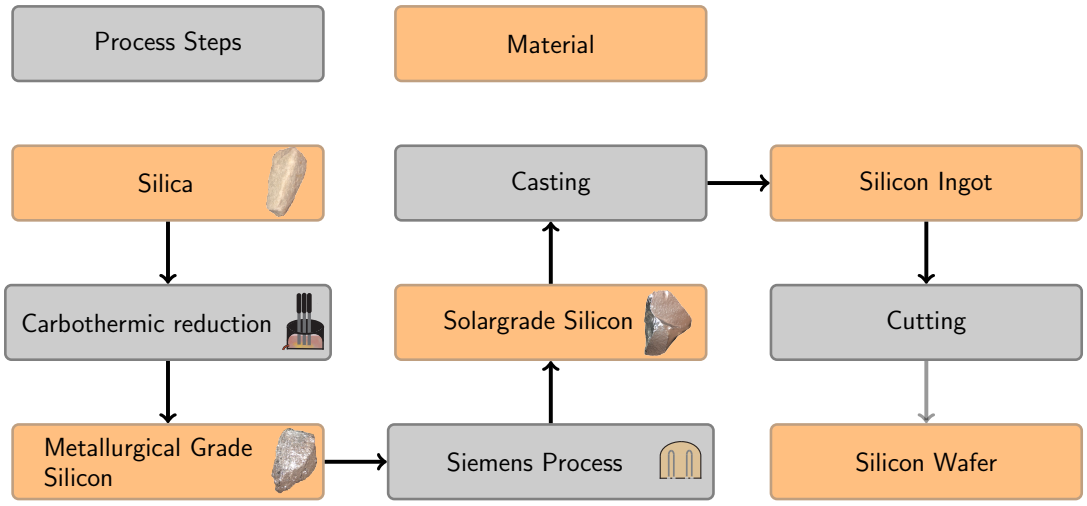

Figure 5.2: Silicon processes and material steps: The gray shaped boxes indicate process steps whereas the orange colored boxes describe the material property

(SiO_2) then to silicon with carbon as reducing agent under the following reactions:

$$SiO_2 + C \longrightarrow SiO + CO \tag{5.1}$$

$$SiO + 2\,C \longrightarrow SiC + CO \tag{5.2}$$

$$SiC + SiO \longrightarrow 2\,Si + CO \tag{5.3}$$

It is understood, that the resulting carbon monoxide from eq. 5.1-5.3 leads to CO_2 when exposed to the atmosphere. In addition, electric arcs supply the heat with electricity and the CO_2 emissions are dependent on the electricity source used. Typically, three electrodes are submerged into the crucible and the electric ground is located at the bottom. Liquid silicon at temperature of above 2000°C starts to accumulate in the inner zone of the furnace while other components gather at the outer zone [216]. The liquid metalloid is then poured into the container with impurities in the silicon (between 10% - 20%) [217], which would then require further refining. The silicon is treated in liquid phase enabling elements, less noble than silicon, to react with the remaining oxygen and float to the top as slag. The purified silicon is tapped and flows into casting molds, where it cooled and solidifies as mc-Si. It is subsequently crushed for further treatment [218, 219].

5.2.2 Purification of metallurgical grade silicon

For photovoltaic and semiconductor applications, impurities must not exceed a concentration in the rate of parts-per-billion (ppb). This is achieved with several different approaches, though only some are industrialized, while other processes became outdated or lost economic competitivity [220, 221]. Among them, the Siemens process is the most common technology for purifying MG-Si to produce mc-Si as end-product. It accounts for the majority of the produced mc-Si but also 50% of the total energy consumption of the SG-Si production [222, 223]. First, trichlorosilane ($SiHCl_3$), a mixture from metallurgical grade silicon and hydrochloric acid (HCl) is created. Next, the

mixture is purified by by fractionally distilling twice. In the first run, heavier components resulting from direct synthesis are removed and in a second run, all components that are lighter than trichlorosilane are extracted. In order to obtain pure silicon, trichlorosilane has to be decomposed back into silicon and hydrochloric acid. Therefore trichlorosilane is vaporized, diluted with hydrogen and then fed into deposition reactors, where the silicon deposits onto silicon rods while the stream of byproducts leaves the reactor. Besides, alternative processes exists that produce silicon of high purity at different process complexities, while partly avoiding the usage of harmful material $SiCl_3$. However, the current overall energy consumption does not vary significantly among different approaches [224, 222, 225, 226, 227].

5.2.3 Casting and cutting

Silicon is removed from the rods, causing it to break. However, the production of wafers for solar panels requires perfectly shaped structures, out which thin slices can be cut. The silicon chunks obtained from the rods are further melted and then cast as ingots. During the casting process, the grade of silicon can easily be decline by contamination through impurities [228]. Finally, the solidified silicon blocks from the cast are cut into thin slices. The most common technique to cut multi-crystalline as well as mono-crystalline silicon is wire slicing. The wire used for this process step is very thin and has an abrasive surface. Newer developments aim to decrease kerf losses and enhance the surface quality, as well as to reduce the need of chemical coolants and lubricants [229].

5.3 Hydrogen as reduction agent for SiO_2

From eq. 5.1-5.3, it is obvious that the carbothermic reduction, using coal as a reduction agent, will lead to CO_2 emissions. A similar process based on coal is also used for reducing iron ore in steel industry, where significant progress has been made to enable substituting coal with hydrogen in recent years. Considering this alternative process for reducing iron ore leads to the investigation whether substituting coal with hydrogen is possible in the production of solar grade silicon. The Ellingham-Richardson diagram is a tool to depict stability in terms of thermodynamic equilibrium [230]. Usually, coal is used for reducing the different types of iron-oxide at temperatures around 600 °C which is indicated by the intersection (C) between the brown and the thick black curve in Figure 5.3 (marked with a red circle). From the perspective of this diagram, the thin green hydrogen curve ($2\,H_2 + O_2$) is close to the iron oxide route ($2\,Fe + O_2$) and could be used as reduction agent around 1700 °C. The thick orange colored silicon ($2\,SiO + O_2$) route clearly shows the intersection (A) with the commonly used route of carbon reduction agent at 1600 °C. In contrast, no intersection between the silicon route and the hydrogen route can be observed, meaning that H_2 does not work as a reducing agent in this range of temperature [231]. From this point of view, SiO_2 cannot be reduced theoretically by using gaseous hydrogen even at high temperatures. However, conditions change when a sufficient proportion of the hydrogen is shifted to plasma state plotted as the thick green line (H_2+2H+O_2). The reduction potential of hydrogen in plasma state increases to such extent that it intersects with the silicon line as seen in the diagram marked with a (B). This demonstrates the theoretical possibility to reduce SiO_2 to MG-Si using a hydrogen plasma. The notation $2H + H_2$ on the reactant side of

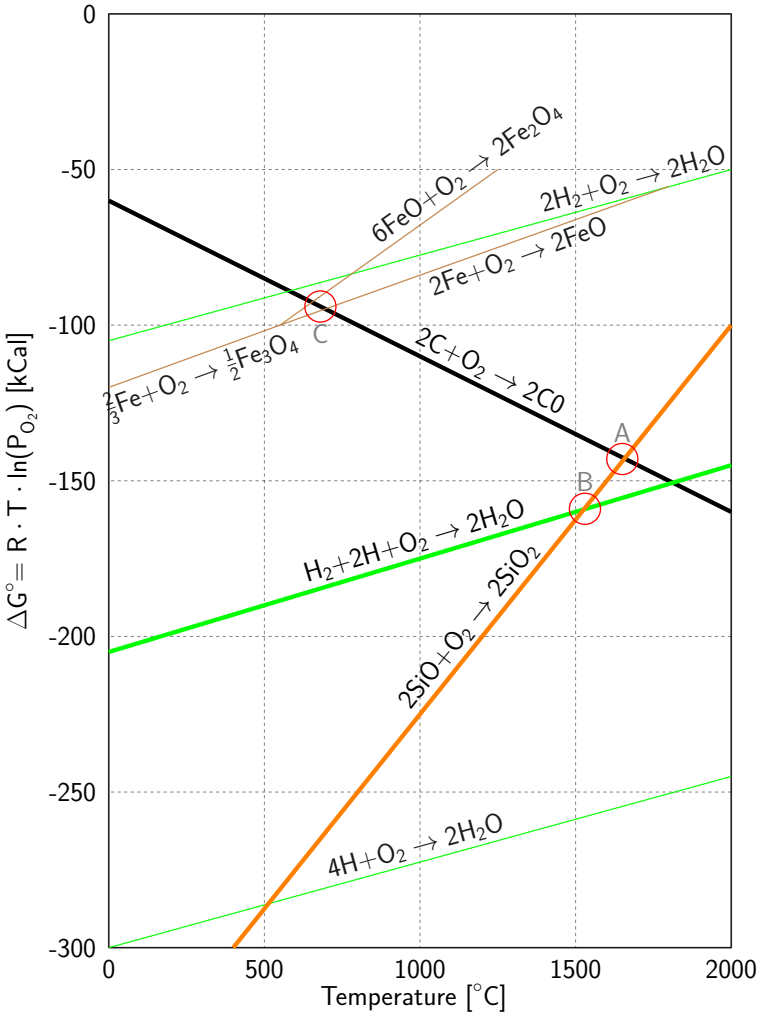

Figure 5.3: Ellingham-Richardson Diagram. The free energy line for $H_2 + {}_2H + O_2 \longrightarrow 2\,H_2O$ is tentatively drawn in the middle between the full plasma 4H and the hydrogen $2H_2$ based reactions. Its exact position depends on the details of the plasma process used. The intersection with the silica line for the formal reaction in eq. 5.4 lies in the correct temperature regime even with this simplistic assumption.

eq. 5.4 indicates that thermodynamically, the cleavage of a single H-H bond is sufficient to drive the reaction:

$$SiO_2 + 2\,H + H_2 \longrightarrow Si + 2H_2O \tag{5.4}$$

So far, this method is not being used in industry, although there are already patents and investigations ongoing [232, 233]. Laure [234, 235] proved in recent DBU projects, the feasibility of this process by successfully reducing SiO_2 with a hydrogen-argon plasma. For In this project, silica-oxide is fed into the plasma reactor as grains with a size of 40-80 µm. The plasma stream heats the SiO_2 grains to such an extent that the thin surface melts. A Figure 5.4 depicts the inside of such a silicon reduction plasma reactor. By using hydrogen-plasma no CO_2 emissions occur from the reduction process directly, whereas the reference process with coal creates 3 units of CO for 2 units of Si as stated in eq. 5.1-5.3. Assuming that the carbon monoxide is released to

the atmosphere without further treatment, 2.36 kg CO_2 per 1 kg of Si are emitted. As stated by Demin [236], 44 kg of MG-Si are needed for the production of a kW_p mc-Si PV panel, so that the carbothermic process will lead to about 104 kg CO_2 per kW_p mc-Si PV panel:

$$\frac{44\frac{g_{CO_2}}{mol_{CO_2}} \cdot 3mol_{CO_2}}{28\frac{g_{Si}}{mol_{Si}} \cdot 2mol_{Si}} \cdot 44\frac{g_{Si}}{W_p} = 104\frac{g_{CO_2}}{W_p} \tag{5.5}$$

When carbon is substituted by hydrogen, the carbon path can be bypassed and water vapor is formed. Since hydrogen is a very pure reducing agent, further purification steps, such as the Silicon tetrachloride treatment, as in the case of carbon, are not needed [235]. In addition, 3700 kWh of electrical energy are needed during the entire process chain [234], as presented in Figure 5.2. By using electricity, further CO_2 emissions will occur depending on the source of energy. Assuming the current German electricity mix of 500 g_{CO_2} per kWh, 185 kg per kW_p mc-Si solar panel will be additional emitted. These emissions, which occur during manufacturing processes, are called indirect emissions and can have a severe impact on the assessment of a technology during lifetime.

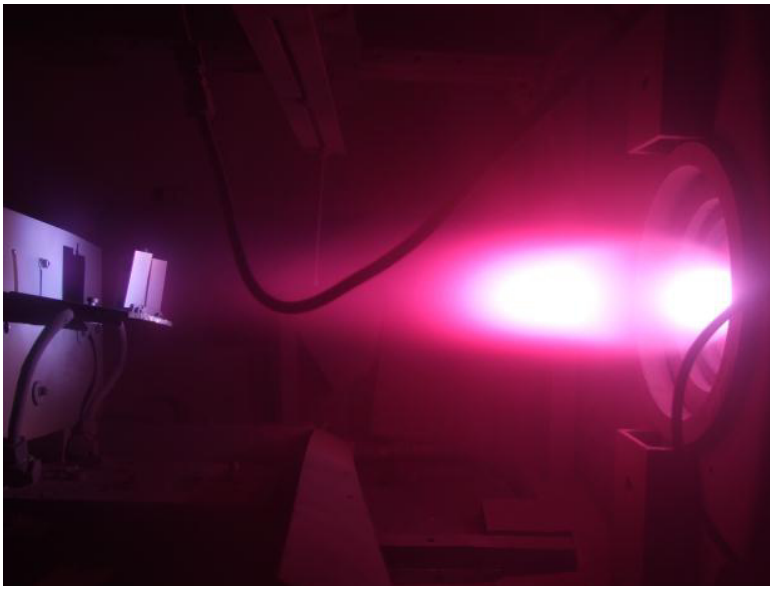

Figure 5.4: Hydrogen-silicon-plasmastream (Copyright © Dr. Laure Plasma Technologie GmbH)

5.4 Modeling indirect emissions as a dynamical *PV-unit* process

To implement the indirect emissions from manufacturing of technologies dynamically in urbs, a new process "PV-unit" is defined as shown in Figure 5.5 whose components will be explained in detail in this section. This PV-unit is then integrated in the known energy system of this work and will replace the existing technology "PV-system".

The electricity output of the **PV-unit** is based, as usual, on an hourly solar time-series used as input for the "PV-cell capacity" which has the unit "kW_p", and therefore,

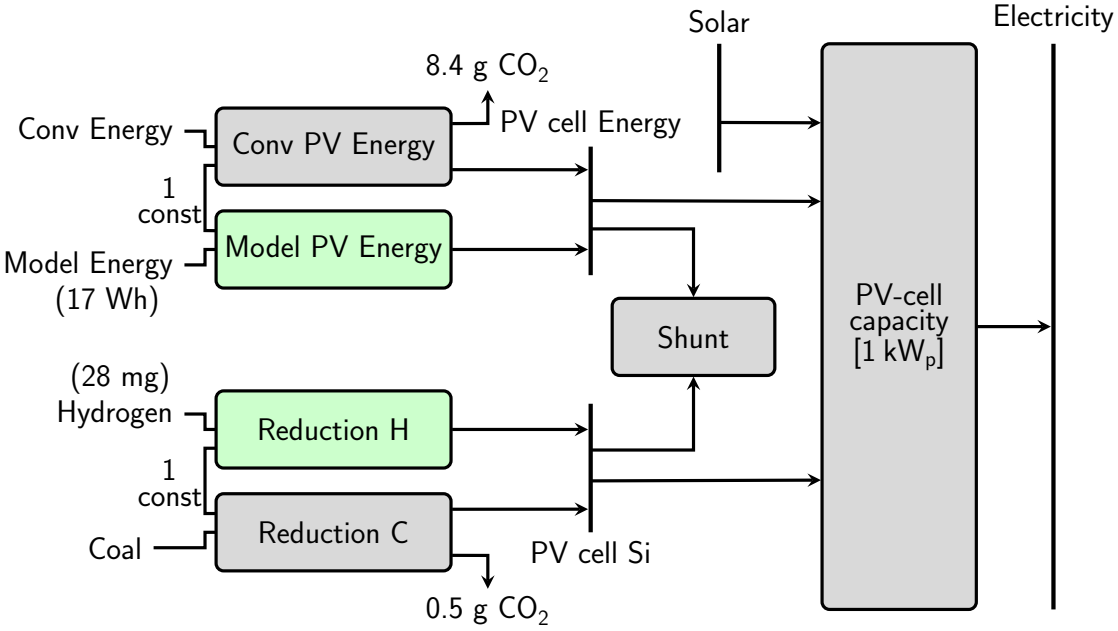

Figure 5.5: Reference energy system of the dynamic implementation of the indirect CO_2 emissions (from LCA) of the renewable technology *PV-unit* in a linear optimization problem with urbs. The components highlighted in green represent the dynamic process whereas the gray shaped processes are symbolizing the reference case including steady CO_2 emissions.

defines the solar harvest. In addition to the time-series, two further input variables are used: (i) The reduction agents which are a necessary input variable for the material path and (ii) energy needed for the production of PV cells. In case of the reduction agent, the model can choose between the two options: hydrogen or carbon. As explained, the established reference process ("Reduction C") is based on carbon for which 0.5 g CO_2 will be emitted every hour of an simulated year for each kW_p PV cell capacity installed by the energy system model. This number is calculated by allocating the emissions which derive from the carbothermic reduction, stated in eq. 5.5 over 25 years lifetime, each with 8760 hours.
Hydrogen is the alternative reduction agent which can be used to reduce emissions during the production process of PV-cells ("Reduction H"). Choosing this path results in further model decisions, such as the point in time when this additional hydrogen demand is produced by PEMWE. These electrolyzers are installed by the model, whereby the capacity is based on their unit commitment. An overcapacity of PEMWE will lead to higher investment cost but might use surplus power from renewable energy technologies to produce hydrogen for later use (H_2-storage presumed). Additional electricity storage, for example, will add a further complexity to the model decisions, as even electricity for covering PEMWE demand can be shifted in time beside hydrogen. Based on these decisions, model endogenous electricity will define the inherent CO_2 emissions of hydrogen as they varies hourly, as extensively described in Chapter 3. Moreover, this solution leads to additional costs due to investment in processes and storage to cover this demand. To summarize, in contrast to the gray shaped processes in Figure 5.6, using the green colored processes, will result in the need of additional commodities

which in turn increases costs at first. Reference processes have no additional costs as these are already included in the investment costs of PV panels as stated in Table 3.8. The amount of hydrogen needed for reducing SiO_2 to solar graded mc-Si can be calculated from the stoichiometry in eq. 5.4 which states that 0.14 kg of hydrogen are needed to create 1 kg of MG-Si. As 44 kg of MG-Si are used to create 1 kg of mc-Si, 6 kg of hydrogen are needed in total for a 1 kW_p panel. This corresponds, allocated over a lifetime of 25 years and 8760 hours per year, to 28 mg H_2 per hour of lifetime. However, the functional unit of hydrogen in urbs is not a gravimetric unit, as hydrogen is used as an energy carrier to power FCVs or as energy storage for later reconversion to electricity. Thus, the hydrogen demand is transformed into the energy unit kWh by using the LHV of hydrogen with 33.3 kWh/kg.

$$\frac{3700\mathrm{Wh/W_p}}{8760\mathrm{h/a}\cdot 25\mathrm{a}} = 0.017\frac{\mathrm{W_{elec}}}{W_\mathrm{p}} \tag{5.6}$$

For the energetic consideration, a choice can be made between using a conventional static electricity mix ("Conv. Energy") or the model endogenous energy ("Model Energy") for PV cell production. As stated previously, the energy for mc-Si production is mainly electricity, wherefore as simplification only electricity is taken into account. It is further implemented, that using the conventional energy will results into additional costs of 50 €/MWh electricity to make this path comparable with that of taking endogenous energy, which will also result into additional costs for the model. The process "Model PV Energy" is modeled such, that 0.017 kWh/kW_p of electricity per hour, over a lifetime of 25 years is needed, independent of the utilization of the PV-cell (see eq. 5.6). It is assumed that PV-cells will experience a degradation over time whether electricity is produced or not. When "Conv Energy" is used as an input, static CO_2 emissions occur with 500g/kWh. Thus, the specific CO_2 emissions of PV (1000 full-load hours) are defined by the reduction (0.47 g_{CO_2}/kW_p) as well as the energy path (8.4 g_{CO_2}/kW_p) to 78 g_{CO_2}/kWh_{el}. With this approach, already 78% of the value previously mentioned from the LCA in Figure 5.1 is achieved, by just modeling the two processes with the main impact.
For each pair (1=conventional, 2=alternative process) of process (p) of a commodity (PV Energy, Reduction agent), the output ratio between these pairs stays constant. Thus, once the value of these processes (MW_p) are determined by the model, they will not be changed during one scenario. This is done by using a supply intermittent (SupIm) variable (C_{supIm}) provided by urbs, which is usually used for defining the capacity factor of renewable technologies over a timeframe (y), providing a fluctuating time-series. This factor is set to the constant value of "1" for each hour, which means that process capacities (κ_p) which use these time-series as input must run at their maximum capacity as stated in eq. 5.7. For this reason, a shunt process is introduced, so that energy-equilibrium holds true by curtailing surplus process output C_{yp}^{out}. This shunt process becomes especially active when there is no sunshine (Solar = 0) as no further input for the "PV-cell capacity" from "Reduction" and "PV Energy" set is needed. The constant SupIm factor forces these processes to run and therefore, produce an output >0. In case of using conventional processes, this will generate emissions. Thus, the model decisions of installing additional PV capacities will lead to steady emissions (from production process) even at the time of no electricity production, e.g. at night or when surplus power from PV-cells needs to be dissipated, to keep

energy-equilibrium, by curtailing as it is of no use.

$$C_{yp}^{out} = (\kappa_{p_1} + \kappa_{p_2}) \cdot C_{supIm} \tag{5.7}$$

This approach of linking processes in a fixed ratio is reminiscent of Chapter 2, in which the heating sector of individual energy suppliers (single-family houses) in a pool (municipality) is modeled for Greifswald (see eq. 3.30).

The new **PV-unit** is implemented in Figure 5.6 and replaces the original PV-system. In contrast to the previous RES, the dynamic indirect emissions of the PV-unit is implemented as an output besides to electricity. On the input side, model endogenous electricity and hydrogen are modeled in addition to the solar time-series, which are highlighted as green dashed lines. This novel approach of connecting an indirect emission path, in addition to a static one, enables a detailed analysis in different setups:

- no indirect CO_2:
  Here, no indirect emissions are taken into account from upstream-processes during manufacturing for renewable energy technologies. Thus, using electricity from wind farms and PV-systems does not result in any CO_2 emissions during a lifetime as shown in Figure 3.7.

- static CO_2:
  With this approach, static indirect emissions are introduced for wind farms and PV-systems. Emissions over a lifetime are taken from ecoinvent database with 20 g_{CO_2}/kWh_{el} coming from onshore wind farms and roughly 100 g for mc-Si PV-systems [237], [238].

- dynamic CO_2:
  As stated in the chapter, this approach will consider emissions occurring during manufacturing in a dynamic way. Regarding the modeled scenario as stated in Figure 5.5, the impact of manufacturing changes over time and thus is a suitable way to model a realistic view of future energy systems. In contrast to the approach of modeling indirect static emissions, the impact is allocated to every hour of the year and not only to those which coincide with the hours of electricity production.

5.5 Temporal aspects

Two approaches are justified when solving the implementation of CO_2 emissions during lifetime in an hourly based optimization model. An **intertemporal** approach with implemented CO_2 budget will give the model a wide degree of freedom and take latest discussions of climate policy into account. Due to long solving times of such a model and the intensive demand for computational power, a second approach is chosen initially. The model is run several times while being optimized in one step for the whole year (8760 hours) by changing the yearly amount of allowed CO_2 emissions to the corresponding value of the climate protection goal of Germany. The benefit of this **snapshot** method is the very fine granularity which enables the possibility to observe minute changes in the system.
All CO_2 reduction targets are made in reference to 1990, so that a 95% reduction of emissions will only allow emission in amount of 5% of those emitted in 1990. The

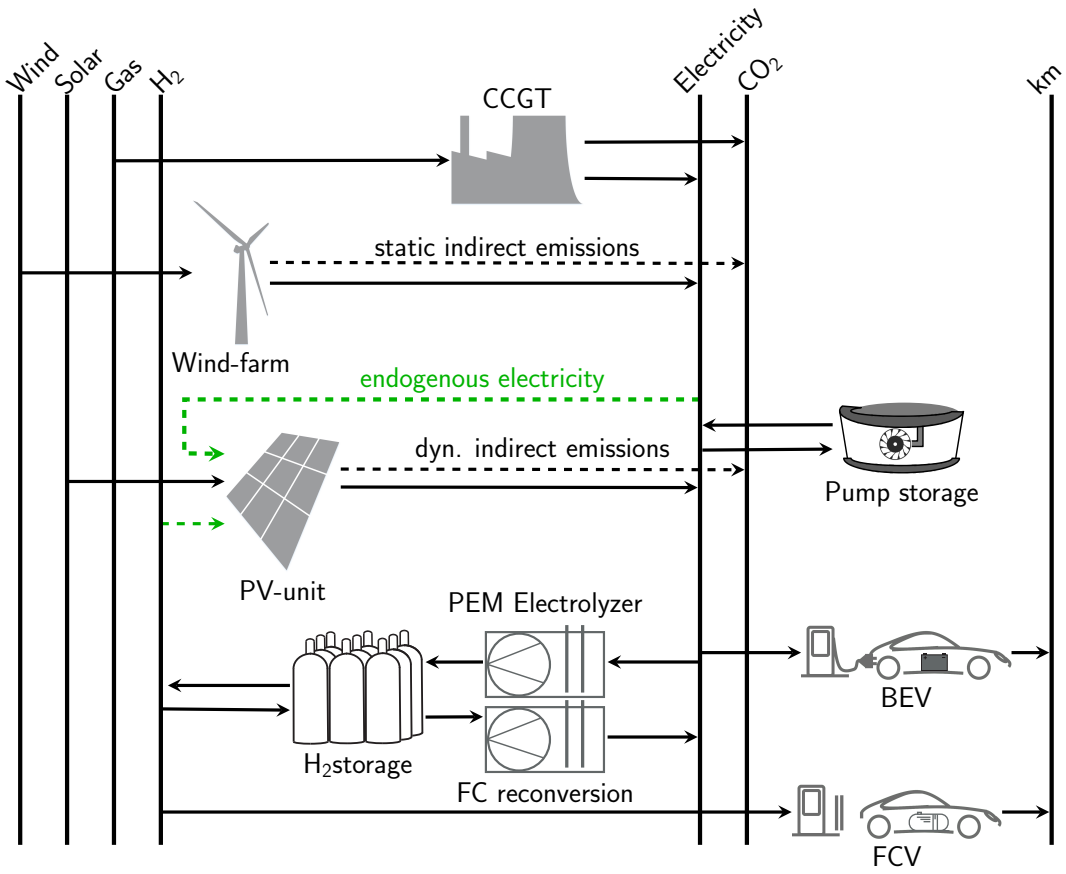

Figure 5.6: Reference energy system as presented in Chapter 3.7 with the implemented dynamic PV-unit (from Figure 5.5), replacing the static PV-system.

comparison of the three model-setups, listed above, starts with a 70% CO_2 reduction until a 95% reduction in 5% steps. As an ambitious CO_2 reduction of 40-95% is targeted by the government between the years 2020 and 2050, one 5% step corresponds to a time period of roughly 2 years. Later, for the dynamic CO_2 scenario, model runs with 8760 hours and a smaller step range of 0.05 percent points will be performed, to make the tipping point of model decisions visible and zoom into the chosen path of PV-production. Hence, this change can even occur quasi sub-yearly for some modeled CO_2 limits as these points might not align with a full year. The following example illustrates this behavior and provides a visualization in Figure 5.7:
A CO_2 reduction goal is set as a limit which does not coincide with the end of a modeled year of e.g. 71% where the initial change in PV-production occur. A full year of 8760 hours is modeled as represented in blue font with the constraint of -71% CO_2. However, the simulation period does not merge with a normalized calendar year, as the starting point is shifted (in this case to the right). Thus, for reasons of simplification, the following results will no longer be connected to years but to CO_2 reduction targets, as this allows to zoom into certain points of time to make tipping points visible.

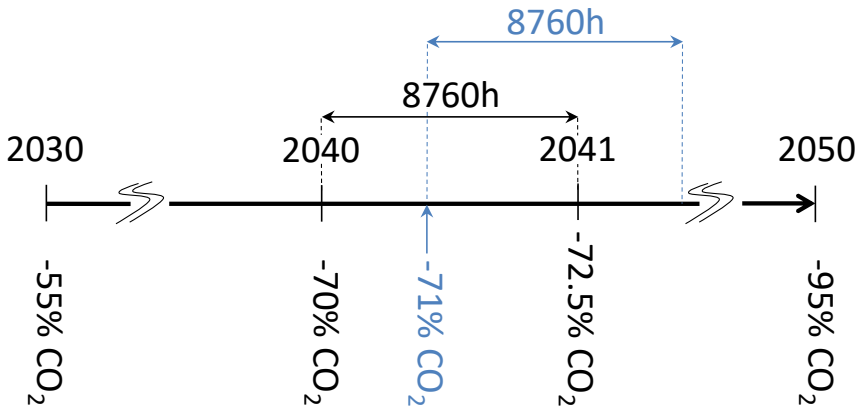

Figure 5.7: The difference between simulation time (blue) and time of a year (black). For some CO_2 reduction scenarios, the simulation time does not match the hours of the year.

5.6 Results of the dynamic approach

In this section, the behavior of the three different model setups as listed before are investigated. Figure 5.8 includes the CO_2 reductions on the x-axis and the total installed PV system by the model on the left y-axis in GW_p. On the secondary y-axis, the abatement costs in the unit €/t are plotted. The first obvious result is that a 95% CO_2 reduction is not feasible using static emissions, as using electricity from renewable energy sources will already exceed the CO_2 boundary. Second, the amount of PV installation at the beginning (70% CO_2 reduction) is similar between the dynamic and the static approach as the dynamic model is using the conventional route (as shown later) and therefore, electricity from PV has the same environmental impact in both models. On the other hand, for very high reduction scenario, the dynamic model gives similar results to the one with static indirect emissions in case of PV installation. For further investigation, the absolute value of negative CO_2 abatement costs are plotted by using dual variables, which can be interpreted as an indicator of the incentive of reducing CO_2 emission. For each ton of saved CO_2, the cost of the model will decrease by the corresponding value as this is the marginal cost.

Calculating marginal costs is a method, used in economics, which describes the increase/decrease in costs per product unit [239]. In industry production costs are usually connected to several parameters such as variable costs and production capacity of utilities which define the price per unit. Producing an additional unit thus might affect the unit price, as e.g production capacity might be exceeded and new facilities are needed. Mathematically, this corresponds to the first derivative of the costs function (eq. 3.3) with respect to a product unit (u)

$$\zeta' = \frac{d\zeta}{du}. \tag{5.8}$$

A strong limitation of CO_2 will lead to more ambitious model results, which increases total system costs. Thus, in this particular case, the effect of decreasing one unit of

CO_2 is subject of interest, as an increase of marginal costs is expected.

In future emitting CO_2 can be seen as a costly process, as the total budget of emitting it becomes very restricted. Thus, the first impression is that the value of preventing CO_2 emissions increases strongly with the limitation of the CO_2 budget, which makes sense from the law of supply and demand. Furthermore the fact that the curve of CO_2 abatement costs of the dynamic approach lies in between the static approach and the one without emissions strengthens the validity of the results, as our expectations are fulfilled. In addition, the overall costs of CO_2 emissions gives a hint at the realistic future price CO_2 certificates should be rated on. It is obvious, that these values will not align with the current price of CO_2 certificates and also exceed, with the value of 1,400 €, the expectations of some scenarios that have predicted future social costs of carbon for the year 2050 with \$69-\$417 [240, 241]. The impact of carbon costs is getting distinct, when having a closer look at the order and time, when substitution of conventional production path of the **PV-unit** occurs as shown in Figure 5.9 and 5.10.

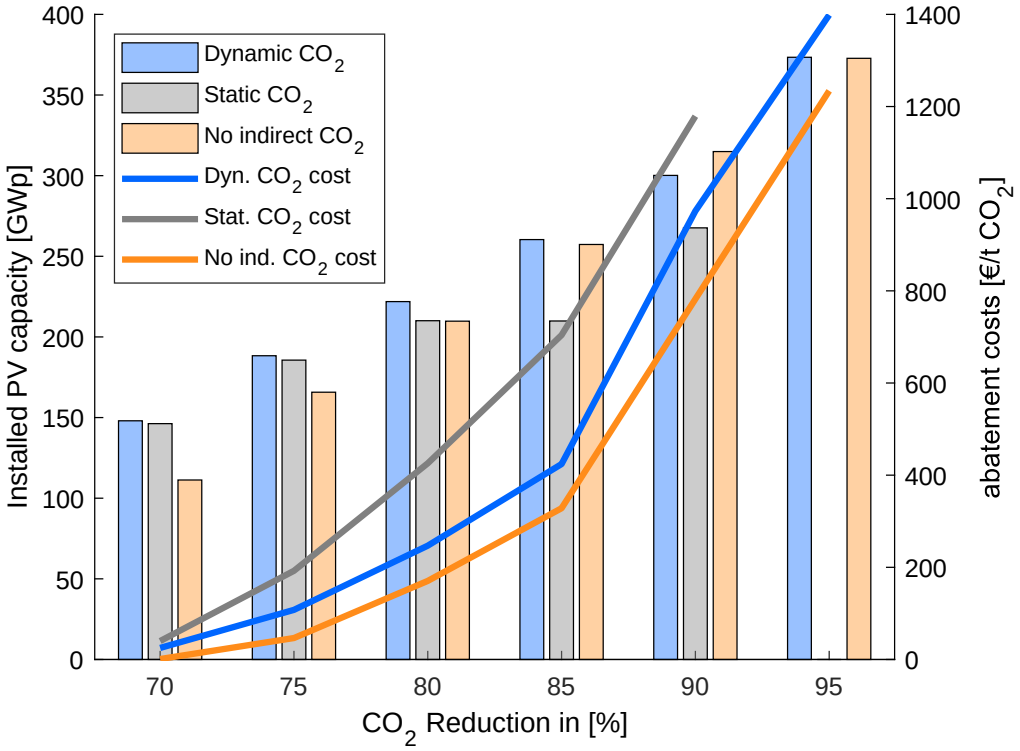

Figure 5.8: Installed PV capacities for static, dynamic and without direct CO_2 emissions of PV panels.

From Figure 5.9 it is observed that the change in the PV production occurs first time at a CO_2 reduction of 71% by using a small share of model-endogenous electricity. Additional model runs between the 70% and 75% CO_2 reduction scenario are conducted with a 0.5% step-length in Figure 5.9 and between 81.8% and 82.3% with a 0.05% range in Figure 5.10. With an increase of CO_2 reduction (between 70% and 71%), the model reacts initially with an increase of PV installation. More intense CO_2 limitation will keep installed PV capacities nearly constant, while changing the manufacturing

process. First, a switch is observed from the conventional PV energy (500 g_{CO_2}/kWh) to the model endogenous energy mix, as this solution has the minimum costs.

By investigating Figure 5.9, its is obvious, that PV capacities stay constant between the 71% and 74% scenario. Additional capacity is built from the point at which PV cells are produced exclusively with endogenous electricity (>74%). Before that, marginal costs for CO_2 remain constant within this technology change (71% and 74%), as represented by the horizontal red line. This effect is reminiscent of a phase transition, as it occurs when materials undergo structural changes due to external influences. If this effect is mirrored on the **PV unit**, an area can be interpreted, at which the transition from "conventional energy" to "model energy" takes place, which is described by a phase boundary (CO_2 marginal costs).

This results in constant value of CO_2 abatement costs at 61 €/t. After the share of the conventional PV energy vanishes, abatement costs rise and further PV cells are installed until 81.8% CO_2 reduction. In Figure 5.10, a similar picture is given but his time for hydrogen used as a reduction agent. Another phase transition appears by keeping overall installed PV capacity constant. It is interesting that the model is able to keep the value of CO_2 constant by using the changes in the carbon reduction process of PV-cells. The CO_2 abatement costs lie in a range of 274 € to 275 € per tonne during this process. Obviously, changing the material is more expensive as changing the electricity. This allegeable, as electric energy is needed by PEMWE to produce hydrogen, which is more costly due to the fact that losses occur during electrolysis caused by conversion losses. Additionally investement costs of the PEMWE and storage costs of hydrogen affecting the system costs. It must be noticed that the ratio of the chosen path for manufacturing PV-cells must stay constant during every hour of the year, which was explained in detail in Chapter 3.5. This prevents the model to switch during certain hours between the PV-energy path and the chosen reduction material. From this point of view, it can be stated that PV-production will change with stricter CO_2 limits in future. First, a shift of the electricity used will happen and later even hydrogen will be used to make PV production more environmental-friendly to reduce valuable CO_2 budget.

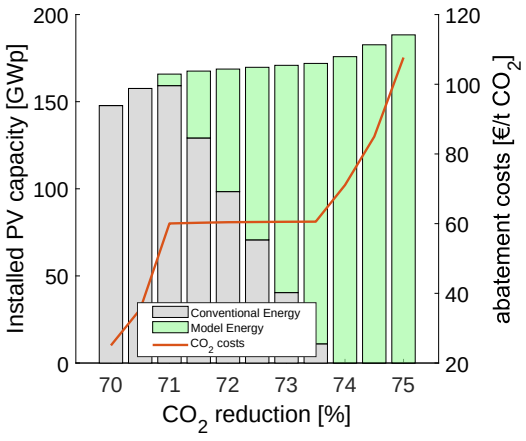

Figure 5.9: Installed solar PV capacity (bars, left) with the respective shares of exogenous (gray) and a endogenous (green) energy used for the manufacturing and CO_2 abatement costs (line, right) as a function of the CO_2 emission targets.

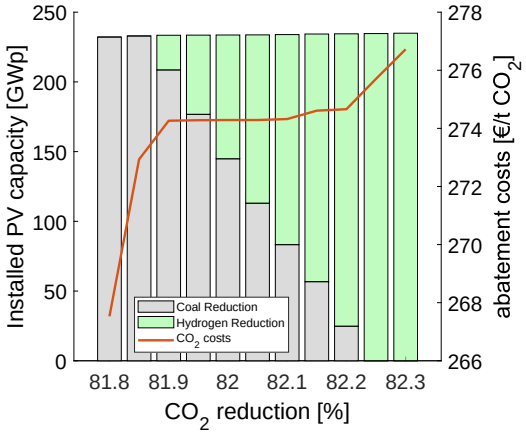

Figure 5.10: Installed solar PV capacity (bars, left) with the respective shares of carbothermic (gray) and hydrogen plasma (green) reduction used for the manufacturings and CO_2 abatement costs (line, right) as a function of the CO_2 emission targets.

5.6.1 discussion of the results of integrating life-cycle to energy system modeling

In this chapter, the importance of integrating the material sector into energy system modeling. This combines the benefits of LCA, which takes the impact from manufacturing into account and the possibility to make predictions of future energy-systems. As in todays available LCA tools, only the composition of an electricity mix on the highest level (e.g 40% PV) is possible but not the change within manufacturing, LCA thinking was integrated into energy system modeling and not the other way around. From the results it is deduced, that this is a very important new feature for energy system modeling, as changes in production of PV units occur and thus, especially for higher CO_2 reduction targets, validity of modeling results might get inaccurate. A strong increase in CO_2 abatement costs over time, which resulted from the annual modeling of every single year leads to the question: "which costs are representative". If advising policy makers, the way these costs increase, could be an indication for the further development of CO_2 prices as they were introduced in 2019 by the German government. Currently this price is set to 25 € per ton of emitted CO_2 for some energy carriers in specific sector such as heating or transportation [242] until 2025. Future prices are not clearly set yet, but a corridor is defined with a lower boundary of 30 € and a maximum of 60 €. The results from the presented model are between 1200 € and 1400 € for each ton of saved CO_2 emissions. This implies, that a ton of CO_2 which is not emitted reduces costs of production and thus is valuable for the emitter. However for the year 2050, the calculated CO_2 abatement costs of the model are 20 times higher than the one given by the government today.

With this presented proceeding, only snapshots of the years are taken. For this reason,

the following chapter will reduce this uncertainty by modeling over a whole timeframe of 20 years, from 2030 until 2050.

6 Introducing *PV-unit* into an intertemporal optimization

An intertemporal approach introduces another degree of freedom to the model. Beside the hourly timestep "t" which connects energy and power, an additional time domain connection is expected. With an intertemporal approach all time periods are solved simultaneously [243, 244]. Especially for modeling a long time horizon, intertemporal models can be used to make the change in an energy system visible over the years, instead of just taking the snapshot of one year. The difference is that not every year is optimized on its own but an optimal solution is found for the whole period of interest. From version 1.0.0 on, urbs does support intertemporal functionality which can be used with basically the same input sheet as used for the annual model. However due to the more complex optimization as well as the bigger amount of data needed to be processed, calculation time increases strongly. Calculating each year as a snapshot with individual CO_2 emission constraints, as presented in previous chapter 5, took approximately 10 minutes per run. Modeling a time frame of 30 years (2020 - 2050) leads to 200 hours on the same computer to find an optimum solution. For this reason, every fifth year is introduced as a support year to get insight into the model. As urbs has already embedded a "weighting function" in the snapshot model, which is used to extrapolate the time horizon of modeled timeperiods smaller than one year up to a full year with 8760 timesteps. This is important when years with a time period smaller than 8760 h are modeled, as urbs finds the minimal solutions of the system-costs which will be otherwise calculated wrong. Similar to the "weighting function", in the intertemporal problem, a factor ("k") on an annual level is implemented, which repeats a modeled year k-times where "k" is the difference between the actual year and the nearest next year with an input-file. Every input file contains an identifier for the model-year, yearly CO_2 limit and a budget allowed to be emit over the full time frame. Input data are valid until the next support time frame is reached, which enables, for example, the mapping of efficiency increases of technologies over time, whereby the point in time at which the efficiency increases is introduced will be controlled via the input files. Therefor the parameters of the variable vector "x", as stated in eq. 3.2, changes by an additional index for the year "y" to:

$$x^T = (\zeta, \rho_{yct}, \kappa_{yp}, \hat{\kappa}_{yp}, \tau_{ypt}, \epsilon^{in}_{ycpt}, \epsilon^{out}_{ycpt}) \tag{6.1}$$

Beside the "depreciation" in Table 3.8 a remaining lifetime is asked when introducing the initial year, needed for already installed processes to determine their run-out period. Here, the same value as for the depreciation is chosen, which means, that the process are new at beginning of the modeling period. Most of the constraints hold true for **intertemporal** modeling as well as for modeling one full year as a **snapshot**. However, in contrast to yearly CO_2 limits, making use of a CO_2 budget over the whole model

horizon, does make models more realistic and thus increases their relevance for policy makers.

6.1 CO_2 constraint dependence on time

For modeling of the known energy system with the PV-unit presented in Chapter 5, each year of CO_2 reduction is not individually optimized, but a period of 30 years in 5 year increments including a discount rate of 3% for calculating system-costs. The total budget of permitted CO_2 emissions is calculated over this entire period as shown in Figure 6.1. The x-axis shows the individual years as well as the corresponding CO_2 reduction targets in accordance with Germany's climate protection. The modeling period starts with the year 2030, which corresponds to 55% CO_2 savings compared to the reference value, and ends with a 95% saving in the year 2050. The absolute reference value differs from the generally accepted reference value, as it is based on agreed literature in the P2X project. Here the assumed values for the energy demand and power plants of the year 2050 (KSZ80) were used (Table.5-98, [41]) and calculated back to a reference value without any CO_2 reduction. In respect to the corresponding scenarios, CO_2 reductions are assumed in the transportation sector as well [171]. As this sector amounts with a share of 61% [245] of the total emissions in transportation (163 Mt CO_2), the budget for the KSZ80 scenario will result in 20 Mt per year. The total budget for the entire period is set to 1.7 Pt, which may be emitted, whereas the decision on the use of that budget is being made within the model.
In contrast, emissions constraints of the annual-model are calculated for each modeled year itself and can therefore only be used exactly for this single modeled year. This excludes the possibility of achieving a global optimum over the whole horizon of modeled years. Modeling a CO_2 budget instead will allow the model for additional savings in CO_2 during one year and carry those over into later years. As its was previously shown in Figure 5.9 this would make sense to some extent since the abatement costs of CO_2 will increase in future, from which the intertemporal model can benefit.

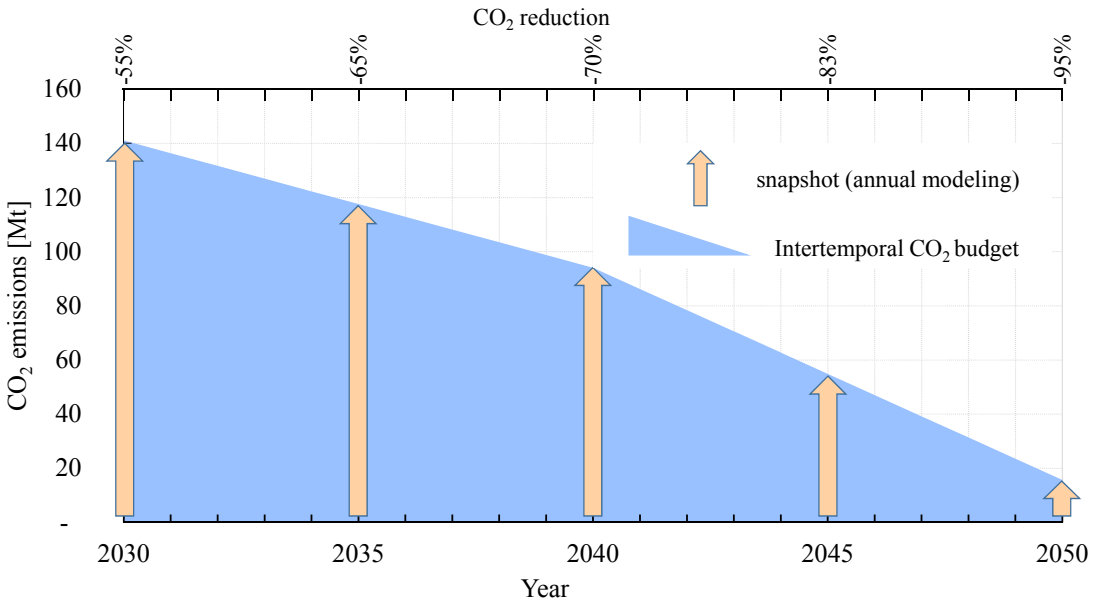

Figure 6.1: Sketch of the difference in calculating CO_2 emissions for the intertemporal model as a budget (blue area) and the arrows for the annual modeling as a snapshot.

6.2 Comparison of intertemporal and annual method

In the Figure 6.2 the installed PV capacities of the annual model, with snapshots of each year, are plotted. The increase of PV capacities over time is clearly visible. Starting at 150 GW_p in the year 2040 overall installation is exceeding 350 GW_p until 2050 in a scenario with a reduction of 95% of CO_2 emissions. In the case of more moderate ambitions resulting into a reduction of 80%, 300 GW_p of PV will be sufficient to reach that goal. In contrast, results look completely different for the intertemporal approach. In Figure 6.3 slightly more PV is installed by the year 2030 and nearly no changes are seen in overall PV installation through the years. In addition only the path of using model energy is taken in the PV-unit. The option of using hydrogen as reduction agent is not even used in case of strong CO_2 reduction in the year 2050. These results are surprising, as the constraints for the intertemporal approach seems to be less difficult to reach. This assertion is underlined by the CO_2 abatement costs at around 50€ which is far less as the costs in the annual approach. This leads to the question, in which way energy system modeling should be conducted as results of the intertemporal model are different to the annual one. It is clear, that the intertemporal abatement costs stay constant over the whole period, as only one CO_2 constraint is set in the form of a budget and not for each single modeled year. As only one CO_2 constraint is active for the whole modeled horizon, marginal costs will not change (see equation 5.8). Another difference compared to the annual mode is, that hydrogen as reducing agent is not used during the entire modeling time period, whereas endogenous "model-energy" is already used from beginning to produce PV-cells with lower emissions.

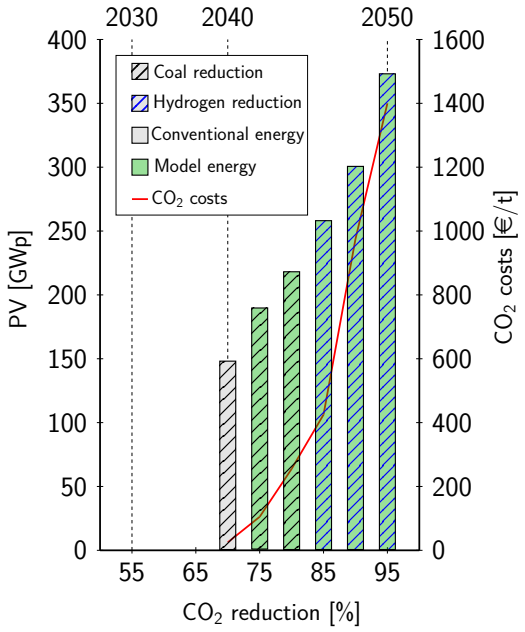

Figure 6.2: Results for the annual (snapshot) model. The total installed PV capacity, CO_2 abatement costs as well as energy and material paths of the PV unit are plotted for different years.

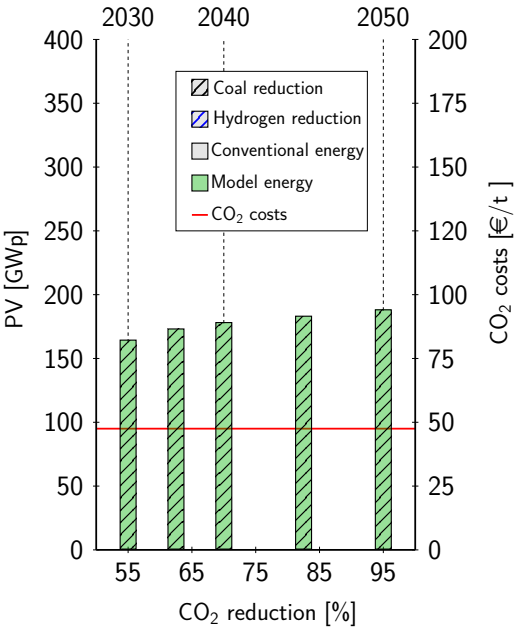

Figure 6.3: Results of the intertemporal model are plotted for the different scenarios. In contrast to the previous graph, only one number for CO_2 abatement cost (constant) are given

It is interesting that in the annual model, CO_2 abatement costs are 25 € and thus only half the price of the intertemporal approach. This leads to the question of how the latter approach handles the budget of CO_2 emissions over the whole modeling horizon. For this reason Figure 6.1 is extended by the real **emitted** CO_2 emissions over the modeled years. In addition the specific CO_2 emissions per kWh electricity are plotted on the secondary y-axis, highlighted with rectangles. The dotted lines are a linear regression of the the specific emissions of the two different model approaches. It is obvious that the intertemporal model is emitting its budget of emissions differently to keep the specific CO_2 emissions to a constant level. These emissions are calculated by taking also the curtailed electricity into account, as energy from renewable electricity will have emissions due to the their manufacturing process, which are allocated over lifetime. The change of the shape occures from a triangle towards rectangular one, regarding the actual intertemporal CO_2 emissions. This is an indication, that the overall budget is not as limiting as it is for the snapshot approach. This is due to the shift of unused CO_2 budget between the years 2030 and 2040 for later use. Thus with a long term planing, actions that need to be taken are less drastic. This inference is substantiated by the moderate PV installation and the constant CO_2 abatement costs. As the specific CO_2 emissions per kWh electricity are constant around 120 g in the intertemporal model, the chosen premise, a model horizon from 2030 until 2050, must be scrutinized. Thus, the horizon is extended from 2050 until 2100. For reasons of computational performance, a resolution of 10 years is chosen.

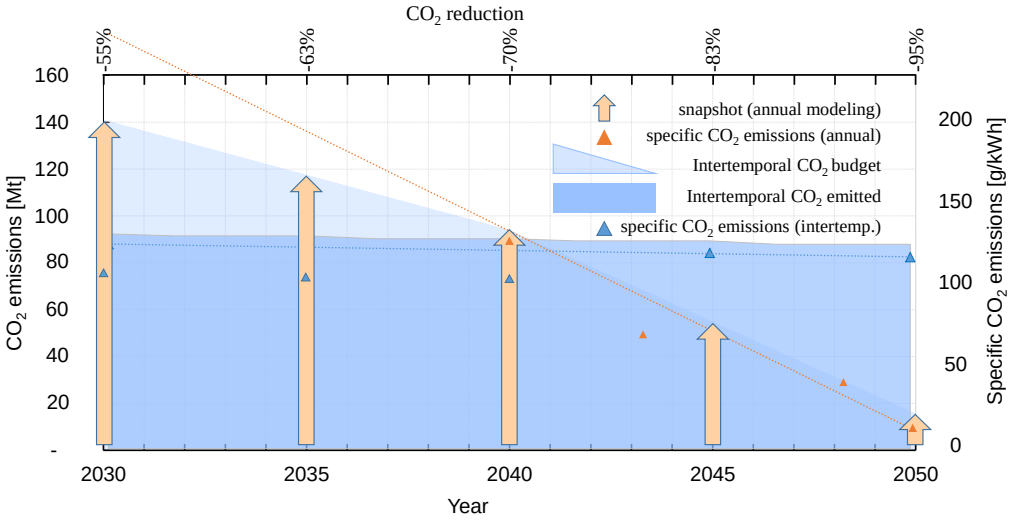

Figure 6.4: Different modeling approaches for the energy system. The arrows describe the emissions allowed in the snapshot method. The light blue shape represents the CO_2 budget regarding to the climate protection goals. The blue rectangle are the true emission from the intertemporal modeling approach. The specific CO_2 emissions of both approaches are marked with triangles whereas a linear regression curve is used for earlier years of the snapshot method.

6.3 Extended time horizon until 2100

With the extension of the modeling period to 2100, CO_2 budget is increased from 1.7 Pt to 2.6 Pt, as from the year 2050 on, the yearly CO_2 budget is set constant to 19 Mt. Figure 6.5 depicts the emissions over the extended horizon. Here, the green shape represents the emissions of the intertemporal model whereas the blue shape shows the targets from the government (the same as in Figure 6.1). It is surprising, that it is more favorable for the model to reduce CO_2 emissions more slightly over time and end with half of the emissions which are allowed in 2100 (10 Mt). Also the CO_2 abatement costs are now substantial higher with a value of 240 € per tonnes. This observation leads to the conclusion that in an intertemporal approach the modeling period is essential to make a statement about future CO_2 prices. The main difference between the intertemporal approach with an observation period of 20 years and the one with an observation period of 70 years is the following. With the former approach, the states exceeding the year 2050 do not exist under modeling perspective, so that the given CO_2 budget can thus be distributed evenly over this shorter period of 20 years. Efficient technologies which were installed earlier leading to CO_2 savings will contribute in a large extent to the later years. For the much longer period until 2100, the influence of the earlier years with few reduction targets is much smaller, as absolute savings in emissions have to be allocated over a much longer period in time. This approach is therefore more realistic, since CO_2 emissions must be severely limited even after 2050 and 2100, and a continuation of 95% CO_2 reduction is therefore certainly realistic. It is therefore clear that an earlier reduction in emissions is advantageous in order to implement a slow

turnaround in the energy system, where CO_2 abatement costs also develop moderately.

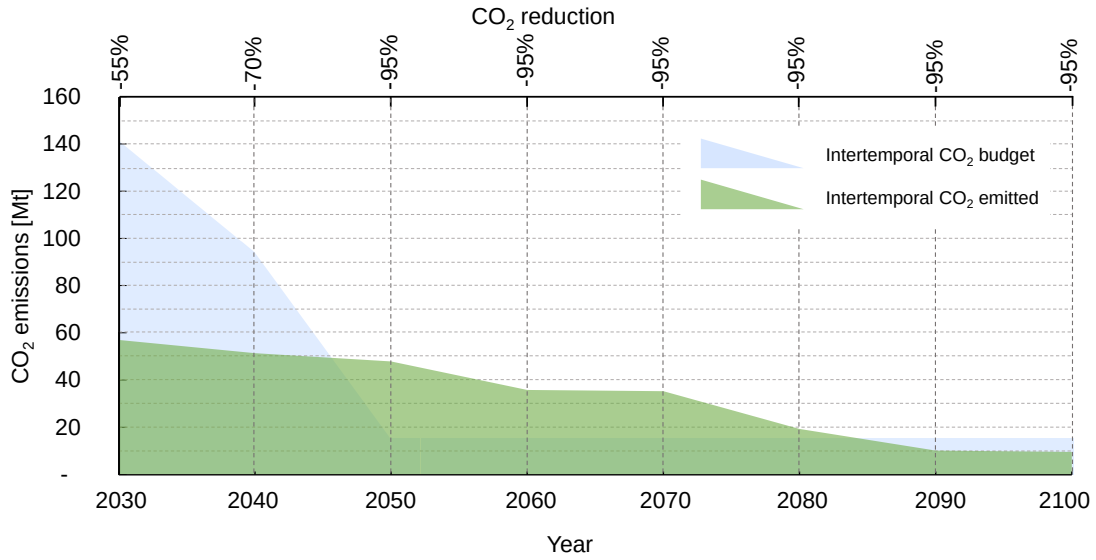

Figure 6.5: Modeling the presented energy system with an extended intertemporal approach until 2100 (green shape). The given CO_2 budget which can be allocated over time is shown in the background as blue shape. For every year exceeding 2050, another 5% is added to the budget

In the later years, when CO_2 budget is decreasing, hydrogen plays a major role as an energy carrier. As hydrogen can be stored cheap, it is used from the year 2060 as a long term storage for later reconversion into electricity. Already in that year, 23 TWh of electricity is used from reconverting hydrogen to supply energy demand. In the year 2100, it is even increased to 87 TWh electricity, which corresponds to approximately $4.5 \cdot 10^9$ kg H_2 before being converted by fuel-cells. This comes along with an expansion in hydrogen storage from 3 TWh to 24 TWh in the same period which corresponds to 13 - 6 complete charging cycles over the year. More detailed insight about the installed capacities of the extended intertemporal approach is provided in Table A.8. The aggregate state of stored hydrogen is not covered by the scope of this work, but of course is associated with further losses, regarding the type of storage used. The liquefaction of hydrogen (LH_2), for example, increases the energy density from 3 kWh/l_g (273.15 K and 0.1013 MPa) up to 2.34 kWh/l_l (LH_2) [25]. However, this technique is very energy intensive and thus requires about 1/3 of the energy stored in the LH_2 to cool the gaseous hydrogen down to -253°C.
Comparing the installed PV capacities between the annual model and the extended intertemporal, capacities are slightly higher for the latter approach at the beginning with 230 GW_p in the year 2030, but lower in the year 2050 with 250 GW_p. It reaches its peak at the end of the modeled horizon in 2100 with 370 GW_p, which is the same as for the result of the previous snapshot method 50 years earlier. It makes sense, that the PV capacities in 2050 are similar between the annual model and the extended intertemporal model, as the CO_2 reduction target from the government is 95% starting from the year 2050 on. This implies the same strong CO_2 constraint as the intertemporal model

with the extended time horizon can transfer less surplus on CO_2 budget to later years. This also explains the fact, that from the very beginning, the innovative path in the presented PV-unit is chosen, both, for the reduction path as well as for the energy related path. To close the loop, which started with the LCA value 100 $g_{CO_2\text{-eq.}}/kWh_{el.}$ from PV (shown in Figure 5.1), the progression of the actual emissions of electricity from PV of the extended intertemporal model is calculated. Again, just 78% of the emissions from the LCA are covered by the PV-unit. As only 28 mg of hydrogen are used per kWp of installed PV and hour of the year, it contributes only with 2% to the specific emissions of electricity from PV. Due to the storages, hydrogen is not been produced constantly over the year. For this reason, the average of the specific CO_2 emissions of electricity was calculated for the hours, hydrogen is produced from PEMWE. Of course, this number is lower than the average specific CO_2 emissions from electricity over the year. In the year 2030, 22 g CO_2 are emitted per energy content of 1 kWh hydrogen (33 kWh/kg_{H_2}). The average of the emissions per kWh electricity produced in the energy system model over all technologies is 74 g in this year. To review, the electricity demand calculated in Chapter 5 for manufacturing 1 kW_p PV cell, results into 0.017 kWh of electricity needed per hour (see 5.6). With an average amount of 1000 full-load hours per year, this amounts to 0.148 kWh of energy needed per 1 kWh electricity output in average, as calculated in eq. 6.2.

$$0.148\text{kWh} = \frac{0.017\text{kWh} \cdot 8760\text{h}}{1000\text{h}} \tag{6.2}$$

Thus, 11 g CO_2 are emitted per kWh of electricity produced by PV, caused by the energy demand of manufacturing supplied by the model electricity-mix (74 g_{CO_2}/kWh). Following Figure A.1 shows the specific CO_2 emissions of the electricity-mix of the energy system for every modeled year in the extended intertemporal model as green bars. In addition, the specific carbon emissions from the installed PV technology are plotted as blue bars. Until the year 2100, emission from PV panels are almost carbon-free (1.5 g_{CO_2}/kWh). Compared to the calculated static emissions of 78 g_{CO_2} per kWh, implementing the innovative PV-unit is a significant improvement of energy system modeling.

In the following Table 6.1 the CO_2 emissions per kWh electricity of the corresponding technologies are stated. In case of CCGT, the emissions are directly coming from burning natural gas. For the renewable energy technologies emissions are indirect and resulting from the whole life-cycle. Only the PV technology is calculated dynamically as mentioned in this chapter.

Table 6.1: specific CO_2 emissions per kWh electricity output

source	$\mathbf{g_{CO_2}}$
Conv. electricity	500
CCGT	333
Strong wind	14
Weak wind	18
Offshore	8
PV	(variable)

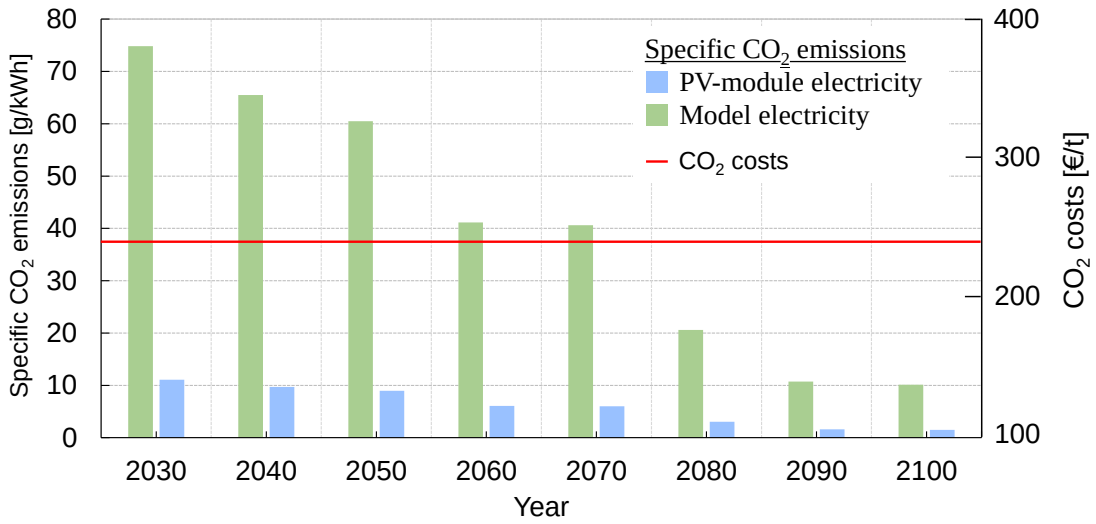

Figure 6.6: Specific CO_2 emissions of the expanded intertemporal approach until 2100. In the green bars the average emissions of the electricity mix per kWh of the model are plotted. Blue bars represent the specific emissions of 1 kWh of electricity from PV for the corresponding year, as the results from the PV-unit method.

7 Conclusion & Outlook

7.1 Conclusion

In this work an energy system model was used to demonstrate that extended sector coupling (PtX) is required not only in the area of energy use, but also in process technology with hydrogen as a reducing agent, in order to achieve Germany's ambitious climate targets. Electrolytically produced hydrogen was chosen both as an energy carrier and as a chemical raw material for the presented analysis. In addition the amount of hydrogen demand for some sectors such as steel industry or agriculture were stated. Already used in pilot projects for steel production (IN4climate.NRW), green hydrogen is a chance of decarbonizing agricultural products by just slightly changing retail prices. Other advantages of hydrogen include low cost seasonal storage, potential to be converted back into electricity and an existing industrial market. However, due to efficiency losses and current cost-intensive technologies, many competing technologies (PtH, BEV) can be initially integrated from an economics standpoint. Particularly when the main focus is on the use of surplus renewable electricity, high investment costs are an obstacle due to low plant utilization. The model results show that hydrogen as a seasonal energy storage, in TWh scale, would be viable only from the year 2050. As electricity from renewable energy technologies is limited, it will not be sufficient to decarbonize all sectors. Thus, the most favorable ones should be selected. Either they might be chosen by the readiness of implementation, economic issues, overall impact or further considerations.

In the course of the P2X project, a discrepancy was observed between the LCA methodology and the approach to energy modeling. This was described in Chapter 4 along with a proposed solution to avoid this blindspot. Life Cycle Assessment (LCA) is a well recognized tool for assessing technologies from an environmental point of view. The approach is described in the ISO 14040 and 14044 standards, which allows for the comparison with similar studies for other components. The LCA is based on a detailed inventory database of relevant process data but so far there has been none proposed for the promising hydrogen producing technology PEMWE (Proton-exchange-membrane water electrolyzer). The general evaluation of PEMWE technology shows that the global warming potential (GWP) is worse than expected when compared to the established SMR (Steam-methane reformer) process. An electrolyzer operating with 100% PV based electricity would produce 5.5 kg CO_2-eq. per kg H_2 which corresponds to about half of the GWP of the reference process SMR. This still seems overestimated while comparing a completely renewable energy based method to another derived from fossil fuels. The reason being that current attempts in literature have only been made to implement static indirect emissions. To mitigate this, a novel approach was developed by dynamically considering the production of renewable technologies in an energy system model.

Photovoltaic was chosen as an application example to validate the developed model, as it emits up to 100 g of CO_2-eq. per kWh electricity generation in the existing LCA for Germany. With this value it is immediately noticeable that a 95% CO_2 saving compared to 1990 levels, as required for the year 2050, is not possible. Therefore the indirect emissions were implemented dynamically, so that the possibility exists to provide the energy-intensive wafer production with improved electricity mix endogenously by the energy system model. This option is favored by the model after the CO_2 savings goes beyond 70%, which in this case corresponds to the levels mandated for the year 2040. In addition to the possibility of reconverting hydrogen to electricity, it is also possible to use it as a climate-friendly reducing agent. Since this is the more cost-intensive solution, a change of the reducing agent from coal to hydrogen only takes place in the model after the CO_2 abatement costs of 275 euro per ton, to meet the climate protection targets. From modeling result it was stated, that the validity of a static LCA is limited and especially not adequate to assess power-intensive processes in the energy transition power systems of the future.

In a further step, the symbiosis of static life cycle analysis and energy system modeling, which is optimized annually, was transformed into an intertemporal problem. In contrast to the annual method it was allowed to accept not only snapshots but also the approach of an independent distribution of a given CO_2 budget over a defined period of time. It turned out that an early change of energy production from fossil fuels to renewable technologies and the associated CO_2 savings provides an unused budget, which can be used to carry out a gradual change of the energy system and at low costs. In contrast, the CO_2 abatement costs are considerably higher if portions of the currently still quite high budget are not saved and postponed to later years.

With regard to grid stabilization, hydrogen storage on a large scale is certainly one way of compensating for fluctuations in electricity generation from renewable sources. The predicted costs of PEM electrolyzers vary greatly between studies. In this work, the costs of the technology is based on the current state of the art for the entire modeling period. Should strong cost reductions occur in future, hydrogen usage will turn more widespread as a stored energy-carrier. In general, however, it has been shown that hydrogen also plays an important role outside the energy economy, as emissions can be saved in agriculture (fertilizer), heavy industry (steel production), transportation (FCV) and also in the manufacturing of renewable technologies (PV) which inherently improves emissions of electricity generation.

7.2 Discussion

In conclusion, the core statements made in this work were based on the modeling results and their respective assumptions. However, it is worth discussing whether a drastic change in the German energy system is the desired way forward. Just taking into account the approximately 200 GW_p capacities of onshore wind turbines, which should be realized as a model result from the year 2080 onwards, is already more than tripling the current installed capacity. In addition, the amount of offshore wind farms increase sixfold from the present day installation of 6 GW_p. Photovoltaics have relaxed regional limitation as compared to wind farm. Due to their lower visibility, they can also be

Figure 7.1: Energy transition also reaches Tomerdingen, a village with a history reaching far back to the medieval time.

better integrated into the landscape. Yet with the projected 370 GW_p the installed PV, the total capacity increases eightfold from today.
In addition, the modeled energy system is limited, as in its scope, hydrogen connects only the electricity sector with the private transportation sector. In the domain of an extended PtX perspective, further sectors have to be integrated which also have a significant energy demand and associated emissions to be reduced. This will not lead to a proportional increase in renewable energy technologies, but will still aggravate the situation. The change of landscape is already seen in some parts of Germany as e.g. in the Swabian Alps where Figure 7.1 was taken. As in this work the critical materials were discussed in Chapter 4, the amount of platinum groups, especially iridium for PEMWE was stated. However, it should not be neglected, that also the amount of naturally occurring lithium is limited and mining is not sustainable as huge amount of water, a rare resource at the mining location (Atacama dessert, Chile), is needed.
Compared to Germany, the United Stated of America are less dense populated and thus e.g. wind parks are easier to be embedded into natural landscape. Texas for example, who has access to large oil deposit, now starts an energy transition toward sustainable energy supply. The following picture in Figure 7.2 was taken during the research stay in Austin and proofs a change in thinking as well as a good way of integrating these technologies in the landscape.

7.3 Outlook

In the wake of the "Energiewende", the electricity sector will change significantly in the next decades to such an extent that associated energy-intensive manufacturing pro-

Figure 7.2: Photograph taken in the western part of Texas showing the contrast between conventional crude oil pumps and modern windturbines

cesses will emit less CO_2. For this reason, the currently validated LCA data-sets will lose their relevance and will no longer be accurate for the future. Either these data-sets should be revised, or tools should be provided to easily adapt data-sets across all the level of detail in the implemented manufacturing processes. Currently this can only be done efficiently at the highest level, such as defining the electricity-mix which is needed by a technology as a direct input. However, changing the data-sets will lead to a lack in the comparability of results, since data records of the same processes would be no longer uniform and exist in different versions.
On the side of energy system modeling, the integration of indirect emissions lead to a more realistic assessment of future energy systems. This aspect also promotes the basic idea of sector coupling, which was demonstrated with the example of PV in this work. The failure to take indirect emissions into account leads to an underestimation of the total emissions. A static analysis of direct emissions leads to infeasible results under the ambitious climate protection targets of 2050. Since a model always represents an interpretation of real processes, it is certainly a balancing act between complexity and computing time for energy system modeling.
A logical next step would be to find technologies for which the presented modeling techniques will improve results and give additional insights. Due to their nature, it is obvious that the electricity-generating technologies have the most impact in an energy system model. In this work mc-Si PV cells were selected, as a significant amount of energy demand and emissions are associated with their manufacturing. A further technology could be wind turbines which have a high steel demand, although the question of recycling also needs to be addressed for this case. By including the manufacturing process, not only the quality of energy system modeling will be improved, but also the potential sector coupling will be more realistically represented.
Finally, the potential of hydrogen, which can be used in case of iron-ore reduction, energy storage, power generation and fuel or process-heat supply, seems to be underestimated in most current studies. In order to fully demonstrate the potential of hydrogen, future models should be designed to be as flexible as possible, with regard to the coupling of sectors. In case, the central research question relates to aspects of sector coupling or even the potential of PtX, first, relevant sectors, must be identified. One good examples is, using hydrogen as a reduction agent for oxide in case of further mined ores. By using PtX as a fully integrated method through the whole value chain

of energy related products, a simple load flow calculation at energy level is no longer sufficient in this case. The material flow, another key element, must be introduced to increase the significance of future energy system models.

Bibliography

[1] Etheridge, D.M., et al. Law dome atmospheric co2 data: Igbp pages/world data center for paleoclimatology, 2001. URL: https://www1.ncdc.noaa.gov/pub/data/paleo/icecore/antarctica/law/law_co2.txt.

[2] Z. Zong-Ci, L. Yong, and H. Jian-Bin. A review on evaluation methods of climate modeling. *Advances in Climate Change Research*, 4(3):137–144, 2013. doi:10.3724/SP.J.1248.2013.137.

[3] L. Caesar, S. Rahmstorf, A. Robinson, G. Feulner, and V. Saba. Observed fingerprint of a weakening atlantic ocean overturning circulation. *Nature*, 556(7700):191–196, 2018. URL: https://www.nature.com/articles/s41586-018-0006-5.pdf, doi:10.1038/s41586-018-0006-5.

[4] Marco Bindi, Sally Brown, Ines Camilloni, Arona Diedhiou, Riyanti Djalante, Kristie L. Ebi, Francois Engelbrecht, Joel Guiot. Impacts of 1.5 °c of global warming on natural and human systems. URL: https://www.ipcc.ch/site/assets/uploads/sites/2/2019/06/SR15_Chapter3_Low_Res.pdf.

[5] United nations framework convention on climate change, 1992. URL: https://treaties.un.org/Pages/ViewDetailsIII.aspx?src=TREATY&mtdsg_no=XXVII-7&chapter=27&Temp=mtdsg3&clang=_en.

[6] Presse- und Informationsamt der Bundesregierung. Co2-emission, 2019. URL: https://www.bundesregierung.de/breg-de/themen/energiewende/co2-kohlenstoffdioxid-oder-kohlendioxid-emission-614692.

[7] Amtsblatt der Europäischen Union. Übereinkommen von paris: (Übersetzung), 2016.

[8] J. Rogelj, G. Luderer, R. C. Pietzcker, E. Kriegler, M. Schaeffer, V. Krey, and K. Riahi. Energy system transformations for limiting end-of-century warming to below 1.5 °c. *Nature Climate Change*, 5:519 EP –, 2015. URL: https://doi.org/10.1038/nclimate2572, doi:10.1038/nclimate2572.

[9] Council of the European Union. Tackling climate change in the eu, 2016. URL: https://www.consilium.europa.eu/en/policies/climate-change.

[10] Bundesministerium für Umwelt and Naturschutz und nukleare Sicherheit. Klimaschutzplan 2050: Klimaschutzpolitische grundsätze und ziele der bundesregierung, 2016. URL: www.bmu.de.

[11] M. Crippa, D. Guizzardi, M. Muntean, J. Olivier, E. Schaaf, E. Solazzo, and E. Vignati. *Fossil CO2 emissions of all world countries: 2018 report*, volume 29433 of *EUR, Scientific and technical research series*. Publications Office of the European Union, Luxembourg, 2018.

[12] IEA. *CO2 Emissions from Fuel Combustion 2018*. OECD, 2018. doi:10.1787/co2{\textunderscore}fuel-2018-en.

[13] European Comission. Tackling climate change in the eu - consilium, 2018. URL: https://www.consilium.europa.eu/en/policies/climate-change/.

[14] Bundesministerium für Wirtschaft und Energie. Gesetz für den ausbau erneuerbarer energien: Erneuerbare-energien-gesetz-eeg 2014, 2014.

[15] F. Ausfelder, H. E. Dura, K. Bareiß, K. Schönleber, and T. e. a. Hamacher. P2x roadmap 1.0 optionen für ein nachhaltiges energiesystem mit power-to-x technologien: Herausforderungen - potenziale - methoden - auswirkungen, 2018. URL: https://www.kopernikus-projekte.de/lw_resource/datapool/systemfiles/cbox/672/live/lw_pdf/p2x_roadmap_a4_v2.pdf;Power-to-X1.Roadmap.

[16] Forschungszentrum Jülich/Tricklabor. Mit power in die energiewende: Kopernikus-projekt „power-to-x“ #p2x, 2016. URL: https://www.youtube.com/watch?v=Eoip2nMapz0.

[17] T. Haas, R. Krause, R. Weber, M. Demler, and G. Schmid. Technical photosynthesis involving co 2 electrolysis and fermentation. *Nature Catalysis*, 1(1):32–39, 2018. URL: https://www.nature.com/articles/s41929-017-0005-1.pdf, doi:10.1038/s41929-017-0005-1.

[18] Aleksandar Lozanovski. Lca of co2 direct air capture: Beniver workshop, 2019.

[19] J.-O. Weidert, J. Burger, M. Renner, S. Blagov, and H. Hasse. Development of an integrated reaction–distillation process for the production of methylal. *Industrial & Engineering Chemistry Research*, 56(2):575–582, 2017. doi:10.1021/acs.iecr.6b03847.

[20] C. J. Baranowski, A. M. Bahmanpour, and O. Kröcher. Catalytic synthesis of polyoxymethylene dimethyl ethers (ome): A review. *Applied Catalysis B: Environmental*, 217:407–420, 2017. URL: http://www.sciencedirect.com/science/article/pii/S0926337317305507, doi:10.1016/j.apcatb.2017.06.007.

[21] S. Deutz, D. Bongartz, B. Heuser, A. Kätelhön, L. S. Langenhorst, A. Omari, M. Walters, J. Klankermayer, W. Leitner, A. Mitsos, S. Pischinger, and A. Bardow. Cleaner production of cleaner fuels: wind-to-wheel – environmental assessment of co2-based oxymethylene ether as a drop-in fuel. *Energy & Environmental Science*, 11(2):331–343, 2018. URL: https://pubs.rsc.org/en/content/articlepdf/2018/ee/c7ee01657c, doi:10.1039/C7EE01657C.

[22] Florian Ausfelder et al. Sektorkopplung – untersuchungen und Überlegungen zur entwicklung eines inteegrierten energiesystems.

[23] Kay Bareiß, Sarah Deutz, Susanne Forster, and Thomas Fröhlich, Cornela Merz, Andreas Paty, Dominik Poncette, Moritz Raab, Andreas Schreiber, Jürgen Sutter, Nils Tenhumberg, Petra Zapp. Technischer anhang p2x: Optionen für ein nachhaltiges energiesystem mit power-to-x technologien.

[24] M. Härtl, P. Seidenspinner, E. Jacob, and G. Wachtmeister. Oxygenate screening on a heavy-duty diesel engine and emission characteristics of highly oxygenated oxymethylene ether fuel ome1. *Fuel*, 153:328–335, 2015. URL: http://www.sciencedirect.com/science/article/pii/S0016236115002938, doi:10.1016/j.fuel.2015.03.012.

[25] Linde Engineering. Hydrogen, 2018. URL: https://www.linde-gas.at/de/images/1007_rechnen_sie_mit_wasserstoff_v110_tcm550-169419.pdf.

[26] Daniel Teichmann. Hydrogenious technologies: Systeme zur sicheren und effizienten wasserstoffspeicherung und -logistik mit lohc: Foliensatz, 2016.

[27] S. Brynolf, M. Taljegard, M. Grahn, and J. Hansson. Electrofuels for the transport sector: A review of production costs. *Renewable and Sustainable Energy Reviews*, 81:1887–1905, 2018. URL: http://www.sciencedirect.com/science/article/pii/S1364032117309358, doi:10.1016/j.rser.2017.05.288.

[28] C. Xue and C. Cheng. Chapter two - butanol production by clostridium. *Advances in Bioenergy*, 4:35–77, 2019. URL: http://www.sciencedirect.com/science/article/pii/S246801251830018X, doi:10.1016/bs.aibe.2018.12.001.

[29] European Comission. Eur-lex - 32000d1753 - de: Entscheidung nr. 1753/2000/eg des europäischen parlaments und des rates vom 22. juni 2000 zur einrichtung eines systems zur Überwachung der durchschnittlichen spezifischen co2 -emissionen neuer personenkraftwagen: Amtsblatt nr. l 202 vom 10/08/2000 s. 0001 - 0013, 2000. URL: https://eur-lex.europa.eu/legal-content/DE/TXT/HTML/?uri=CELEX:32000D1753&qid=1568212325131&from=DE.

[30] F. Ausfelder, H. E. Dura, K. Bareiß, K. Schönleber, and T. e. a. Hamacher. P2x roadmap 2.0 optionen für ein nachhaltiges energiesystem mit power-to-x technologien: Nachhaltigkeitseffekte - potenziale -entwicklungsmöglichkeiten, 2019.

[31] European Comission. Critical raw materials - internal market, industry, entrepreneurship and smes - european commission, 2019. URL: https://ec.europa.eu/growth/sectors/raw-materials/specific-interest/critical_en.

[32] G. A. Blengini, D. Blagoeva, J. Dewulf, C. Baranzelli, C. Torres De Matos, D. Pennington, B. Vidal-Legaz, E. Tzimas, L. Talens Peirò, C. Pavel, P. Nuss, V. Nita, F. Mathieux, A. Marmier, S. Manfredi, L. Mancini, C. E. Latunussa, Y. Kayam, P. Alves-Dias, and C. Ciupagea. *Assessment of the methodology for establishing the EU list of critical raw materials: Background report*, volume 28654 of *EUR. Scientific and technical research series*. Publications Office, Luxembourg, 2017.

[33] Bundesministerium für Wirtschaft und Forschung. Kopernikus-projekt p2x, 2016. URL: https://www.kopernikus-projekte.de/projekte/power-to-x.

[34] K. Bareiß, C. de La Rua, M. Möckl, and T. Hamacher. Life cycle assessment of hydrogen from proton exchange membrane water electrolysis in future energy systems. *Applied Energy*, 237:862–872, 2019. doi:10.1016/j.apenergy.2019.01.001.

[35] J. C. Koj, C. Wulf, and P. Zapp. Environmental impacts of power-to-x systems - a review of technological and methodological choices in life cycle assessments. *Renewable and Sustainable Energy Reviews*, 112:865–879, 2019. URL: http://www.sciencedirect.com/science/article/pii/S1364032119304228, doi:10.1016/j.rser.2019.06.029.

[36] Antje Wörner. Zukünftige speicher- und flexibilitätsoptionen durch power-to-x, 2014. URL: https://www.dlr.de/tt/Portaldata/41/Resources/dokumente/ess_2014/DLR-ESS-2014-Woerner_Zukuenftige_Speicher-_und_Flexibilitaetsoptionen_durch_Power-to-X.pdf.

[37] A. Sternberg and A. Bardow. Power-to-what? – environmental assessment of energy storage systems. *Energy & Environmental Science*, 8(2):389–400, 2015. URL: https://pubs.rsc.org/en/content/articlepdf/2015/ee/c4ee03051f, doi:10.1039/C4EE03051F.

[38] V. Neisch, R. Klar, and M. Aufleger, editors. *Powertower - Hydraulischer Energiespeicher*, 2012.

[39] M. Sterner and I. Stadler, editors. *Energiespeicher - Bedarf, Technologien, Integration*. Springer Vieweg, Berlin, 2. korrigierte und ergänzte auflage edition, 2017. doi:10.1007/978-3-662-48893-5.

[40] Andreas Jossen. Batteriespeichersysteme 1: Skript. 2010.

[41] Öko-Institut e.V. und Fraunhofer ISI. Klimaschutzszenario 2050.

[42] Fabio Gemelli. Tatsächlicher verbrauch: Mercedes eqc im test, 2019. URL: https://de.motor1.com/reviews/369022/tatsachlicher-verbrauch-mercedes-eqc-reichweite-test/.

[43] A. García, J. Monsalve-Serrano, D. Villalta, R. Lago Sari, V. Gordillo Zavaleta, and P. Gaillard. Potential of e-fischer tropsch diesel and oxymethylether (omex) as fuels for the dual-mode dual-fuel concept. *Applied Energy*, 253:113622, 2019. URL: http://www.sciencedirect.com/science/article/pii/S0306261919312966, doi:10.1016/j.apenergy.2019.113622.

[44] E. V. Kondratenko, G. Mul, J. Baltrusaitis, G. O. Larrazábal, and J. Pérez-Ramírez. Status and perspectives of co2 conversion into fuels and chemicals by catalytic, photocatalytic and electrocatalytic processes. *Energy & Environmental Science*, 6(11):3112–3135, 2013. URL: https://pubs.rsc.org/en/content/articlepdf/2013/ee/c3ee41272e, doi:10.1039/C3EE41272E.

[45] DIN e. V. Luftkonditionierer, flüssigkeitskühlsätze und wärmepumpen für die raumbeheizung und -kühlung und prozess-kühler mit elektrisch angetriebenen verdichtern - teil 1: Begriffe; deutsche fassung, 2019. URL: 27.01.2020.

[46] emobicon. Elektromobilität: Die post war schon früher elektrisch unterwegs, 2018. URL: https://emobicon.de/elektromobile-geschichte-der-berliner-post/.

[47] Volker Quaschning. Sektorkopplung durch die energiewende. URL: https://www.volker-quaschning.de/publis/studien/sektorkopplung/index.php.

[48] Exxon mobile. Primärenergieverbrauch in deutschland nach energieträger bis 2040 — statista. URL: https://de.statista.com/statistik/daten/studie/173855/umfrage/primaerenergieverbrauch-in-deutschland-seit-2000/.

[49] Marie-Luise Plappert, Manuel Rudolph, Carla Vollmer. Auswirkungen von mindestabstaenden zwischen windenergieanlagen und siedlungen auswertung im rahmen der uba-studie flaechenanalyse windenergie an land.

[50] IEA. Offshore wind outlook 2019. URL: https://www.iea.org/reports/offshore-wind-outlook-2019.

[51] G. B. Andresen, R. A. Rodriguez, S. Becker, and M. Greiner. The potential for arbitrage of wind and solar surplus power in denmark. *Energy*, 76:49–58, 2014. doi:10.1016/j.energy.2014.03.033.

[52] F. Wagner. Surplus from and storage of electricity generated by intermittent sources. *The European Physical Journal Plus*, 131(12):20, 2016. doi:10.1140/epjp/i2016-16445-3.

[53] B. Bundesnetzagentur. Monitoringbericht 2018.

[54] Länderarbeitskreis Energiebilanzen. Primärenergieverbrauch in terajoule — 2016, 2016. URL: http://www.lak-energiebilanzen.de/primaerenergieverbrauch-in-terajoule-2016/.

[55] Suedlink bewegt, 2016. URL: https://www.tennet.eu/de/unser-netz/onshore-projekte-deutschland/suedlink/dialog/mediathek/suedlink-bewegt/.

[56] C. Pellinger and T. Schmid. *Verbundforschungsvorhaben Merit Order der Energiespeicherung im Jahr 2030: Teil 1: Hauptbericht.* FFE Forschungsstelle für Energiewirtschaft e.V, München, Mai 2016.

[57] Christian Heilek. *Modellgestützte Optimierung des Neubaus und Einsatzes von Erzeugungsanlagen und Speichern für elektrische und thermische Energie im deutschen Energiesystem.* Dissertation, TUM, München, 2015.

[58] N-ERGIE Aktiengesellschaft. N-ergie kraftwerksstandort nürnberg: Unsere anlagen, 11.3.2020.

[59] Alexander Rosenkranz. Heizstab für pufferspeicher: Anwendung, 11.3.2020. URL: https://heizung.de/heizung/wissen/heizstab-fuer-pufferspeicher-die-anwendung/.

[60] D. Fischer. *Integrating heat pumps into smart grids.* Dissertation, Kungliga Tekniska Högskolan, 2017.

[61] Dohr. Grundwassertemperaturen münchen: Messungen 2009-2010. URL: https://www.muenchen.de/rathaus/Stadtverwaltung/Referat-fuer-Gesundheit-und-Umwelt/Wasser_und_Boden/Grundwasserdaten.html.

[62] Bayrisches Landesamt für Umwelt. Lufttemperatur: Jahresgrafik münchen stadt, 2010. URL: http://download.gkd.bayern.de/de/meteo/lufttemperatur/isar/muenchen-stadt-10865/jahreswerte?zr=jahr&art=&beginn=01.01.2010&ende=31.12.2010.

[63] Jörg Adolf, Christopher H. Balzer, Jurgen Louis, Uwe Schabla. and amfred Fischedick, Karin Arnold, Andreas Pastowski, Dietmar Schüwer. Shell hydrogen study: Energy of the future? sustainable mobility through fuel cells and h2, 2019. URL: https://www.dvgw.de/medien/dvgw/forschung/berichte/g3_01_12_tp_b_d.pdf.

[64] Frank Graf, Manuel Götz, Marco Henel, Tanja Schaaf, Robert Tichler. Technoökonomische studie von power-to-gas-konzepten teilprojekte b-d abschlussbericht.

[65] IEA. Technology roadmap hydrogen and fuel cells - technologyroadmaphydrogenandfuelcells-(1).aspx, 2015. URL: http://ieahydrogen.org/pdfs/TechnologyRoadmapHydrogenandFuelCells-(1).aspx.

[66] L. Weger, A. Abánades, and T. Butler. Methane cracking as a bridge technology to the hydrogen economy. *International Journal of Hydrogen Energy*, 42(1):720–731, 2017. URL: http://www.sciencedirect.com/science/article/pii/S0360319916333213, doi:10.1016/j.ijhydene.2016.11.029.

[67] A. Buttler and H. Spliethoff. Current status of water electrolysis for energy storage, grid balancing and sector coupling via power-to-gas and power-to-liquids: A review. *Renewable and Sustainable Energy Reviews*, 82:2440–2454, 2018. URL: http://www.sciencedirect.com/science/article/pii/S136403211731242X, doi:10.1016/j.rser.2017.09.003.

[68] Linde Group. Wasserstoff- und synthesegasanlagen. URL: https://www.linde-engineering.com/de/process_plants/hydrogen_and_synthesis_gas_plants/index.html.

[69] Linde Group. Petrochemical processing, 2016. URL: https://www.linde-engineering.com/de/process_plants/petrochemical-plants/index.html.

[70] Alan D. McNaught and Andrew Wilkinson. *IUPAC Compendium of Chemical Terminology*. IUPAC, Research Triagle Park, NC, 2009.

[71] X. D. Peng. Analysis of the thermal efficiency limit of the steam methane reforming process. *Industrial & Engineering Chemistry Research*, 51(50):16385–16392, 2012. doi:10.1021/ie3002843.

[72] Robert EDWARDS, Jean-François, LARIVÉ, David RICKEARD, Werner Weindorf. Well-to-tank report version 4.a: Jec well-to-wheels analysis: Jrc technical report.

[73] S. Müller, M. Stidl, T. Pröll, R. Rauch, and H. Hofbauer. Hydrogen from biomass: large-scale hydrogen production based on a dual fluidized bed steam gasification system. *Biomass Conversion and Biorefinery*, 1(1):55–61, 2011. URL: https://doi.org/10.1007/s13399-011-0004-4, doi:10.1007/s13399-011-0004-4.

[74] M. Ni, D. Y. Leung, M. K. Leung, and K. Sumathy. An overview of hydrogen production from biomass. *Fuel Processing Technology*, 87(5):461–472, 2006. URL: http://www.sciencedirect.com/science/article/pii/S0378382005001980, doi:10.1016/j.fuproc.2005.11.003.

[75] D. M. F. Santos, C. A. C. Sequeira, and J. L. Figueiredo. Hydrogen production by alkaline water electrolysis. *Química Nova*, 36(8):1176–1193, 2013. doi:10.1590/S0100-40422013000800017.

[76] T. Smolinka, M. Gu¨nther, J. Garche. Stand und entwicklungs- potential der wasserelektrolyse zur herstellung von wasserstoff aus regenerativen energien: Now-studie.

[77] Luca Bertuccioli, Alvin Chan, David Hart, Franz Lehner, Ben Madden, Eleanor Standen. Study on development of water electrolysis in the eu.

[78] O. Schmidt, A. Gambhir, I. Staffell, A. Hawkes, J. Nelson, and S. Few. Future cost and performance of water electrolysis: An expert elicitation study. *International Journal of Hydrogen Energy*, 42(52):30470–30492, 2017. URL: http://www.sciencedirect.com/science/article/pii/S0360319917339435, doi:10.1016/j.ijhydene.2017.10.045.

[79] F. Ausfelder, C. Beilmann, M. Bertau, S. Bräuninger, A. Heinzel, R. Hoer, W. Koch, F. Mahlendorf, A. Metzelthin, M. Peuckert, L. Plass, K. Räuchle, M. Reuter, G. Schaub, S. Schiebahn, E. Schwab, F. Schüth, D. Stolten, G. Teßmer, K. Wagemann, and K. Ziegahn. Energiespeicherung als element einer sicheren energieversorgung. *Chemie Ingenieur Technik*, 87(1-2):17–89, 2015. URL: https://onlinelibrary.wiley.com/doi/full/10.1002/cite.201400183, doi:10.1002/cite.201400183.

[80] Anika Regett, Christoph Pellinger und Sebastian Eller. Power2gas – hype oder schlüssel zur energiewende? - forschungsstelle für energiewirtschaft e.v., 2014. URL: https://www.ffe.de/publikationen/veroeffentlichungen/522-power2gas-hype-oder-schluessel-zur-energiewende.

[81] K. Schoots, F. Ferioli, G.J. Kramer, and B.C.C. van der Zwaan. Learning curves for hydrogen production technology: An assessment of observed cost reductions. *International Journal of Hydrogen Energy*, 33(11):2630–2645, 2008. URL: http://www.sciencedirect.com/science/article/pii/S0360319908002954, doi:10.1016/j.ijhydene.2008.03.011.

[82] O. Vozniuk, N. Tanchoux, J.-M. Millet, S. Albonetti, F. Di Renzo, and F. Cavani. Chapter 14 - spinel mixed oxides for chemical-loop reforming: From solid state to potential application. In S. Albonetti, S. Perathoner, and E. A. Quadrelli, editors, *Studies in Surface Science and Catalysis : Horizons in Sustainable Industrial Chemistry and Catalysis*, volume 178, pages 281–302. Elsevier, 2019. URL: http://www.sciencedirect.com/science/article/pii/B9780444641274000148, doi:10.1016/B978-0-444-64127-4.00014-8.

[83] P. H. Stefan Schütz. Klimaschutz und regenerativ erzeugte chemische energieträger – infrastruktur und systemanpassung zur versorgung mit regenerativen chemischen energieträgern aus in- und ausländischen regenerativen energien.

[84] V. Smil. *Enriching the earth: Fritz Haber, Carl Bosch, and the transformation of world food production*. MIT, Cambridge, Mass. and London, 2001.

[85] Ewald Günther. Stickstoff: Grundlage des stickstoffeinsatzes in der landwirtschaft.

[86] IEA. The future of hydrogen, 2019.

[87] IPTS - JRC. Anorganischer grundchemikalien: Ammoniak, säuren und düngemittel, 2007.

[88] Hydrogen in industry — hydrogen, 20.07.2019. URL: `https://hydrogeneurope.eu/hydrogen-industry`.

[89] M. Felgenhauer and T. Hamacher. State-of-the-art of commercial electrolyzers and on-site hydrogen generation for logistic vehicles in south carolina. *International Journal of Hydrogen Energy*, 40(5):2084–2090, 2015. `doi:10.1016/j.ijhydene.2014.12.043`.

[90] Johannes TöplerJochen Lehmann. *Wasserstoff und Brennstoffzelle: Technologien und Marktperspektiven*. Springer Vieweg, Berlin and Heidelberg, 2., aktualisierte und erweiterte auflage edition, 2017.

[91] Industrieverband Agrar e.V. Wichtige zahlen: Düngemittel- produktion-;arktlandwirtschaft, 2016. URL: `www.iva.de`.

[92] J. C. U. Brunke. Energieeinsparpotenziale von energieintensiven produktionsprozessen in deutschland : eine analyse mit hilfe von energieeinsparkostenkurven. URL: `https://elib.uni-stuttgart.de/handle/11682/9259`, `doi:10.18419/OPUS-9242`.

[93] Bayrisches Staatsministerium für Wirtschaft, Landesentwicklung und Energie. Energiedaten.bayern-kompakt. URL: `https://www.stmwi.bayern.de/energie-rohstoffe/daten-fakten/`.

[94] Bundesinformationszentrum Landwirtschaft:. Wie viel getreide benötigt man für ein brot?, 2019. URL: `https://www.iva.de/sites/default/files/benutzer/uid/publikationen/stick.pdf`.

[95] YARA GmbH & Co. KG. Beispiel einer düngebedarfs-berechnung, 2019. URL: `https://www.effizientduengen.de/kulturen_/beispiel-einer-duengebedarfs-berechnung/`.

[96] F.-X. Maidl, E. Sticksel, F. Retzer, and G. Fischbeck. Effect of varied n-fertilization on yield formation of winter wheat under particular consideration of mainstems and tillers. *Journal of Agronomy and Crop Science*, 180(1):15–22, 1998. `doi:10.1111/j.1439-037X.1998.tb00363.x`.

[97] Die große stahl-statistik 2017 - stahlmarkt. URL: `https://www.stahleisen.de/stahlmarkt/crossmedia/die-grosse-stahlstatistik-2017/`.

[98] Ralph Diermann. Grüner wasserstoff als klimaschützer: Der sauberstoff. *Spiegel Online*, 2019. URL: https://www.spiegel.de/wissenschaft/technik/gruener-wasserstoff-soll-die-industrie-klimaneutral-machen-a-1266023.html.

[99] P. Vogt. Co2-bilanz stahl: Ein beitrag zum klimaschutz.

[100] Marlies Uken. Deutschland ist europas gaszentrale. *ZEIT*, 2014, 30.Juni 2014. URL: https://www.zeit.de/wirtschaft/2014-06/erdgasspeicher.

[101] O. Schmidt, A. Hawkes, A. Gambhir, and I. Staffell. The future cost of electrical energy storage based on experience rates. *Nature Energy*, 2(8):17110, 2017. URL: https://www.nature.com/articles/nenergy2017110.pdf, doi:10.1038/nenergy.2017.110.

[102] R. Lee, S. Homan, N. Mac Dowell, and S. Brown. A closed-loop analysis of grid scale battery systems providing frequency response and reserve services in a variable inertia grid. *Applied Energy*, 236:961–972, 2019. doi:10.1016/j.apenergy.2018.12.044.

[103] Eebatt: Dezentrale stationäre batteriespeicher zur effizienten nutzung erneuerbarer energien und unterstützung der netzstabilität: Zwischenbericht.

[104] Christopher Schrader. Der netzschrittmacher. *Süddeutsche Zeitung*, 2019. URL: www.sueddeutsche.de/wissen/hamburg-curslack-strom-netz-frequenz-speicher-puffer-atomkraftwerke-1.4525360.

[105] Stefan Preiß. 48-mw-batteriespeicher geht in jardelund in betrieb. *EUWID Neue Energie Nachrichten*, 2018. URL: https://www.euwid-energie.de/48-mw-batteriespeicher-geht-in-jardelund-in-betrieb/.

[106] Philipp Kuhn. *Iterative model for the optimisation of storage capacity additions and operation in a power system with increasingly fluctuating generation.* Dissertation, TUM, München, 2013.

[107] D. G. Caglayan, N. Weber, H. U. Heinrichs, J. Linßen, M. Robinius, P. A. Kukla, and D. Stolten. Technical potential of salt caverns for hydrogen storage in europe. *International Journal of Hydrogen Energy*, 45(11):6793–6805, 2020. doi:10.1016/j.ijhydene.2019.12.161.

[108] M. Deutsch. Nachfrage und angebotsflexibilitäten insbesondere speicher: Impulsvortrag für den energiegipfel bayern - arbeitsgruppe 3.

[109] U.S. Energy Information Administration. International energy outlook 2016, 2016.

[110] H. Appel. Der grüne weg. *Frankfurter Allgemeine Zeitung*, 24.11.2016. URL: https://www.faz.net/aktuell/technik-motor/elektroautos-elektromobilitaet-nimmt-langsam-fahrt-auf-14537062.html.

[111] D. Kunde. Elektromobilität: Steht der durchbruch für elektroautos bevor? *Die Zeit*, 16.8.2019. URL: https://www.zeit.de/mobilitaet/2019-08/elektromobilitaet-e-autos-elektroautos-verkehrswende-marktzahlen.

[112] J. Becker. Der kampf um die zellen der zukunft. *Süddeutsche Zeitung*, 27.11.2019. URL: https://www.sueddeutsche.de/auto/elektromobilitaet-die-zellen-der-zukunft-1.4686781.

[113] C. B. Brian Cox. Background report: The environmental burdens of passenger cars: today and tomorrow, 2018.

[114] Supercharger — tesla deutschland, 21.2.2020. URL: https://www.tesla.com/de_DE/supercharger?redirect=no.

[115] A. Meintz, J. Zhang, R. Vijayagopal, C. Kreutzer, S. Ahmed, I. Bloom, A. Burnham, R. B. Carlson, F. Dias, E. J. Dufek, J. Francfort, K. Hardy, A. N. Jansen, M. Keyser, A. Markel, C. Michelbacher, M. Mohanpurkar, A. Pesaran, D. Scoffield, M. Shirk, T. Stephens, and T. Tanim. Enabling fast charging – vehicle considerations. *Journal of Power Sources*, 367:216–227, 2017. doi:10.1016/j.jpowsour.2017.07.093.

[116] Introducing v3 supercharging — tesla deutschland, 21.2.2020. URL: https://www.tesla.com/de_DE/blog/introducing-v3-Supercharging.

[117] Wolfgang Rudschies. Mercedes glc f-cell 2018 (x 253): Test, daten, preis — adac, 21.2.2020. URL: https://www.adac.de/rund-ums-fahrzeug/autokatalog/marken-modelle/mercedes/mercedes-glc-fuel-cell/.

[118] H. Eichlseder and M. Klell. *Wasserstoff in der Fahrzeugtechnik*. Vieweg+Teubner, Wiesbaden, 2010. doi:10.1007/978-3-8348-9674-2.

[119] L. David Roper. Tesla model s, 2019. URL: http://www.roperld.com/science/TeslaModelS.htm.

[120] Der glc f-cell: Erstes elektrofahrzeug mit brennstoffzelle und plug-in-hybrid-technologie, 2019. URL: https://www.daimler.com/produkte/pkw/mercedes-benz/glc-f-cell.html.

[121] K. Nagasawa, F. T. Davidson, A. C. Lloyd, and M. E. Webber. Impacts of renewable hydrogen production from wind energy in electricity markets on potential hydrogen demand for light-duty vehicles. *Applied Energy*, 235:1001–1016, 2019. doi:10.1016/j.apenergy.2018.10.067.

[122] I. Staffell, D. Scamman, A. Velazquez Abad, P. Balcombe, P. E. Dodds, P. Ekins, N. Shah, and K. R. Ward. The role of hydrogen and fuel cells in the global energy system. *Energy & Environmental Science*, 12(2):463–491, 2019. doi:10.1039/C8EE01157E.

[123] Frankfurter Allgemeine Zeitung GmbH. Unterwegs mit wasserstoff: Hessen plant größte brennstoffzellen-flotte der welt, 21.05.2019.

[124] Gustav Tuschen. Wolfgang prokopp daimler buses - citaro e-mobility platform mannheim, 09. november 2015.

[125] Susanne Adler, Martin Fuhrmann, Werner Stützel. Newsletter wasserstoff + brennstoffzelle: Interview mit dr.-ing. frank koch. (KW 28), 2019.

[126] M. Bareiß and D. Vorgerd. Thermomanagement für elektrisch angetriebene stadtbusse. *ATZ - Automobiltechnische Zeitschrift*, 121(2):52–55, 2019. URL: https://doi.org/10.1007/s35148-018-0227-9, doi:10.1007/s35148-018-0227-9.

[127] Klaus Schulte. Microsoft word - e-journ al-04 fliegen mit wasserstoff.doc, 2007. URL: http://klspublishing.de/fr_ejourns.htm.

[128] G.D. Brewer, R.E. Morris, R.h. Lange and J.W. Moore. Study of the application of hydrogen fuel to long-range subsonic transport aircraft.

[129] Heinz G. Klug. Cryoplane: Hydrogen fuelled aircraft.

[130] Regina Egelhofer. *Aircraft design driven by climate change*. Dissertation, TUM, München, 2008.

[131] F. Haglind, A. Hasselrot, and R. Singh. Potential of reducing the environmental impact of aviation by using hydrogen part i: Background, prospects and challenges. *The Aeronautical Journal*, 110(1110):533–540, 2006. doi:10.1017/S000192400000141X.

[132] F. Online. Wasserstoffbetriebene flugzeuge wären eine klimapest, 08.07.2012. URL: https://www.focus.de/wissen/klima/klimaprognosen/tid-26430/odenwalds-universum-erhitzt-wasserdampf-das-klima-wasserstoffbetriebene-flugzeuge-waeren-eine-klimapest_aid_778254.html.

[133] Climate change 2013: The physical science basis working group i contribution to the fifth assessment report of the intergovernmental panel on climate change, 2013.

[134] Hoffman, K. C, Palmedo, P. F. Reference energy systems and resources: Data for use in the assessment of energy technologies.

[135] S. C. Bhattacharyya and G. R. Timilsina. A review of energy system models. *International Journal of Energy Sector Management*, 4(4):494–518, 2010. doi:10.1108/17506221011092742.

[136] H.-K. Ringkjøb, P. M. Haugan, and I. M. Solbrekke. A review of modelling tools for energy and electricity systems with large shares of variable renewables. *Renewable and Sustainable Energy Reviews*, 96:440–459, 2018. URL: http://www.sciencedirect.com/science/article/pii/S1364032118305690, doi:10.1016/j.rser.2018.08.002.

[137] O. Kraan, G. J. Kramer, and I. Nikolic. Investment in the future electricity system - an agent-based modelling approach. *Energy*, 151:569–580, 2018. URL: http://www.sciencedirect.com/science/article/pii/S0360544218305012, doi:10.1016/j.energy.2018.03.092.

[138] S. Pfenninger, A. Hawkes, and J. Keirstead. Energy systems modeling for twenty-first century energy challenges. *Renewable and Sustainable Energy Reviews*, 33:74–86, 2014. URL: http://mediatum.ub.tum.de/doc/1285570/1285570.pdf, doi:10.1016/j.rser.2014.02.003.

[139] HOMER Energy. Homer- hybrid renewable and distributed generation system, 2014. URL: http://www.homerenergy.com.

[140] IES-ETSAP. Times modelling tool, 2001. URL: (https://iea-etsap.org/index.php/etsap-tools/model-generators/times.

[141] Johannes Dorfner, Magdalena Dorfner, Soner Candas, Sebastian Müller, Yunus Özsahin, Thomas Zipperle, Simon Herzog, Okan Akca, and Leonhard Odersky. urbs v0.7.3, 2017. URL: https://url.org/10.5281/zenodo.1228851.

[142] M. Howells, H. Rogner, N. Strachan, C. Heaps, H. Huntington, S. Kypreos, A. Hughes, S. Silveira, J. DeCarolis, M. Bazillian, and A. Roehrl. Osemosys: The open source energy modeling system: An introduction to its ethos, structure and development. *Energy Policy*, 39(10):5850–5870, 2011. URL: http://www.sciencedirect.com/science/article/pii/S0301421511004897, doi:10.1016/j.enpol.2011.06.033.

[143] Stefan Pfenninger. a multi-scale energy systems (muses) modeling framework, 2014. URL: http://www.callio.pe.

[144] S. Pfenninger and J. Keirstead. Renewables, nuclear, or fossil fuels? scenarios for great britain's power system considering costs, emissions and energy security. *Applied Energy*, 152:83–93, 2015. URL: http://www.sciencedirect.com/science/article/pii/S0306261915005656, doi:10.1016/j.apenergy.2015.04.102.

[145] O. Y. Edelenbosch, K. Kermeli, W. Crijns-Graus, E. Worrell, R. Bibas, B. Fais, S. Fujimori, P. Kyle, F. Sano, and D. P. van Vuuren. Comparing projections of industrial energy demand and greenhouse gas emissions in long-term energy models. *Energy*, 122:701–710, 2017. URL: http://www.sciencedirect.com/science/article/pii/S0360544217300178, doi:10.1016/j.energy.2017.01.017.

[146] H.-K. Ringkjøb, P. M. Haugan, and I. M. Solbrekke. A review of modelling tools for energy and electricity systems with large shares of variable renewables. *Renewable and Sustainable Energy Reviews*, 96:440–459, 2018. doi:10.1016/j.rser.2018.08.002.

[147] J. F. C. Dorfner. *Open Source Modelling and Optimisation of Energy Infrastructure at Urban Scale*. PhD thesis, TUM, München, 2015. URL: http://mediatum.ub.tum.de/doc/1506225/590329440273.pdf.

[148] Stephan Richter. Entwicklung einer methode zur integralen beschreibung und optimierung urbaner energiesysteme: Erste anwendung am beispiel augsburg.

[149] Wolfgang Mauch, Roger Corradini, Karin Wiesemeyer, Marco Schwentzek. Allokationsmethoden für spezifische co2-emissionen von strom und wärme aus kwk-anlagen. *Energiewirtschaftliche Tagesfragen*, 2010(9):12–14, 2010.

[150] Kay Bareiß and Thomas Hamacher. Klimaschutzteilkonzept - kapitel wärme. URL: https://www.greifswald.de/de/wirtschaft-bauen-verkehr/umwelt-und-klimaschutz/klimaschutz/index.html.

[151] Kay Bareiß. Power-to-heat for decarbonizing municipal district heating with high shares of wind energy: (proceedings), 12.06.2019.

[152] K. Bareiß. Potential of power-to-heat from excess wind energy on the city level. *Energy Sources, Part B: Economics, Planning, and Policy*, 31(9):1–18, 2020. doi:10.1080/15567249.2020.1740358.

[153] TransnetBW, TenneT, 50Hertz and Amprion. Onshore netzentwicklungplan 2024, erster entwurf der Übertragungsnetzbetreiber, szenario b2024, 2014. URL: https://www.netzentwicklungsplan.de/de/netzentwicklungsplaene/netzentwicklungsplaene-2024.

[154] Axel Holst. Netzintegration der erneuerbaren energien im land mecklenburg-vorpommern (netzstudie m-v i 2009). doi:10.13140/RG.2.1.4786.1362.

[155] Dr. Kurt Rohrig, Christoph Richts, Dr. Stefan Bofinger, Malte Jansen, Malte Siefert, Sebastian Pfaffel, Michael Durstewitz. Energiewirtschaftliche bedeutung der offshore-windenergy für die energiewende: Langfassung, 2012.

[156] Christoph Kost, Johannes N. Mayer, Jessica Thomsen, Niklas Hartmann, Harlotte Senkpiel, Simon Phillips, Sebastian Nold , Simon Lude, Thomas Schlegl. Studie: Stromgestehungskosten erneuerbare energien (november 2013), 2013.

[157] W. X. Jin Hao. Extended transmission line loadability curve by including voltage stability constrains. *2008 IEEE Canada Electric Power Conference*, 2008. doi:10.1109/EPC.2008.4763379.

[158] Turan Gönen. *Electrical Power Transmission System Engineering: Analysis and Design: Analysis and Design.* CRC Press, 2014. URL: https://site.ieee.org/northern-canada-pesias/files/2013/01/Transmission-Lines-Presentation.pdf.

[159] H. Martin, T. Hamacher, T. A. Deetjen, and M. E. Webber. Reduced transmission grid representation using the st. clair curve applied to the electric reliability council of texas. In *2017 14th International Conference on the European Energy Market (EEM): 6-9 June 2017, Dresden, Germany*, pages 1–5, Piscataway, NJ, 2017. IEEE. doi:10.1109/EEM.2017.7981961.

[160] Bill Kennedy. Transmission lines electricity's highways, 14.01.2013. URL: https://site.ieee.org/northern-canada-pesias/files/2013/01/Transmission-Lines-Presentation.pdf.

[161] 50hertz. Netzbelastung in der regelzone, 2018. URL: https://www.50hertz.com/de/Transparenz/Kennzahlen/Netzdaten/Netzbelastung/.

[162] Johannes Dorfner. implement proportional processes (still untested) · ojdo/urbs@0257631 · github, 2015. URL: https://github.com/ojdo/urbs/commit/0257631280621f511041a9077cd30b0a27ac580f.

[163] L. S. Karin Fuchs. Maximale energieeffizienz im bestand: Zeigen, was möglich ist. *Die Wohnungswirtschaft*, (30):32–35, 2015.

[164] Technische Universität München. Leitfaden energienutzungsplan, 2011.

[165] Agora Energiewende. Stromspeicher in der energiewende, 2014.

[166] Thomas Bründlinger, Julian Elizalde König, Oliver Frank, Dietmar Gründig, Christoph Jugel, Patrizia Kraft, Oliver Krieger, Stefan Mischinger, Dr. Philipp Prein, Hannes Seidl, Stefan Siemund, Christian Stolte, Mario Teichmann, Jakob Willke, Mareike Wolke. dena-leitstudie integrierte energiewende: Impulse für die gestaltung des energiesystems bis 2050, 2018.

[167] P. Matschilles. Analyse und aufbereitung der dena-leitstudie integrierte energiewende: Impulse für die gestaltung der energiesysteme bis 2050. *(not published)*, 2019.

[168] Kay Bareiß and Konrad Schönleber. Hydrogen from electrolyzers as an energy carrier for sector coupling in germany: Poster.

[169] Alexis Michael Bazzanella, Florian Ausfelder. *Low carbon energy and feedstock for the European chemical industry.* 2017.

[170] A. P. Hans-Martin Henning. Was kostet die energiewende? - wege zur transformation des deutschen energiesystems bis 2050, 2015.

[171] Umweltbundesamt. Entwicklung der energiebedingten treibhausgas-emissionen nach quellgruppen, 2017. URL: `https://www.umweltbundesamt.de/daten/energie/energiebedingte-emissionen#textpart-1`.

[172] Kais Siala. Increasing the spatial resolution of merra-2 reanalysis data for energy system modeling, 12.04.2019. URL: `http://www.donellameadows.org/wp-content/userfiles/Limits-to-Growth-digital-scan-version.pdf`.

[173] Felix Chr. Matthes, Franziska Flachsbarth, Charlotte Loreck, Hauke Hermann, Hanno Falkenberg, and Vanessa Cook. *Zukunft Stromsystem II - Regionalisierung der erneuerbaren Stromerzeugung vom Ziel her denken.*

[174] Umweltbundesamt. *Potenzial der Windenergie an Land*, volume 2013. 2013. URL: `https://www.umweltbundesamt.de/publikationen/potenzial-windenergie-an-land`.

[175] Karl Albert Janker. *Aufbau und Bewertung einer für die Energiemodellierung verwendbaren Datenbasis an Zeitreihen erneuerbarer Erzeugung und sonstiger Daten.* Dissertation, TUM.

[176] K. Bareiß, K. Schönleber, and T. Hamacher. Szenarien für den strommix zukünftiger, flexibler verbraucher am beispiel von p2x-technologien. URL: `https://mediatum.ub.tum.de/node?id=1436016`.

[177] infas and DLR. Mobilität in deutschland 2008, tabellenband, 2008. URL: `http://www.mobilitaet-in-deutschland.de/mid2008-publikationen.html`.

[178] Kraftfahrt-Bundesamt. Verkehr in kilometern der deutschen kraftfahrzeuge im jahr 2017. URL: `https://www.kba.de/DE/Statistik/Kraftverkehr/VerkehrKilometer/verkehr_in_kilometern_node.html`.

[179] Volker Busack, Manfred Veenker, Ulrich Hoffmann, Albert Großmann. Power to gas: Neues gas in alten leitungen - werkstofffragen. *Energie — Wasser-Praxis*, (9), 2014.

[180] Holger Dörr, Kerstin Kröger, Frank Graf, Wolfgang Köppel. Untersuchungen zur einspeisung von wasserstoff in ein ergasnetz. *Energie — Wasser-Praxis*, 2016.

[181] Peter Wasserscheid. Lohc vortrag jülich, 2018. URL: https://www.youtube.com/watch?v=sjiB5kwRUvQ.

[182] IFA. Gestis-stoffdatenbank (dibenzyltoluol), 2019. URL: http://gestis.itrust.de/nxt/gateway.dll/gestis_de/492182.xml?f=templatesfn=default.htm3.0.

[183] R. G. Hunt, W. E. Franklin, and R. G. Hunt. Lca – how it came about. *The International Journal of Life Cycle Assessment*, 1(1):4–7, 1996. URL: https://doi.org/10.1007/BF02978624, doi:10.1007/BF02978624.

[184] Donella H. Meadows and Dennis L. Meadows, Jorgen Randers, William W. Behrens. *The Limits to growth: A Report for the Club of Romes's Project on the predicament of Mankind*. Universe Books, 1972.

[185] F. Zeman. *Metropolitan Sustainability: Understanding and Improving the Urban Environment*, volume no. 34 of *Woodhead Publishing series in energy*. Woodhead Pub Ltd, Cambridge, UK and Philadelphia, PA, 2012. URL: http://search.ebscohost.com/login.aspx?direct=true&scope=site&db=nlebk&db=nlabk&AN=680495.

[186] R. G. Hunt, J. D. Sellers, and W. E. Franklin. Resource and environmental profile analysis: A life cycle environmental assessment for products and procedures. *Environmental Impact Assessment Review*, 12(3):245–269, 1992. URL: http://www.sciencedirect.com/science/article/pii/019592559290020X, doi:10.1016/0195-9255(92)90020-X.

[187] DIN Deutsches Institut für Normung e.V. Umweltmanagement - Ökobilanz - grundsätze und rahmenbedingungen (iso 14040:2006); deutsche und englische fassung en iso 14040:2006, 2009-11. URL: https://www.din.de/de/mitwirken/normenausschuesse/nagus/normen/wdc-beuth:din21:122442325.

[188] M. A. Curran. Life-cycle assessment. In S. E. Jørgensen, editor, *Encyclopedia of ecology*, pages 2168–2174. Elsevier, Amsterdam, 2008. doi:10.1016/B978-008045405-4.00629-7.

[189] J. Ellsmoor. Electric vehicles are driving demand for lithium - with environmental consequences, 2019. URL: https://www.forbes.com/sites/jamesellsmoor/2019/06/10/electric-vehicles-are-driving-demand-for-lithium-with-environmental-consequences/.

[190] L. A.-W. Ellingsen, B. Singh, and A. H. Strømman. The size and range effect: lifecycle greenhouse gas emissions of electric vehicles. *Environmental Research Letters*, 11(5):054010, 2016. doi:10.1088/1748-9326/11/5/054010.

[191] A. Katwala. The spiralling environmental cost of our lithium battery addiction, 2018. URL: https://www.wired.co.uk/article/lithium-batteries-environment-impact.

[192] IPCC. Climate change 2013: The physical science basis, 2013. URL: http://www.ipcc.ch/report/ar5/wg1/.

[193] M. Z. Hauschild, R. K. Rosenbaum, and S. I. Olsen. *Life Cycle Assessment: Theory and Practice*. Springer International Publishing, Cham, 2018. doi:10.1007/978-3-319-56475-3.

[194] David R. Lide. *CRC handbook of chemistry and physics: A ready-reference book of chemical and physical data*. CRC Press, Boca Raton, 76. ed. edition, 1996.

[195] P. Trinke, B. Bensmann, and R. Hanke-Rauschenbach. Experimental evidence of increasing oxygen crossover with increasing current density during pem water electrolysis. *Electrochemistry Communications*, 82:98–102, 2017. doi:10.1016/j.elecom.2017.07.018.

[196] M. Dowson, M. Grogan, T. Birks, D. Harrison, and S. Craig. Streamlined life cycle assessment of transparent silica aerogel made by supercritical drying. *Applied Energy*, 97:396–404, 2012. URL: http://www.sciencedirect.com/science/article/pii/S0306261911007446, doi:10.1016/j.apenergy.2011.11.047.

[197] GmbH SV. Drying by adsorption, 2017. URL: https://silica.berlin/en/air-and-gas-drying.html.

[198] M. Bernt and H. A. Gasteiger. Influence of ionomer content in iro 2 /tio 2 electrodes on pem water electrolyzer performance. *Journal of The Electrochemical Society*, 163(11):F3179–F3189, 2016. doi:10.1149/2.0231611jes.

[199] Qi Feng, Xiao Zi Yuan, Gaoyang Liu, Bing Wei, Zhen Zhang, Hui Li, and Haijiang Wang. A review of proton exchange membrane water electrolysis on degradation mechanisms and mitigation strategies. *Journal of Power Sources*, 366:33–55, 2017. doi:10.1016/j.jpowsour.2017.09.006.

[200] M. Bernt, A. Siebel, and H. A. Gasteiger. Analysis of voltage losses in pem water electrolyzers with low platinum group metal loadings. *Journal of The Electrochemical Society*, 165(5):F305–F314, 2018. doi:10.1149/2.0641805jes.

[201] U. Babic, M. Suermann, F. N. Büchi, L. Gubler, and T. J. Schmidt. Critical review–identifying critical gaps for polymer electrolyte water electrolysis development. *Journal of The Electrochemical Society*, 164(4):F387–F399, 2017. doi:10.1149/2.1441704jes.

[202] M. Eypasch, M. Schimpe, A. Kanwar, T. Hartmann, S. Herzog, T. Frank, and T. Hamacher. Model-based techno-economic evaluation of an electricity storage system based on liquid organic hydrogen carriers. *Applied Energy*, 185:320–330, 2017. URL: http://www.sciencedirect.com/science/article/pii/S0306261916315094, doi:10.1016/j.apenergy.2016.10.068.

[203] M. Wagner and I. Lewandowski. Relevance of environmental impact categories for perennial biomass production. *GCB Bioenergy*, 9(1):215–228, 2017. doi:10.1111/gcbb.12372.

[204] Edgar Neumann. Feinstaubalarm und zur luftreinhalteplanung in stuttgart, 2018. URL: https://vm.baden-wuerttemberg.de/de/mensch-umwelt/luftreinhaltung/feinstaubalarm/faq-luftreinhaltung-stuttgart/?type=98.

[205] W. Chen, J. Hong, X. Yuan, and J. Liu. Environmental impact assessment of monocrystalline silicon solar photovoltaic cell production: a case study in china. *Journal of Cleaner Production*, 112:1025–1032, 2016. URL: http://www.sciencedirect.com/science/article/pii/S0959652615011130, doi:10.1016/j.jclepro.2015.08.024.

[206] J. Lieberei and S. H. Gheewala. *Resource depletion assessment of renewable electricity generation technologies–comparison of life cycle impact assessment methods with focus on mineral resources*, volume 22. 2017. URL: https://doi.org/10.1007/s11367-016-1152-3, doi:10.1007/s11367-016-1152-3.

[207] actionaid. Human rights in wind turbine supply chains: Towards a truly sustainable energy transition, 2018. URL: https://www.somo.nl/wp-content/uploads/2018/01/Final-ActionAid_Report-Human-Rights-in-Wind-Turbine-Supply-Chains.pdf.

[208] W. McDowall, B. Solano Rodriguez, A. Usubiaga, and J. Acosta Fernández. Is the optimal decarbonization pathway influenced by indirect emissions? incorporating indirect life-cycle carbon dioxide emissions into a european times model. *Journal of Cleaner Production*, 170:260–268, 2018. doi:10.1016/j.jclepro.2017.09.132.

[209] R. Dufo-López, J. L. Bernal-Agustín, J. M. Yusta-Loyo, J. A. Domínguez-Navarro, I. J. Ramírez-Rosado, J. Lujano, and I. Aso. Multi-objective optimization minimizing cost and life cycle emissions of stand-alone pv-wind-diesel systems with batteries storage. *Applied Energy*, 88(11):4033–4041, 2011. doi:10.1016/j.apenergy.2011.04.019.

[210] F. You, L. Tao, D. J. Graziano, and S. W. Snyder. Optimal design of sustainable cellulosic biofuel supply chains: Multiobjective optimization coupled with life cycle assessment and input-output analysis. *AIChE Journal*, 58(4):1157–1180, 2012. URL: https://aiche.onlinelibrary.wiley.com/doi/full/10.1002/aic.12637, doi:10.1002/aic.12637.

[211] M. Pehl, A. Arvesen, F. Humpenöder, A. Popp, E. G. Hertwich, and G. Luderer. Understanding future emissions from low-carbon power systems by integration of life-cycle assessment and integrated energy modelling. *Nature Energy*, 2(12):939–945, 2017. doi:10.1038/s41560-017-0032-9.

[212] Pamela L. Spath, Margaret K. Mann, Dawn R. Kerr. Life cycle assessment of coal-fired power production.

[213] D. H. Filsinger and D. B. Bourrie. Silica to silicon: Key carbothermic reactions and kinetics. *Journal of the American Ceramic Society*, 73(6):1726–1732, 1990. doi:10.1111/j.1151-2916.1990.tb09820.x.

[214] Y. Jiao, A. Salce, W. Ben, F. Jiang, X. Ji, E. Morey, and D. Lynch. Siemens and siemens-like processes for producing photovoltaics: Energy payback time and lifetime carbon emissions. *JOM*, 63(1):28–31, 2011. doi:10.1007/s11837-011-0007-4.

[215] A. M. Zhilkashinova, S. K. Kabdrakhmanova, A. V. Troyeglazova, and M. B. Abilev. Structure and properties of metallurgical-grade silicon. *Silicon*, 10(5):2201–2210, 2018. doi:10.1007/s12633-017-9751-6.

[216] S. G. Hutchison, L. S. Richardson, and C. M. Wai. Carbothermic reduction of silicon dioxide– a thermodynamic investigation. *Metallurgical Transactions B*, 19(2):249–253, 1988. doi:10.1007/BF02654209.

[217] Y. Sakaguchi, M. Ishizaki, T. Kawahara, M. Fukai, M. Yoshiyagawa, and F. Aratani. Production of high purity silicon by carbothermic reduction of silica using ac-arc furnace with heated shaft. *ISIJ International*, 32(5):643–649, 1992. doi:10.2355/isijinternational.32.643.

[218] A. Schei, J. K. Tuset, and H. Tveit. *Production of high silicon alloys*. TAPIR, Trondheim, 1998.

[219] Klevan Ole Svein. Removal of c and sic from si and fesi during ladle refining and solidification, 1997. URL: http://hdl.handle.net/11250/248844.

[220] J. Safarian, G. Tranell, and M. Tangstad. Processes for upgrading metallurgical grade silicon to solar grade silicon. *Energy Procedia*, 20:88–97, 2012. URL: http://www.sciencedirect.com/science/article/pii/S1876610212007412, doi:10.1016/j.egypro.2012.03.011.

[221] F. Chigondo. From metallurgical-grade to solar-grade silicon: An overview. *Silicon*, 10(3):789–798, 2018. URL: https://doi.org/10.1007/s12633-016-9532-7, doi:10.1007/s12633-016-9532-7.

[222] C. L. Yaws, K.-Y. Li, T. C. Chu, C. S. Fang, R. Lutwack, and A. Briglio. New technologies for solar energy silicon–cost analysis of dichlorosilane process. *Solar Energy*, 27(6):539–546, 1981. doi:10.1016/0038-092X(81)90049-9.

[223] C. L. Yaws, K. Y. Li, and S. M. Chou. Economics of polysilicon processes, 1986. URL: https://ntrs.nasa.gov/search.jsp?R=19860017211.

[224] R. Lutwack. A u.s. view of silicon production processes. In W. Palz and W. Palz, editors, *Photovoltaic Solar Energy Conference: Proceedings of the International Conference, held at Cannes, France, 27-31 October 1980*, pages 220–227, Dordrecht, 1981. Springer Netherlands. doi:10.1007/978-94-009-8423-3\textunderscore.

[225] A Ciftja, T Engh, M Tangstad. Refining and recycling of silicon: A review. URL: http://hdl.handle.net/11250/244462.

[226] W. O. Filtvedt, M. Javidi, A. Holt, M. C. Melaaen, E. Marstein, H. Tathgar, and P. A. Ramachandran. Development of fluidized bed reactors for silicon production. *Solar Energy Materials and Solar Cells*, 94(12):1980–1995, 2010. doi:10.1016/j.solmat.2010.07.027.

[227] D. Y. Goswami and Y. Zhao. *Proceedings of ISES World Congress 2007 (Vol. I - Vol. V)*. Springer Berlin Heidelberg, Berlin, Heidelberg, 2009. doi:10.1007/978-3-540-75997-3.

[228] J. C. Anglézio, C. Servant, and F. Dubrous. Characterization of metallurgical grade silicon. *Journal of Materials Research*, 5(9):1894–1899, 1990. doi:10.1557/JMR.1990.1894.

[229] N. Watanabe, Y. Kondo, D. Ide, T. Matsuki, H. Takato, and I. Sakata. Characterization of polycrystalline silicon wafers for solar cells sliced with novel fixed-abrasive wire. *Progress in Photovoltaics: Research and Applications*, 18(7):485–490, 2010. doi:10.1002/pip.923.

[230] K. C. Sabat, P. Rajput, R. K. Paramguru, B. Bhoi, and B. K. Mishra. Reduction of oxide minerals by hydrogen plasma: An overview. *Plasma Chemistry and Plasma Processing*, 34(1):1–23, 2014. doi:10.1007/s11090-013-9484-2.

[231] J. F. Plaul, W. Krieger, and E. Bäck. Reduction of fine ores in argon-hydrogen plasma. *steel research international*, 76(8):548–554, 2005. doi:10.1002/srin.200506055.

[232] Siegfried Strämke and Herbert Wilhelmi. Verfahren zur herstellung von silicium für solarzellen: Offenlegungsschrift, 18.06.1979.

[233] Jochem Hahn, Uwe Kerat, Christina Schmid. Verfahren zur herstellung von hochreinem silizium: Veröffentlichung der int. anmeldung, 15.09.2011.

[234] Dr.- Ing. Stefan Laure. Hochleistungsplasmaverfahren für die wirtschaftliche produktion von solargrade-silizium. URL: https://www.dbu.de/projekt_23845/01_db_2848.html.

[235] Dr.- Ing. Stefan Laure. Hochreine, kristalline silizium-absorber.

[236] A. Demin. Reaktionstechnische untersuchungen zur hydrochlorierung von metallurgischem silicium. doi:10.18419/OPUS-1357.

[237] Karin Treyer. Ecoinvent 3.3 dataset documentation: electricity production, photovoltaic, 570kwp open ground installation, multi-si - de.

[238] Niels Jungbluth, Matthias Stucki, Karin Flury, Rolf Frischknecht, and Sybille Büsser. Life cycle inventories of photovoltaics.

[239] Brockhaus Enzyklopädie, editor. volume 9. Mannheim, 19 edition, 1989.

[240] U. S. EPA, OAR, OAP, and CCD. The social cost of carbon, 14.02.2017. URL: https://19january2017snapshot.epa.gov/climatechange/social-cost-carbon_.html.

[241] K. Ricke, L. Drouet, K. Caldeira, and M. Tavoni. Country-level social cost of carbon. *Nature Climate Change*, 8(10):895, 2018. URL: https://www.nature.com/articles/s41558-018-0282-y.pdf, doi:10.1038/s41558-018-0282-y.

[242] M. Uken and K. Schuler. Koalitionsausschuss: Das steht im klimaprogramm der koalition. *Die Zeit*, 20.9.2019. URL: https://www.zeit.de/politik/2019-09/koalitionsausschuss-klimaschutz-klimakabinett-klimapolitik-co2-steuer#co2-preis.

[243] G. S. Latta, J. S. Baker, R. H. Beach, S. K. Rose, and B. A. McCarl. A multi-sector intertemporal optimization approach to assess the ghg implications of u.s. forest and agricultural biomass electricity expansion. *Journal of Forest Economics*, 19(4):361–383, 2013. URL: http://www.sciencedirect.com/science/article/pii/S1104689913000226, doi:10.1016/j.jfe.2013.05.003.

[244] M. R. Kühne. *Drivers of energy storage demand in the German power system: an analysis of the influence of methodology and parameters on modelling results.* Dissertation, TUM, München.

[245] Bundesministerium für Umwelt, Naturschutz, Bau und Reaktorsicherheit. Klimaschutz in zahlen - fakten, trends und impulse deutscher klimapolitik, ausgabe 2017, 2017. URL: www.bmub.bund.de.

[246] T. H. Florian Botzenhart. A roadmap for the future energy infrastructure in salzburg.

[247] P.L. Spath and M.K. Mann. Life cycle assessment of hydrogen production via natural gas steam reforming.

[248] Volkswagen. Ökobilanz im volkswagen konzern, 21.08.2019. URL: https://www.volkswagenag.com/de/news/stories/2019/04/from-the-well-to-the-wheel.html.

A Appendix

A.1 PtH: case study

The costs for differently technologies of the case-study are listed in Table A.1.

Table A.1: Costs for energy in the PtH case-study

Technology	**Investment (1000 €/MW)**	**Variable (€/MWh)**
Gas heater	300	80
Photovoltaic system	1,920	0
Heat pump	900	Electricity
Solar thermal system	1,920	0
District heat	Installed	65
Surplus power (PtH)	0	0
Electricity (Grid)	0	253
centralized heat storage	11.3	0
decentralized heat storage	88	0

In case of the renovation scenario, different assumptions from earlier work was taken from [246]. In Figure A.1 the costs for different degree of renovations is plotted. It is assumed, that in average, 18% of heat demand is saved during the 1st renovation cycle. The second cycle with further reduce heat demand by 28% compared to a building of the corresponding class and age without an renovation cycle.

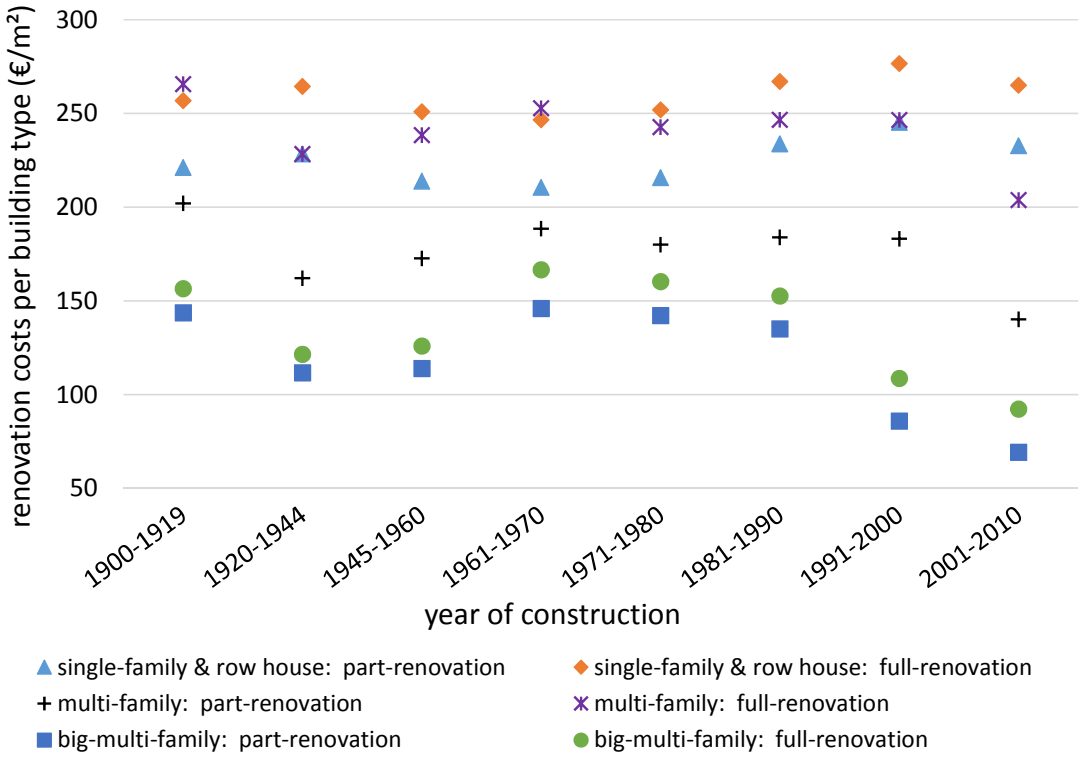

Figure A.1: Renovation costs for different building types and year of construction used for the corresponding scenarios

In the year 2030 following technologies are installed as solved by the model, stated in Table A.2 and Table A.3. Numbers in brackets are not ought to summed up for calculating the total.

Table A.2: NDH technologies used in 2030

Technology	Power (MW)	Energy (MWh)	CO_2 (tonne)
Gas heater	51	133,419	32,152
Heat pump[a]	13.6	37,596	2,597
Electricity (Grid)	-	(8,324)	(2,597)
Electricity (PV)	(1.5)	(1,075)	0
Total	66.1	171,015	34,649

[a] $COP = 4$

Table A.3: DH technologies used in 2030

Technology	Power (MW)	Energy (MWh)	CO_2 (tonne)
CHP	Already installed	155,356	32,158
Electric heaters	101	61,130	0
Electricity (Grid)	-	0	0
Excess power	-	(61,130)	0
Electricity (PV)	From NDH	(250)	0
Storage	(96)	(944)	0
Total	66.1	216,736	32,158

A.2 Full-load hours used for the energy-system model

Following heatmaps are representing the full load hours of wind and PV installations used for the energy system model. They are itemized by each federal state of Germany as well as the quality of the location which is rated by the numbers 1-8.

Full-load hours	1	2	3	4	5	6	7	8
'Baden-Württemberg'	928	1136	1021	1033	1038	990	1026	1065
'Bayern'	893	1007	957	976	982	912	951	982
'Berlin'	872	874	874	874	874	0	0	0
'Brandenburg'	846	933	881	892	897	860	869	906
'Bremen'	879	879	879	879	879	0	0	0
'Hamburg'	861	850	861	850	850	0	0	0
'Hessen'	859	995	925	941	948	892	915	973
'MV'	876	868	872	881	883	855	881	888
'Niedersachsen'	861	910	879	884	885	872	881	886
NRW	881	969	904	919	927	876	898	939
'Rheinland.	859	1047	962	971	975	914	955	1004
'Saarland'	951	1011	967	988	994	951	973	1011
'Sachsen-Anhalt'	863	926	900	912	916	874	894	929
'Sachsen'	888	937	911	909	909	916	911	901
'Schleswig-Holstein'	905	897	880	887	889	870	880	894
'Thüringen'	876	930	897	902	902	897	876	916

Figure A.2: full-load hours for mc-si PV panels on the norther hemisphere for different qualities of locations. Data created from the matlab tool [175] by following configuration: azimuth: 80% south, 10% east/west, 30° inclination. 1= Worst location, 2= Best location, 3= Equal distribution, 4= Linear distribution, 5= Slightly exponential distribution, 6= Worst third, 7= Middle third, 8= Best third

Full-load hours	1	2	3	4	5	6	7	8
'Baden-Württemberg'	615	1764	1370	1486	1506	962	1441	1607
'Bayern'	277	1909	1353	1478	1509	783	1406	1677
'Berlin'	2506	2515	2514	2515	2515	0	0	0
'Brandenburg'	2358	2880	2527	2606	2637	2411	2537	2708
'Bremen'	2870	2870	2870	2870	2870	0	0	0
'Hamburg'	2878	2910	2910	2910	2910	0	0	0
'Hessen'	1264	2510	1914	2021	2058	1607	1929	2229
'MV'	2647	4120	3080	3300	3407	2814	2983	3476
'Niedersachsen'	1835	4413	2810	2932	2977	2411	2795	3171
NRW	1988	2852	2546	2583	2597	2337	2574	2735
'Rheinland.	1362	2492	1933	2035	2062	1601	1969	2221
'Saarland'	1362	1890	1789	1850	1853	1362	1792	1890
'Sachsen-Anhalt'	1835	2775	2411	2457	2474	2253	2442	2649
'Sachsen'	1504	2390	2128	2210	2228	1711	2128	2328
'Schleswig-Holstein'	2878	4629	3393	3651	3747	3129	3586	4050
'Thüringen'	1474	2216	1911	2033	2057	1643	1920	2116
Nordsee'	3152	4316	3866	3997	4034	3331	3815	4136
Ostsee'	3001	4909	4422	4530	4564	3704	4416	4767

Figure A.3: full-load hours for different wind locations of a Vestas V112/3000. Data created from the matlab tool [175] by following configuration: azimuth: 80% south, 10% east/west, 30° inclination. 1= Worst location, 2= Best location, 3= Equal distribution, 4= Linear distribution, 5= Slightly exponential distribution, 6= Worst third, 7= Middle third, 8= Best third

A.3 LCA: Impact categories of the PEMWE

In the following Table A.4 all impact categories for the PEMWE are listed according to their scenarios. The values of most categories reduce with and increased share of renewable energy in the electricity. However the value for metal depletion (MD) increases, as described in Chapter 4. Also the value for human toxicity (HT) is an outlier in the scenario 2050 (80) in baseload. Here, still 40% of the electricity is produced by CCGT with a very low specific HT number in contrast to coal. As the production of PV and windturbines works with harmful materials (e.g. $SiCl_4$), the HT value increases again with the increase of renewable energy.

Table A.4: Impact categories for PEMWE in 2017, 2030 and 2050 (CC= Climate change, OD= Ozone depletion, TA= Terrestrial acidification, HT= Human toxicity, POF= Photochemical oxidant formation, PM= Particulate matter formation, MD= Metal depletion)

Impact category (unit)	2017 baseload	2030 baseload	2030 renewable	2050 (80) baseload	2050 (80) renewable	2050 (90) baseload	2050 (90) renewable
CC (kg CO_2-eq.)	29.5	16.2	3.4	11.6	3.0	3.9	2.9
OD (10^{-6} kg CFC-11eq.)	2.6	1.7	6.3	2.6	2.3	1.2	1.2
TA (10^{-2} kg SO_2 eq.)	4.7	2.7	2.2	2.5	2.1	2.0	1.9
HT (kg 1,4-DB eq.)	24.8	9.3	6.3	3.9	5.6	5.5	5.7
POF (10^{-2} kg NMVOC)	3.4	2.1	1.3	2.0	1.3	1.3	1.2
PM (10^{-2} kg PM10 eq.)	1.6	1.3	1.1	1.2	1.1	1.0	1.0
MD (kg Fe-eq.)	0.5	1.0	1.6	1.4	1.4	1.6	1.5

For completion, the cumulative energy demand (CED) is shown in the following Table A.5 in addition to the impact categories. The CED describes the totality of primary energetically evaluated expenditure that arises in connection with production, use and disposal of an economic good (product or service). In contrast to gray energy, the CED also includes the energy consumption during use phase and is therefore more comprehensive. The energy expenditure can be differentiated according to renewable and non renewable components whereas the non renewable represents energy from fossil or nuclear power sources. The CED for the SMR is stated with 183 MJ/kgH_2 (LHV basis) by Spath [247], from which almost 90% originate from the natural gas feedstock.

Table A.5: cumulative energy demand (CED) for PEMWE in 2017, 2030 and 2050 separated by renewable and non-renewable energy

CED (MJ/kg H_2)	2017 baseload	2030 baseload	2030 renewable	2050 (80) baseload	2050 (80) renewable	2050 (90) baseload	2050 (90) renewable
renewable	128	214	220	134	220	208	220
non renewable	432	149	40	293	39	56	38

A.4 LCA: comparison of vehicle kilometer

By comparing hydrogen as a fuel for FCVs versus conventional petrol-driven vehicles, in a cradle-to-wheel analysis, CO_2 emissions can be greatly reduced in some cases. Of course other impact categories need to be observed when the full spectrum of environmental issues are the scope. The global warming impact of the different scenarios are analyzed by comparing hydrogen from PEMWE, as a fuel in FCV with a petrol driven 1.0 l TSI VW Golf (81 kW). The values for the ICE are taken from the latest P2X roadmap [30], for the FCV from [113] and the BEV values from [248]. The Golf is stated to consume 5 l/100 km today and 3.7 l /100 km in 2050. As petrol has a LHV of 43.2 MJ/km with a density of 745 kg/m^3 this corresponds to 1.6 MJ-1.2 MJ/km. Compared to combustion, a fuel cell vehicle burns hydrogen at a higher efficiency with 1.05 kg H_2 today and 0.86 kg H_2 in future per 100 km or 1.3-1.0 MJ/km. BEV are the third concept of mobility that is used for comparison. In this case, the eGolf with an energy demand of 14 kWh/100km (0.5 MJ/km) are used. This value is assumed to stay constant for future as relevant increase in efficiencies of the comparatively simple drivetrain are not expected. The emissions from the manufacturing of the vehicles are

shaped as gray bars in Figure A.4, allocated to the total mileage, whereas the green bars depict the emissions during usage originated from fuel.

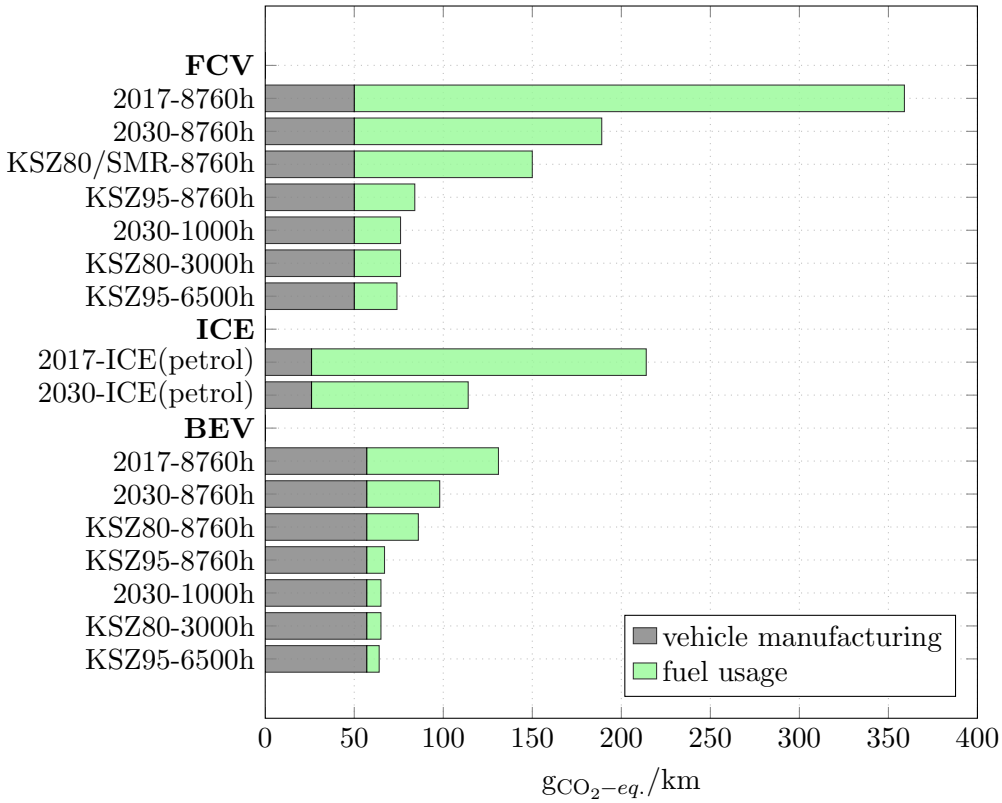

Figure A.4: GWP of 1 km drive range with a mid-size vehicle using hydrogen in a FC from PEMWE versus petrol in an ICE and BEV using electricity from the grid.

It must be mentioned the fuels were not calculated from the perspective of an tank-to-weel approach as only ICE would have direct emission from combustion of fuel. Thus, as BEVs and FCVs do not have direct emissions, the impact of hydrogen from the PEMWE LCA is used in case of the FCV and the corresponding value of the impact of electricity for the usage phase of BEVs. In 2050 with a moderate CO_2 reduction scenario of 80 % the petrol driven car is still environmental friendlier compared to the FCV which uses the electricity mix of the corresponding year, using the presented LCA method. The results are surprising, as the produced hydrogen should be due to the higher efficiency an advantage of the FCV compared to the ICE could be expected. The difference is that burning petrol leads to direct CO_2 emissions during driving, whereas hydrogen does not emit emissions directly but indirect over the whole value chain (mainly through electricity) as presented. From the life-cycle perspective it holds true, that green hydrogen produced solely by renewable energy technologies still has a perceivable CO_2 impact. With regard to a future evaluation of hydrogen as an alternative fuel, this result is worth a discussion.

A.5 Further results: Energy system model

In the following, the maximum value per demand of the modeled year is listed in Table A.6 and is the same for every year. Thus, no change in energy demand is supposed from 2017 until 2050. Regarding the renewable electricity production, the capacity factor represents the workload of the corresponding plant. The capacity factor multiplied with the installed capacity (MW_p) yields the produced electricity (MWh) in that hour. In the third column, the hour of the year is stated in which the maximum value appears the first time. As the hydrogen demand is assumed to be equal during the year, no specific hour is stated.

Table A.6: peak power values of the energy system model

type	max. value	hour of year
Electricity (GW)	78	8,322
H_2 - FCV (GW)	6	-
Electricity - BEV (GW)	13	2,067
Strong wind cap. factor	0.86	25
Weak wind cap. factor	0.84	28
Offshore cap. factor	0.9	20
PV cap. factor	0.7	2,603

A.6 Further results: Intertemporal model

No hydrogen reconversion takes place, thus this parameter is excluded from Table A.7. The maximum capacity on strong-wind turbines is built in all years with 45.5 GW_p and 2500 full load-hours. In this scenario only in the last year additional weak wind turbines are built, in the previous years, the installed capacity is constant with 22 GW_p and 2250 full load hours. Offshore capacities are built to their maximum with 35 GW_p and 4100 full-load hours. A strong shortage in curtailed electricity occurs for the year 2050 which is caused by the increased production of hydrogen.

Table A.7: Installed capacities for the intertemporal approach until 2050

Process	2030	2035	2040	2045	2050
H_2 Storage (GWh)	409	409	409	409	409
PV (GWp)	165	170	176	181	185
Onshore (GWp)	57	57	57	57	59
Offshore (GWp)	35	35	35	35	35
CGGT (GW)	109	109	109	109	109
CGGT (TWh)	236	234	230	227	224
H_2 produced (TWh)	54.6	55.3	56.1	88.9	186.2
PEMWE (GW)	6.5	6.5	6.5	6.5	6.5
H_2 produced (TWh)	52	52	52	52	52
Curtailment (GW)	119	253	253	253	134
Curtailment (TWh)	10.4	11.2	12.3	13.3	14.6

A.7 Further results: Extended intertemporal model

Electricity energy stays constant with 506 TWh/a over the years (same as for all models). Access of using pump storages is also not changed over the different model approaches with an overall capacity of 114 GWh constant over the whole modeling period and 16 GW power of installed turbines for converting water to electricity. BEVs are modeled with 143 GW battery availability with a 1 C rate constant over the whole modeling period. The offshore capacity is reached its maximum already in the first year 2030. More values are available in Table A.8

Table A.8: Installed capacities for the intertemporal approach until 2100

Process	**2030**	**2040**	**2050**	**2060**	**2070**	**2080**	**2090**	**2100**
H_2 Storage (TWh)	1.1	1.7	3	3.1	3.5	12.5	21.5	23.8
PV (GWp)	230	245	248	278	283	322	365	368
Onshore (GWp)	100	111	118	158	156	193	192	193
Offshore (GWp)	35	35	35	35	35	35	35	35
CGGT (GW)	107	107	107	91	91	91	34	34
H_2 reconversion (GW)	0	0	0	7.7	7.8	21.2	38.4	38.4
H_2 produced (TWh)	54.6	55.3	56.1	88.9	91.8	150.2	187.1	186.2
PEMWE (GW)	13.7	15.2	16.6	23.4	24.5	38	48.4	48.2
Curtailment (GW)	193.7	193.7	237.5	237.5	266.7	266.7	280.8	280.8
Curtailment (TWh)	34.9	49.2	53.7	96.3	91.4	111.8	95.7	98.3

List of Figures

List of Tables

Acronyms

a	annum (year).
BEV	battery electric vehicle.
BOP	balance of plant.
CAES	Compressed Air Energy Storage.
CED	cumulative energy demand.
CHP	Combined Heat and Power.
CO_2	Carbondioxide.
CO_2-eq.	CO_2-equivalent.
COP	Coefficient of performance.
DBU	Deutsche Bundesstiftung Umwelt.
FCV	fuel cell vehicle.
GHG	greenhouse gas emissions.
GIS	Geo-Information-System.
GWP	global warming potential.
H_2	hydrogen.
ICE	internal combustion engine.
IPCC	Intergovernmental Panel on Climate Changes.
kWh	kilowatt hour.
LCA	life-cycle assessment.
LCIA	life-cycle-impact assessment.
LCOE	levelized costs of electricity.
LHV	lower heating value.
LOHC	liquid organic hydrogen carriers.
mc-Si	multicrystalline silicon.
MDP	metal depletion.
MEA	membrane electrode assembly.
MG-Si	metallurgical grade silicon.
MIMO	multiplie input multiple output.
MWh	Megawatt hour.

PEMWE	proton-exchange-membrane water-electrolyzer.
PtG	power-to-gas.
PtL	power-to-liquid.
PV	Photovoltaics.
RES	renewable energy sources.
sc-Si	single-crystalline silicon.
SG-Si	solar grade silicon.
SMR	steam methane reformer.
SupIm	supply intermittent.
WLTC	worldwide harmonized light-duty vehicles test cycles.

Acknowledgement

This dissertation was carried out at the Chair for Renewable and Sustainable Energy Systems at the Technical University of Munich (TUM). I started my research on May 1st, 2014 under the supervision of Prof. Dr. Thomas Hamacher, who holds the chair.

First of all I would like to thank my first supervisor Prof. Dr. Thomas Hamacher for giving me the great opportunity to do my research at his chair. Above all, I am grateful to him for his good advises during the whole time. I also appreciate that he always took the time to discuss interesting results and motivated me to carry on. I would also like to thank him for giving me a position as a research assistant working on exciting projects. I learned much.

I would like to thank my mentor, Dr. Philipp Kuhn, for always having constructive suggestions for solving problems. Due to his administrative knowledge and his project experience, the numerous discussions were very valuable for me. In addition to the very good working relationship I would like to thank him for his friendly nature.

I would also like to thank my office colleague Rita Dornmair especially during the final phase of the dissertation. It was the perfect balance of having fun as well as professional discussions in all areas of energy technology during long office hours. Thank you very much!

I would also like to thank Leonhard Odersky for his Python support during my modelling of energy systems in urbs.

Luckily I was able to work with Dr. Cristina de la Rua in the field of LCA together, who was a great support with her expertise in modeling LCAs.
My thanks also go to Anurag Mohapatra, who took the time to proofread my dissertation. Thank you for your great help!

I would like to thank Ms. Angela Brunnbauer for her good solution-oriented suggestions regarding administrative issues.

I would also like to thank Dr. Konrad Schönleber, who supports me in the implementation of new modeling methods and with whom I was able to discuss initial results.

I would also like to thank the other colleagues at the Center for Energy and Information. Johannes Winklmaier, for the pleasant time in Garching-Hochbrück and also the exchange outside working hours. Soner Candas for his support in mathematical questions. I would also like to thank Kais Siala for his candor and helpfulness in exchanging data sets as well as Smajil Halilovic for the pleasant conversations.

I would like to thank the Energy Institute under the direction of Dr. Varun Rai to make a research stay in the USA at the University of Texas at Austin possible. It was a great experience. Above all I would like to thank Dr. Dave Tuttle for the interesting discussions and the support during my time abroad. I would like to thank Ms. Christa J. Hopkins for her incredibly fast response time in organizing my stay abroad despite

the time difference. I would like to thank Todd Davidson and Alan Lloyd for their great support during my time at the Energy Institute. Of course I would also like to thank the Graduate School of the Faculty of Electrical Engineering and Information Technology at TUM for their financial support of this stay abroad.

I would also like to thank my project partners for the professional and good cooperation during the Kopernikus research project P2X. Above all, I would like to thank the project coordinator Dr. Florian Ausfelder for giving me insight into numerous interesting research fields which motivates me. I would also like to thank Ms. Hanna Dura for the uncomplicated and pleasant organization during the project. I would like to thank Maximilian Möckl and Dr. Matthias Rzepka for their help on the subject of PEM-electrolyzer.

I would also like to thank Sebastian Köberle for the good conversations during my time at TUM and Munich. I would also like to thank Tobias Gschnaidtner for his support in questions concerning power plant technology. In addition I also want to thank both of them for the pleasant atmosphere at the Garching campus.

My special thanks go to my parents Carmen and Alexander, who supported me throughout my studies. I would also like to thank my brother Mario for his advice, who, like my parents, also supported me beside my study.

Finally, I gratefully acknowledge the funding by the German Federal Ministry of Education and Research (BMBF) within the Kopernikus Project P2X: Flexible use of renewable resources – exploration, validation and implementation of 'Power-to-X' concepts which made this work possible.